

NPS ARCHIVE
1969
LANDAZURI, R.

SERVO COMPENSATION FOR MECHANICAL
RESONANCES AND FEEDBACK LOOPS

by

Ruben Jaime Landazuri

United States Naval Postgraduate School



THESIS

Servo Compensation for Mechanical
Resonances and Feedback Loops

by

Ruben Jaime Landazuri

December 1969

*This document has been approved for public re-
lease and sale; its distribution is unlimited.*

T133477

LIBRARY
NAVAL POSTGRADUATE SCHOOL
MONTEREY, CALIF. 93940

Servo Compensation for Mechanical

Resonances and Feedback Loops

by

Ruben Jaime Landazuri
Teniente de Fragata, Ecuadorian Navy

Submitted in partial fulfillment of the
requirements for the degree of

MASTER OF SCIENCE IN ELECTRICAL ENGINEERING

from the

NAVAL POSTGRADUATE SCHOOL
December 1969

NPS ARCHIVE

1969

LANDAUZURI, R.

~~41-51-563~~ C 1

ABSTRACT

When the transfer function of a system has at least one pair of complex poles, resonant peaks will occur in the open-loop frequency response at the frequency determined by these complex poles. The resonant peaks may produce instability in the closed-loop system. Cascaded complex-zero compensators are studied in order to cancel the effect produced by the complex poles. Circles of stability are developed and if the complex zeros of the compensator are located inside the circles the system stability is guaranteed. Several locations for the complex zeros in the s-plane are studied and a correlation among frequency-response, transient-response and root-locus techniques is described to aid in the design of the compensator. (Complex poles are often generated by mechanical resonances)

TABLE OF CONTENTS

| | | |
|------|--|----|
| I. | INTRODUCTION ----- | 9 |
| II. | CASCADE COMPLEX-ZERO COMPENSATORS ----- | 13 |
| | A. INTRODUCTION ----- | 13 |
| | B. THE S-PLANE ----- | 14 |
| | C. ANALYSIS OF DATA ----- | 17 |
| | 1. Root Locus ----- | 18 |
| | 2. Bode Diagrams ----- | 22 |
| | 3. Transient Response ----- | 26 |
| III. | APPLICATION OF RESULTS TO DESIGN OF COMPENSATORS ----- | 29 |
| IV. | CONCLUSIONS ----- | 33 |
| | BIBLIOGRAPHY ----- | 87 |
| | INITIAL DISTRIBUTION LIST ----- | 88 |
| | FORM DD 1473 ----- | 89 |

LIST OF ILLUSTRATIONS

| Figure | | Page |
|--------|--|------|
| 1.1 | Block Diagram of the System ----- | 10 |
| 2.1 | Block Diagram of the Plant and Compensator ----- | 15 |
| 2.2 | Root Locus for Plant ----- | 34 |
| 2.3 | Root Locus of the System Showing Exact Cascade Compensation ----- | 35 |
| 2.4 | Root Locus of the Plant Added the Real Poles of the Compensator ----- | 36 |
| 2.5 | Root Locus of a Typical Case Where the Complex Poles are Away from the Complex Poles ----- | 37 |
| 2.6 | Stability Boundaries for Different Gains ----- | 38 |
| 2.7 | Different Location of the Complex Zeros of the Compensator ----- | 39 |
| 2.8a | Root Locus for Point 1 ----- | 40 |
| 2.8b | Bode Diagram for Point 1 ----- | 41 |
| 2.8c | Transient Response for Point 1 ----- | 42 |
| 2.9a | Root Locus for Point 2 ----- | 43 |
| 2.9b | Bode Diagram for Point 2 ----- | 44 |
| 2.9c | Transient Response for Point 2 ----- | 45 |
| 2.10a | Root Locus for Point 3 ----- | 46 |
| 2.10b | Bode Diagram for Point 3 ----- | 47 |
| 2.10c | Transient Response for Point 3 ----- | 48 |
| 2.11a | Root Locus for Point 4 ----- | 49 |
| 2.11b | Bode Diagram for Point 4 ----- | 50 |
| 2.11c | Transient Response for Point 4 ----- | 51 |
| 2.12a | Root Locus for Point 5 ----- | 52 |
| 2.12b | Bode Diagram for Point 5 ----- | 53 |

| Figure | | Page |
|--------|---------------------------------------|------|
| 2.12c | Transient Response for Point 5 ----- | 54 |
| 2.13a | Root Locus for Point 6 ----- | 55 |
| 2.13b | Bode Diagram for Point 6 ----- | 56 |
| 2.13c | Transient Response for Point 6 ----- | 57 |
| 2.14a | Root Locus for Point 7 ----- | 58 |
| 2.14b | Bode Diagram for Point 7 ----- | 59 |
| 2.14c | Transient Response for Point 7 ----- | 60 |
| 2.15a | Root Locus for Point 8 ----- | 61 |
| 2.15b | Bode Diagram for Point 8 ----- | 62 |
| 2.15c | Transient Response for Point 8 ----- | 63 |
| 2.16a | Root Locus for Point 9 ----- | 64 |
| 2.16b | Bode Diagram for Point 9 ----- | 65 |
| 2.16c | Transient Response for Point 9 ----- | 66 |
| 2.17a | Root Locus for Point 10 ----- | 67 |
| 2.17b | Bode Diagram for Point 10 ----- | 68 |
| 2.17c | Transient Response for Point 10 ----- | 69 |
| 2.18a | Root Locus for Point 11 ----- | 70 |
| 2.18b | Bode Diagram for Point 11 ----- | 71 |
| 2.18c | Transient Response for Point 11 ----- | 72 |
| 2.19a | Root Locus for Point 12 ----- | 73 |
| 2.19b | Bode Diagram for Point 12 ----- | 74 |
| 2.19c | Transient Response for Point 12 ----- | 75 |
| 2.20a | Root Locus for Point 13 ----- | 76 |
| 2.20b | Bode Diagram for Point 13 ----- | 77 |
| 2.20c | Transient Response for Point 13 ----- | 78 |
| 2.21a | Root Locus for Point 14 ----- | 79 |

| Figure | | Page |
|--------|---|------|
| 2.21b | Bode Diagram for Point 14 ----- | 80 |
| 2.21c | Transient Response for Point 14 ----- | 81 |
| 2.22a | Root Locus for Point 15 ----- | 82 |
| 2.22b | Bode Diagram for Point 15 ----- | 83 |
| 2.22c | Transient Response for Point 15 ----- | 84 |
| 2.23b | Bode Diagram for Exact Compensation ----- | 85 |
| 2.23c | Transient Response for Exact Compensation ----- | 86 |

ACKNOWLEDGEMENT

The author wishes to express his sincere appreciation to Doctor George J. Thaler for the topic, guidance and assistance which he provided during the pursuit of this study.

I. INTRODUCTION

The structural resonances found in missiles, shaft twisting, fuel sloshing, etc., can be modeled and treated as control-system problems. In these models and in general in systems where the plants have moving mechanical parts, the transfer functions have at least one pair of complex poles whose location is near the imaginary axis.

If the gain of the system is low, the effect of the pair of complex poles is minimum compared with the dominant poles. If the gain of the system has to be maintained high, the effect of the complex poles is no longer negligible and the resonances due to these poles have to be considered. The magnitudes of these resonant peaks are usually 20 to 30 db; in practice peaks as high as 50 db have been encountered. Depending on the relative magnitude of these peaks, the system may be unstable if the resonant frequencies are contained in the bandwidth of the system.

When the system specifications cannot be met by adjusting the open-loop gain, because a decrease in it could permit errors caused by friction, hysteresis, backlash, etc., or because the specifications require a high gain, cascade compensation may be an effective solution to reduce the effect of the resonant peaks produced by the complex poles.

A cascade compensator can be added to the plant in order to cancel part or all the undesirable zeros or poles, and at the same time maintain a higher value of gain. The block diagram of this kind of compensator is shown in Fig. 1.1.

A very versatile technique to improve the performance of the system is to replace undesirable poles with desirable ones. This can be

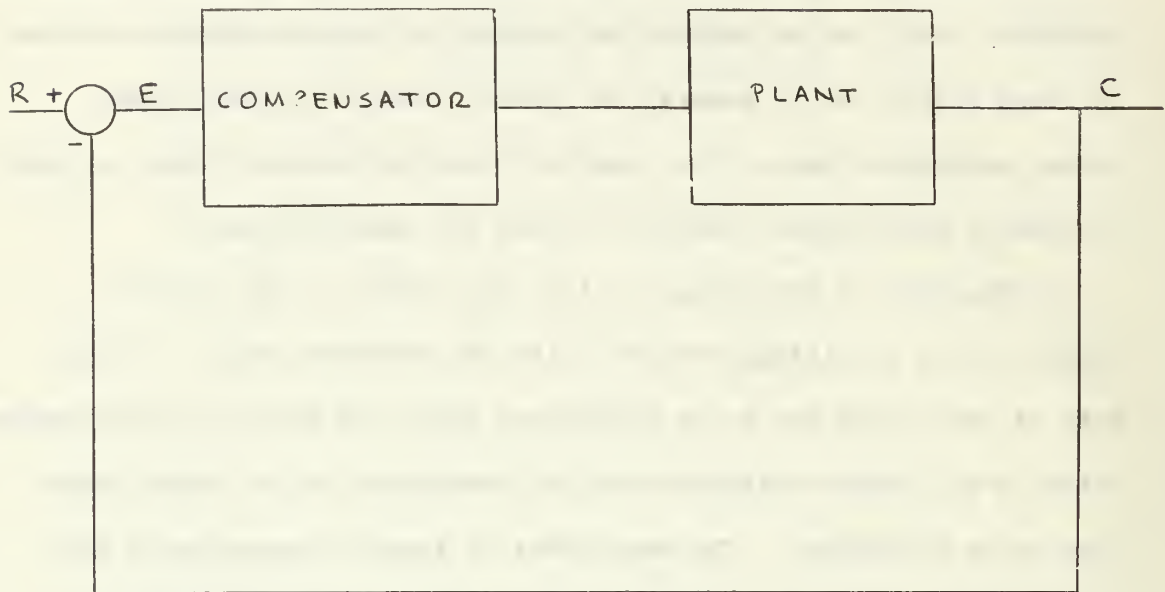


Figure 1.1

accomplished by the classical phase-lead, phase-lag, or phase-lag-lead compensators.

The phase-lead compensator is a high-pass filter. It introduces a positive phase shift and provides attenuation at low frequencies. These characteristics tend to stabilize unstable systems and improve stable systems by increasing damping.

When a phase-lead filter is used, it increases the bandwidth of the system; but it has the disadvantages that if the spacing between pole and zero is large, noise will be added to the system, and the gain of the forward path has to be increased in order to cancel the attenuation of the filter if acceptable accuracy in steady state is expected.

The transfer function of the phase-lead compensator is given by:

$$G_c(s) = \frac{s+z}{s+p} \quad \text{where} \quad |p| \geq |z|$$

The phase-lag compensator is a low-pass filter. It provides attenuation at high frequencies. Whenever a phase-lag compensator is used, the bandwidth of the system is reduced. One advantage of using it is that no additional gain is needed because the filter does not attenuate at low frequencies.

The transfer function of the phase-lag compensator is given by:

$$G_c(s) = \frac{p \left(\frac{s+z}{s+p} \right)}{z \left(\frac{s+p}{s+z} \right)} \quad \text{where} \quad |p| < |z|$$

In practice, there are occasions when the system is highly unstable; neither the phase-lead nor the phase-lag filters alone can give the desired compensation. A phase-lag compensator is used to put the system at the limit of stability and then a phase-lead compensator is used to stabilize the system. These two filters in cascade are known as the lag-lead compensator and when it is used the characteristics described for the lead and lag compensators are applied in conjunction. Its transfer function is given by :

$$G_c(s) = \frac{p_2 (s+z_2) (s+z_1)}{z_2 (s+p_2) (s+p_1)} \quad \text{where} \quad |p_1| \geq |z_1| \quad \text{and} \\ |p_2| < |z_2|$$

When the system has mechanical resonances produced by the presence of complex poles and the system specifications require a high gain, the phase-lead compensator can be used, but as an additional gain is

added to the system, the resonant peaks may produce instability in the system. The phase-lag compensator cannot be used either because the system specifications often require high bandwidth. The solution to the problem of stability is to design a filter that will attempt to cancel the resonant peaks by means of cascading a pair of complex zeros which will neutralize the action produced by the complex poles. This kind of compensator will be widely studied in the next section.

II. CASCADE COMPLEX ZERO COMPENSATORS

A. INTRODUCTION

A system subjected to mechanical resonances may become unstable at high gains, due to the presence of complex poles. Cascade compensation techniques can be used in order to stabilize the system. When this technique is used, the ideal compensation is to have a perfect cancellation, which occurs when the complex zeros of the compensator are exactly superimposed on the complex poles of the plant. Therefore the complex zeros will cancel the effect of the resonances produced by the complex poles. This is the ideal situation; but in practice, most of the time it is almost impossible to build physically this kind of compensator and at other times it is very difficult to know the exact location of the complex poles or their changes of position during operation of the system.

For these reasons the complex zeros should be placed in other locations, in which they will try to achieve the following objectives:

1. provide good compensation characteristics, and
2. be physically and economically realizable.

The possibility of having good compensation, even if perfect cancellation is not achieved leads to the study of the present Thesis.

When the loop gain is increased, the relative area on the s-plane desirable for location of the complex zeros is decreased, namely the higher the gain of the system the harder it is to stabilize.

Bounded areas on the s-plane, inside of which the position of the complex zeros of the compensator will guarantee stability of the system will be determined. To achieve this a procedure of trial and error, using digital computer simulation will be followed.

The real poles of the compensator are arbitrarily located and in such a way that their contribution to the transient response will disappear before the maximum overshoot is reached. Meanwhile the complex zeros will be varied radially until the limit of stability is reached. Repeating this procedure several times, points lying on the limit of stability will be used to bound the area where the complex zeros can be located in order to achieve stability. Areas of stability for different gains will be found in order to appreciate the effect of raising the gain over the area of stability.

Further digital computer simulations will take selected cases where the complex zeros of the compensator will be located at:

1. outside of the area of stability,
2. inside of the area of stability on:
 - a. left hand plane,
 - b. imaginary axis, and
 - c. right hand plane

and a correlation among: s-domain (Root Locus), frequency-domain (Bode diagram) and Transient response will be carried out.

B. THE S-PLANE

The block diagram shown in Fig. 2.1, will be the basic system for the study of the effect of cascaded complex zero compensators. The pair of complex poles in the plant are located very near to the imaginary axis, and as a consequence have a very low damping factor. With a moderate gain k , the system will be unstable. These complex poles typically represent the mechanical resonances that are encountered in real life.

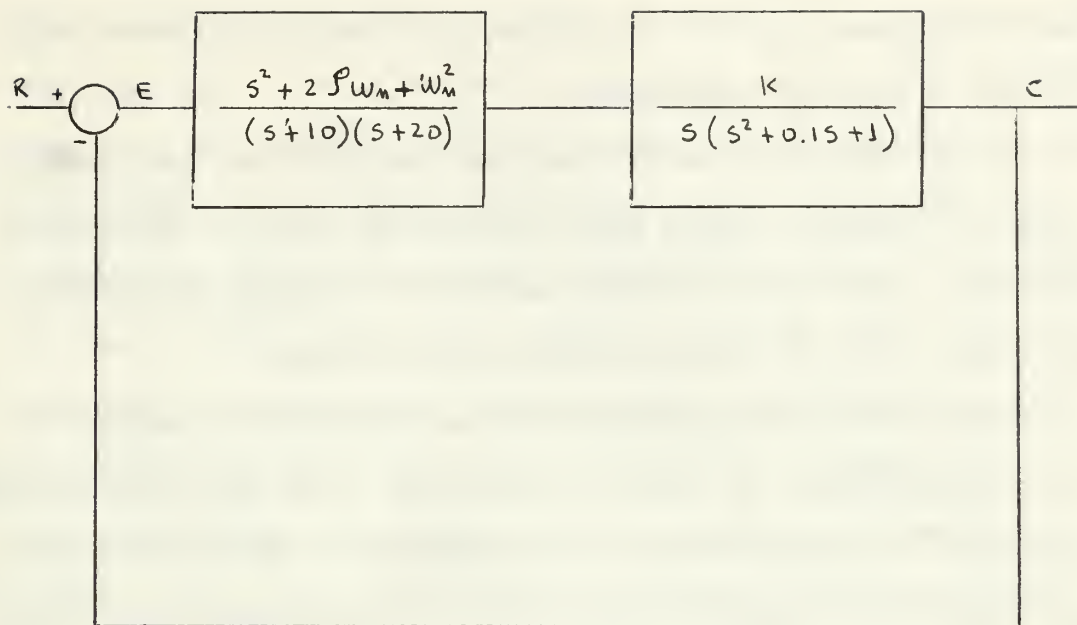


Figure 2.1

Figure 2.2 is the representation of the plant in the s-plane. From this figure it can be seen that the root locus crosses the imaginary axis as soon as the loop gain is increased. Calculations of the gain k at the limit of stability give a value of 0.1. For greater values of gain the system will become unstable.

If the gain is raised to a high value, the performance and the response of the system will be improved. This point of view leads to the problem of how to find a way by which the system will remain stable when the gain is raised.

In Figure 2.2 part of the root loci depart from the complex poles, and as the gain is increased, arrive at the complex zeros that theoretically are located at infinity. If these complex zeros can be relocated in a place near the complex poles, then the gain can be raised and the roots will still be on the left of the imaginary axis,

making the system stable. The relocation of the complex zeros can be achieved by means of compensators.

In this Thesis the use of a cascade compensator has been assumed in order to maintain higher gains than the one found at the limit of stability. The effect on system stability of changing the location of the complex zeros of the compensator will be studied.

Figure 2.3 is a representation on the s-plane of the perfect or exact compensation. The complex poles of the plant have been cancelled exactly by the complex zeros of the compensator. Now the root loci that began on the complex poles and ended on the complex zeros do not exist, except at one point, since the zeros and poles are superimposed. As a consequence, the gain of the system can be increased without affecting the stability, because the branches of the root loci that crossed the imaginary axis and went into the right hand plane have been cancelled by the effect of the cascade compensator.

As was pointed out before, most of the time it is impossible to build an exact compensator. The following discussion will be concerned with kinds of cascaded compensators that are not perfect.

Figure 2.4 shows the root locus of the basic plant cascaded with the real poles of the compensator. From this figure it can be seen that the effect of adding the real poles of the compensator is a slight reshaping of the original root loci starting from the complex poles. Therefore, the problem of instability is still important. From this it is deduced that something has to be added to the compensator besides the real poles in order to improve the stability.

Figure 2.5 illustrates the procedure used to study the effects on stability of the locations of the complex zeros. A pair of complex zeros was located on a chosen radial line ($\sigma = \text{constant}$) giving

rise to a root locus such as is shown on Figure 2.5. The gain at the stability limit, (i.e., the gain at the point of intersection between root locus and imaginary axis) was checked and the stability of system with regard to a prespecified loop gain was thus determined. This procedure was repeated for other locations of the zeros on the chosen ζ -line. In this fashion the stability limit was found, that is, the location of the zeros which placed the roots on the imaginary axis for a specified loop gain. Repeating this for other constant ζ -lines determined a stability boundary for the system, i.e., determined a boundary line on the s-plane such that locating the complex zeros within this boundary guaranteed a stable system.

This process has been repeated for different gains. Figure 2.6 shows these "circles of stability" for selected gains which were chosen as 10, 50 and 100 per cent greater than the gain of the plant at its limit of stability.

C. ANALYSIS OF DATA

An elementary discussion of the stability criteria of any system is given by considering the relative location of the roots of the characteristic equation in the s-plane. Let the system be defined by the matrix equation

$$\dot{\underline{X}}(t) = \underline{A} \underline{X}(t) + \underline{B} u(t) \quad 2.1$$

Assume that for simplification the forcing function $u(t)=0$ and that the initial conditions are given by $\underline{X}(t_0) = \underline{X}_0$, so equations 2.1 is reduced to

$$\dot{\underline{X}}(t) = \underline{A} \underline{X}(t) \quad 2.2$$

whose time solution is

$$\underline{X}(t) = \exp[\underline{A}(t-t_0)] \underline{X}_0 \quad 2.3$$

Thus if the system has its roots in the left-half portion of the s-plane, the time solution $\underline{X}(t)$ will approach zero as time approaches infinity; this means that the system is stable. If the system has

its roots in the right-half portion of the s-plane, the time solution $\underline{x}(t)$ will approach infinity as time approaches infinity due to the positive exponent; this means that the system is unstable. And finally, if the roots are located on the imaginary axis the time function $\underline{x}(t)$ will be oscillatory and the system will be at the limit of stability.

Once the stability problem has been solved, and knowing that the system is stable, does not mean that the optimal solution has been achieved. As discussed earlier, the complex zeros of the compensator that will be used to stabilize the system can be located at any place inside the stability boundaries. In the following analysis, it will be shown how the system responds to the different location of the compensator complex zeros.

Figure 2.7 shows the location in the s-plane of the complex zeros that have been chosen for this study, and Table I indicates their transfer functions and other characteristics. A gain 50 per cent higher than the gain at the limit of stability has been used for these points in order to make the system unstable and therefore require stabilization.

1. Root Locus

The system in Figure 1.1 has a transfer function given by

$$\frac{C(s)}{R(s)} = \frac{G(s)}{1 + G(s)H(s)} \quad 2.4$$

where $G(s)$ and $H(s)$ are fractions whose numerators and denominators are polynomials in s . Formula 2.4 can be rewritten as

$$\frac{C(s)}{R(s)} = \frac{k_1 \prod_{k=1}^m (s + z_k)}{\prod_{k=1}^n (s + p_k)} \quad 2.5$$

where $-z_k$ and $-p_k$ from $k=1$, to $k=m$ and n respectively are the zeros and poles of the closed-loop transfer function. What is usually known is

| Point | Numerator | Denominator | ω_n | ζ |
|-------|----------------------|-------------------|------------|---------|
| 1 | $s^2 + s + 0.5$ | $s^2 + 30s + 200$ | 0.707 | 0.707 |
| 2 | $s^2 + 1.5s + 1.12$ | $s^2 + 30s + 200$ | 1.06 | 0.707 |
| 3 | $s^2 + 2s + 2.0$ | $s^2 + 30s + 200$ | 1.41 | 0.707 |
| 4 | $s^2 + 2.54s + 3.26$ | $s^2 + 30s + 200$ | 1.80 | 0.707 |
| 5 | $s^2 + 0.49$ | $s^2 + 30s + 200$ | 0.7 | 0.0 |
| 6 | $s^2 + 1.21$ | $s^2 + 30s + 200$ | 1.1 | 0.0 |
| 7 | $s^2 + 1.96$ | $s^2 + 30s + 200$ | 1.4 | 0.0 |
| 8 | $s^2 + 3.24$ | $s^2 + 30s + 200$ | 1.8 | 0.0 |
| 9 | $s^2 - 1.5s + 1.12$ | $s^2 + 30s + 200$ | 0.707 | -0.707 |
| 10 | $s^2 - 1.5s + 1.12$ | $s^2 + 30s + 200$ | 1.06 | -0.707 |
| 11 | $s^2 - 2s + 2.0$ | $s^2 + 30s + 200$ | 1.41 | -0.707 |
| 12 | $s^2 - 2.4s + 2.88$ | $s^2 + 30s + 200$ | 1.69 | -0.707 |

TABLE I. Location, transfer function, natural frequency and damping factor of the compensator.

the open-loop transfer function

$$G(s)H(s) = k \frac{\prod_{i=1}^M (s + z_i)}{\prod_{i=1}^M (s + p_i)} \quad 2.6$$

and from 2.6 the characteristic equation is obtained,

$$G(s)H(s) + 1 = 0 \quad 2.7a$$

or

$$\prod_{i=1}^M (s + p_i) + k \prod_{i=1}^M (s + z_i) = 0. \quad 2.7b$$

Thus assigning values to the variable k , a locus of points may be drawn. In other words, the roots of the characteristic equation lie in the s -plane. Using the root locus method it is possible to determine the roots of the closed-loop transfer function and the only requirement is that

$$\left| G(s)H(s) \right| = 1$$

$$\arg G(s)H(s) = (2n + 1) \pi \quad \text{where } n \text{ is an integer.}$$

In figures 2.8a, 2.9a, 2.10a and 2.11a the root-locus plots for points 1 through 4 of Figure 2.7 are shown. A damping factor of 0.707 has been chosen for these points. It can be seen that all the root loci are similar and follow the same pattern.

Note specially that the loci starting on the complex poles do not (in this case) terminate on the complex zeros, but they are bent into the left half plane by these zeros. They eventually re-enter the right half plane because the transfer function has three excess poles, but do so only at very high gain values. Thus, for all normal gain values the system is stabilized and the dominant roots are those on the root loci which terminate on the complex zeros. As the complex zeros are moved away from the origin on the chosen ζ -line, the loci from the complex poles undergo less bending, and on Figure 2.11a it is seen that

these loci enter the right half plane before being bent into the left half plane. This fact, by itself, does not make the loop unstable, but for the gain value specified the roots on these segments happen to be on that portion which is in the right half plane so the system designated by Figure 2.11a is unstable.

Figures 2.12a, 2.13a, 2.14a and 2.15a show the root locus corresponding to points 5, 6, 7 and 8 of Figure 2.7. They are located along the constant ζ -line, whose damping factor value is 0.0. In these figures the loci starting on the complex poles end on the complex zeros of the compensator. It is interesting to note this fact because in the preceeding cases the loci from the complex poles did not end on the complex zeros.

For natural frequencies of the complex zeros lower than the natural frequency of the complex poles, the root locus is bent toward the left of the imaginary axis. Taking into account only this branch of root locus the system is stable even for infinite gain. As soon as the natural frequency of the complex zeros is higher than the natural frequency of the complex poles, the bending of the root loci changes its sense and now is bent to the right hand plane forcing the system to instability for relatively low gains. The gains at the limit of stability for points 6 and 7 are 90.0 and 21.2. Figure 2.15a shows the root of point 8; the system is unstable even for a gain as low as 9.1. The complex roots definitely are located in the right hand plane.

Figures 2.16a, 2.17a, 2.18a and 2.19a illustrate the root locus for points 9, 10, 11, and 12 of Figure 2.7. For this case a constant damping factor of -0.707 was chosen since the complex zeros

of the compensator are located in the right hand s-plane. It can be seen from these figures that the root loci have the same shape whether the natural frequencies of the complex zeros are higher or lower than the natural frequency of the complex poles. The root loci starting at the complex poles end in the complex zeros and in its path bends toward the origin and then leaves to the right, crossing the imaginary axis.

The complex zeros are located on the right hand plane, and for this reason the root locus will not return to the left hand plane and the system will be unstable, because the roots of the system will lie on the right hand plane for values of gains higher than the gain at the limit of stability. The gain at the limit of stability for points 10 and 11 are 44.0 and 18.0 respectively, and as low as 10.5 for point 12.

Figures 2.20a, 2.21a and 2.22a, describe the root locus for points 13, 14 and 15, which were chosen to lie in the s-plane, inside of the circles of stability and at the same relative position with respect to the complex poles; but the gain of the plant was set equal to 0.11, 0.15 and 0.20 respectively. For low values of gain the root loci starting at the complex poles goes to infinity, but as the gain is increased, this root locus changes and instead of going to infinity, it ends at the complex zeros. The same property was achieved by decreasing the damping factor of the compensator. Even for relatively high values of gain, the roots lie entirely on the left hand plane, which guarantees stability of the system.

2. Bode Diagrams

The Bode diagrams are basic logarithmic plots of the open-loop transfer function, and give a curve of magnitude and a curve of phase as a function of angular frequency. These plots give the same information as the Nyquist or polar plot but in a different form. From these

curves of magnitude and phase, a relationship is obtained, namely the Phase Margin, which is of importance when the stability of the system is to be determined.

The phase margin is defined as 180° minus the amount of phase that exists at the angular velocity where the gain of the system has magnitude equal 1, or 0 db. From this definition, a positive phase margin means stability in the system and a negative phase margin signifies that the system is unstable. A phase margin greater than 45° is indicative of good stability. Lower phase margins may be considered unsatisfactory and the system may need to be compensated.

Prediction of stability with Bode plots may not be so easy and specially it becomes rather difficult when poles or zeros are located in the right hand plane. When this occurs, a more detailed look at the corresponding Nyquist plot would be required in order to clarify the problem.

Figures 2.8b, 2.9b, 2.10b and 2.11b show the Bode plots corresponding to points 1, 2, 3 and 4 of Figure 2.7. In these graphs the damping factor is maintained constant at 0.707. It is seen that the zero-db line is crossed three times by the magnitude curve. This means that the system has three different phase margins and if these are not all positive values and higher than 45° to ensure good stability, the system could be unstable if one of these has a negative or low positive value.

As an example in Figure 2.11b which corresponds to the point 4 in Figure 2.7, the first point, where the magnitude curve crosses the zero-db line at frequency 0.2 Hertz, has a corresponding phase margin of 95° . The second crossing is at a frequency of 1.49 Hz. with a

corresponding phase margin of 87° . The third point is at frequency 1.66 Hz. and has a phase margin of -6° . With respect to the last point and looking only at the Bode diagram, it is difficult to measure the low negative phase margin because the slope of the phase curve at frequencies around where the mechanical resonances occurs is very steep; there is a change of 140° . A plot to a larger scale was required to get this value of phase margin. As was discussed above, a system will be unstable if one or more of the three phase margins are negative. In the present case, one is negative and the system is unstable. The instability of this point is clearly shown in the transient response plot in Figure 2.11c.

Figures 2.12b, 2.13b, 2.14b and 2.15b show the Bode diagrams of points 5, 6, 7 and 8 of Figure 2.7. The constant damping factor for these points is 0.0; i.e., the complex zeros lie on the imaginary axis. For lower natural frequencies than the natural frequency of the complex poles, the magnitude curve crosses the zero-db line three times. This is due to the complex zeros are relatively located away from the complex poles and cannot compensate the resonances produced by these complex poles. Figure 2.12b illustrates point 5 which is near the origin; the three gain margins are positive and the system presents good stability.

As the natural frequency of the complex zeros of the compensator is increased, the zeros become close to the complex poles and are able to compensate partially the effect of the resonances due to the complex poles. This is clearly shown in Figure 2.13b where the complex poles and zeros are very close to each other. This is reflected in the magnitude curve where the zero-db line is crossed only at one point, meanwhile the resonant peak almost disappears and is down -10 db.

As the natural frequency of the complex zeros is increased more, the process begins to repeat. The complex zeros are going away from the complex poles again and do not exert much influence in the neutralization of the resonant peak. As a consequence this resonant peak begins to increase in magnitude and again crosses the zero-db line. Point 8 in Figure 2.15b represents an unstable system. It gives the following phase margins: at frequency 0.2 Hz, the phase margin is 86° , at 1.55 Hz, it is -12° and at 1.63 Hz, the phase margin is -33° .

Figures 2.16b, 2.17b, 2.18b and 2.19b represent the Bode diagrams for points 9, 10, 11 and 12 of Figure 2.7. The constant damping factor chosen for the location of the complex zeros of the compensator was -0.707, i.e., the complex zeros are in the right hand plane. For this reason it is not possible to get any information about stability from these diagrams. If information about stability in the frequency domain is required, a careful interpretation of the Nyquist plot will have to be carried out for these specific locations of the complex zeros.

Bode diagrams for points 13, 14, and 15 are shown in Figures 2.20b, 2.21b and 2.22b. These points have the same relative position with respect to the complex poles, but different open-loop gain. It can be seen from these figures that as the gain of the plant is increased from 0.11 to 0.2 so do the resonant peaks which are increased from 1 db to 4.8 db. These points all have phase margins with positive values. The increase in gain produces an increase in phase margins, which means that the system becomes more stable.

3. Transient Response

The transient response is the manner in which a system changes from some initial operating condition to some final condition. Of special interest for stability, is the steady-state performance of the system which is basically given by the roots of the system which are near to the imaginary axis. The roots located far to the left of the imaginary axis have large exponential decaying factors and transients tend to decrease very rapidly to negligible quantities after approximately 5 time constants.

The response of a system to a unit impulse excitation provides a good indication of the general transient behavior of the system. In time, a stable system will return again to its equilibrium position or the output will follow the input if a disturbance is applied.

The classical methods for evaluating the transient response use Laplace transforms or solve the differential equations of the system in time domain. In the present study, digital computer programs like DSL (Digital Simulation Language) and LISA (Linear System Analysis) were used to obtain the transient response.

Figures 2.8c, 2.9c, 2.10c and 2.11c show the transient response for points 1, 2, 3 and 4 of Figure 2.7. These points have the same damping factor 0.707, but different natural frequencies.

As the natural frequency of the complex zeros of the compensator is increased the system passes from an over-damped to an under-damped system. In the same manner the settling time is increased due to the increase of oscillations; but the rise time remains the same. This means that the change in natural frequency of the complex zeros does not affect the basic speed of response of the system.

For point 4, the system becomes so underdamped that the oscillations begin to increase and the system goes unstable; this was not so clearly indicated from the analysis of the Bode diagram, but from the transient response graph it is seen clearly that the system is unstable.

Figures 2.12c, 2.13c, 2.14c and 2.15c show the transient response for points 5, 6, 7 and 8 of Figure 2.7. Zero damping factor was chosen for these points; the complex zeros of the compensator lie on the imaginary axis. Of these points, the ones presenting special interest are points 5 and 6. For these specific points the natural frequency of the complex zeros is lower than the natural frequency of the complex poles. The interesting feature is that even with zero damping factor the time response of the system is overdamped and almost without any oscillations. The rise time is short and the speed of response is fast. In other words, it is as if perfect compensation was accomplished. Increasing the natural frequency of the complex zeros, points 7 and 8 present the same characteristics described for points 3 and 4 in the preceding paragraph.

Figures 2.16c, 2.17c, 2.18c and 2.19c show the transient response for points 9, 10, 11 and 12 of Figure 2.7. A negative value for damping factor of -0.707 was chosen for these points. The complex zeros of the compensator are on the right hand plane. For all natural frequencies of the complex zeros compared with the natural frequency of the complex poles, the system response is underdamped and this characteristic increases with the increase in the natural frequency of the complex zeros; but as this frequency is increased, the settling time is increased and also the amplitude of the oscillations increases until the system goes unstable as shown in Figure 2.19c.

For low natural frequencies of the complex zeros, the transient response initially has only a small positive increment of magnitude, then it goes with negative slope and it reaches a negative value as can be seen in Figure 2.16c.

The transient responses for points 13, 14 and 15 are shown in Figures 2.20c, 2.21c and 2.22c. As was discussed in the root locus and Bode diagrams, these points are located inside of the boundaries of stability; i.e., the system is stable at these locations of the complex zeros of the compensator.

An increase in the gain of the system for these locations results in a better transient response which is reflected in the improvement of rise time, settling time and indeed the system response becomes less oscillatory.

III. APPLICATION OF RESULTS TO DESIGN OF COMPENSATORS

When compensation of a system subjected to mechanical resonances is required, a pair of complex zeros is used to cancel the resonant peaks produced by the complex poles. At the same time that the effect of these poles is neutralized, it is intended to get a new pair of dominant poles for the system and with this there are less constraints imposed and all the system specifications can be achieved, specifications that may not be accomplished if the complex poles still remain the dominant roots of the system.

The ideal situation, when it is physically and economically realizable, is to cancel the complex poles exactly with a pair of complex zeros. The effect of using this kind of compensation is shown in Figures 2.3, 2.23b, and 2.23c. Figure 2.3 is a representation of the root locus and as was discussed in section II; the root loci starting at the complex poles end in the same place, i.e., the root locus is a point.

The gain of the system can be increased without risk of instability, which may be caused by the resonant peak. With the cancellation of the complex poles, the new dominant poles are those located at the origin and the one located on the real axis at -10. The compensated system will be at the limit of stability when the loci of the new dominant roots cross the imaginary axis and this will happen when the root-locus gain will have a value of 6000. Making a comparison with the gain at the limit of stability before compensation, i.e., $k=0.1$, it can be seen that now there is a broad margin for fulfilling the requisites of the system specifications concerned with this higher gain.

Figure 2.23b is the Bode diagram. It can be observed that the resonant peak which would have occurred at the frequency of 1.59 Hz. is completely canceled by the effect of the compensator and the curves of magnitude and phase are smooth curves, in contrast with the ones that describe the other points. The phase margin for this case is equal to 87° , which is indicative that the system presents good stability.

Figure 2.23c describes the transient response for the exact compensation. It can be said that the unit step response of the system is almost critically damped. The rise time is fast, the settling time is short and there are no overshoots or undershoots.

When exact compensation cannot be accomplished because it is physically or economically impractical or because the position of the complex poles changes during the operation of the system due to changes in temperature or changes in the load of the system, etc., then a compensator has to be designed for which the location of the complex zeros is the important feature. In section II the "circles of stability" were developed and it is known that if the complex zeros of the compensator are located inside these circles, the system will be stable. The following discussion will aid in the decision of how to choose the location of the complex zeros in order to satisfy the specifications that have to be met.

If there is an option of choice, it is convenient to choose the damping factor close to the damping factor of the complex poles. Complex zeros with a damping factor far away from the complex poles will give an oscillatory response, which will be more pronounced if the right hand plane is chosen for the location of the complex zeros.

The oscillations will increase as will the settling time with the increase in separation between the damping factors of the zeros and complex poles. In contrast to this fact, where the Bode gain was maintained constant, for lower positive damping factors than the damping factor of the complex poles, the gain of the system at the limit of stability increases with the increase in damping factor. This point has to be kept in mind because if it is possible to raise the system gain, a well behaved response can be obtained.

Once the constant ζ -line has been chosen for the location of the complex zeros of the compensator, i.e., a damping factor close to the one of the complex poles, the natural frequency of the complex zeros may be varied in order to satisfy the requirements of the compensation. From the analysis of the data, it can be seen that a good and quick transient response is always obtained when the natural frequency of the complex zeros is lower than the natural frequency of the complex poles. For these cases, the unit step response of the system is similar to the response of exact compensation. Only when the complex zeros are in the right hand plane is the response oscillatory; but for very low natural frequencies the response can be considered satisfactory.

As the natural frequency of the complex zeros becomes greater than the natural frequency of the complex poles, the transient response changes to underdamped if the location of the complex zeros is on the imaginary axis or in the left half plane. The oscillations of the response increase if the complex zeros are located in the right hand plane.

With the change of the response to underdamped or with the increase in oscillations, the settling time becomes large, but the rise times remain essentially the same.

Another point that has to be considered in the design of the compensator, besides the damping factor and natural frequency of the complex zeros, is the amount of open-loop gain of the plant. As was observed, with the raising of the open-loop gain of the plant, the radius of the circles of stability was reduced. Then, for the same relative position of the complex zeros with respect to the complex poles (i.e., points 13, 14 and 15 for open loop gains of 0.11, 0.15 and 0.20 respectively), the best response is the one that has the highest open-loop gain. This is explained because as the gain is increased, the rise time and the settling time are decreased.

As a conclusion for the location of the complex zeros of the compensator, and taking into account its damping factor, its natural frequency and the open-loop gain of the plant, the optimal compensation, besides the exact compensation, is achieved when the location of the complex zeros fills the following requisites:

1. choose the highest open-loop gain of the plant available.
2. choose the closest damping factor to the one of the complex poles that is higher than the damping factor of the complex poles.
3. choose the highest natural frequency that is lower than the natural frequency of the complex poles.

If these three requisites are followed, the location in the s-plane of the complex zeros of the compensator will be close to the location of the complex poles of the plant. It can be assured that the response of the system will only differ with respect to the response of the exact compensation by the presence of little ripples, which decay quickly. But it can be considered that the settling time and rise time for both cases are in principle the same.

IV. CONCLUSIONS

The presence of complex poles due to mechanical resonances produces resonant peaks in the frequency response of the system and tends to destabilize it. Complex zeros can be put in cascade with the plant to cancel these resonant peaks. Circles of stability can be found for every gain of the system. These circles have center at the origin and radii larger than the natural frequency of the complex poles. The complex zeros located within these circles assure stability. The best compensation is obtained when the complex zeros of the compensator are superimposed on the complex poles of the plant but satisfactory results are achieved when the complex zeros are located close to the complex poles. In particular best results are obtained when the zeros have

$$\zeta_z > \zeta_p \quad \text{and} \quad \omega_z < \omega_p .$$

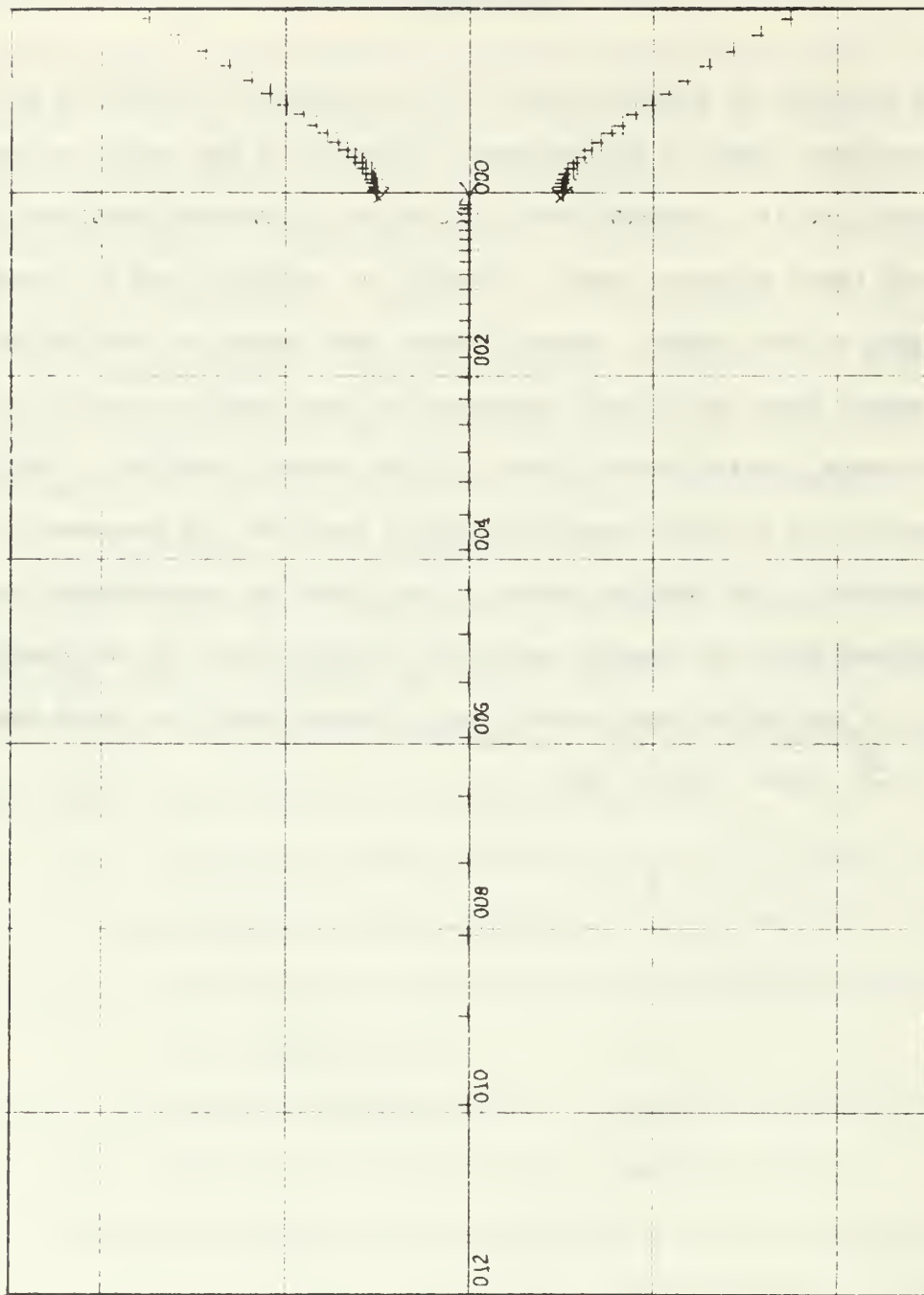


Figure 2.2. Root Locus of the Plant

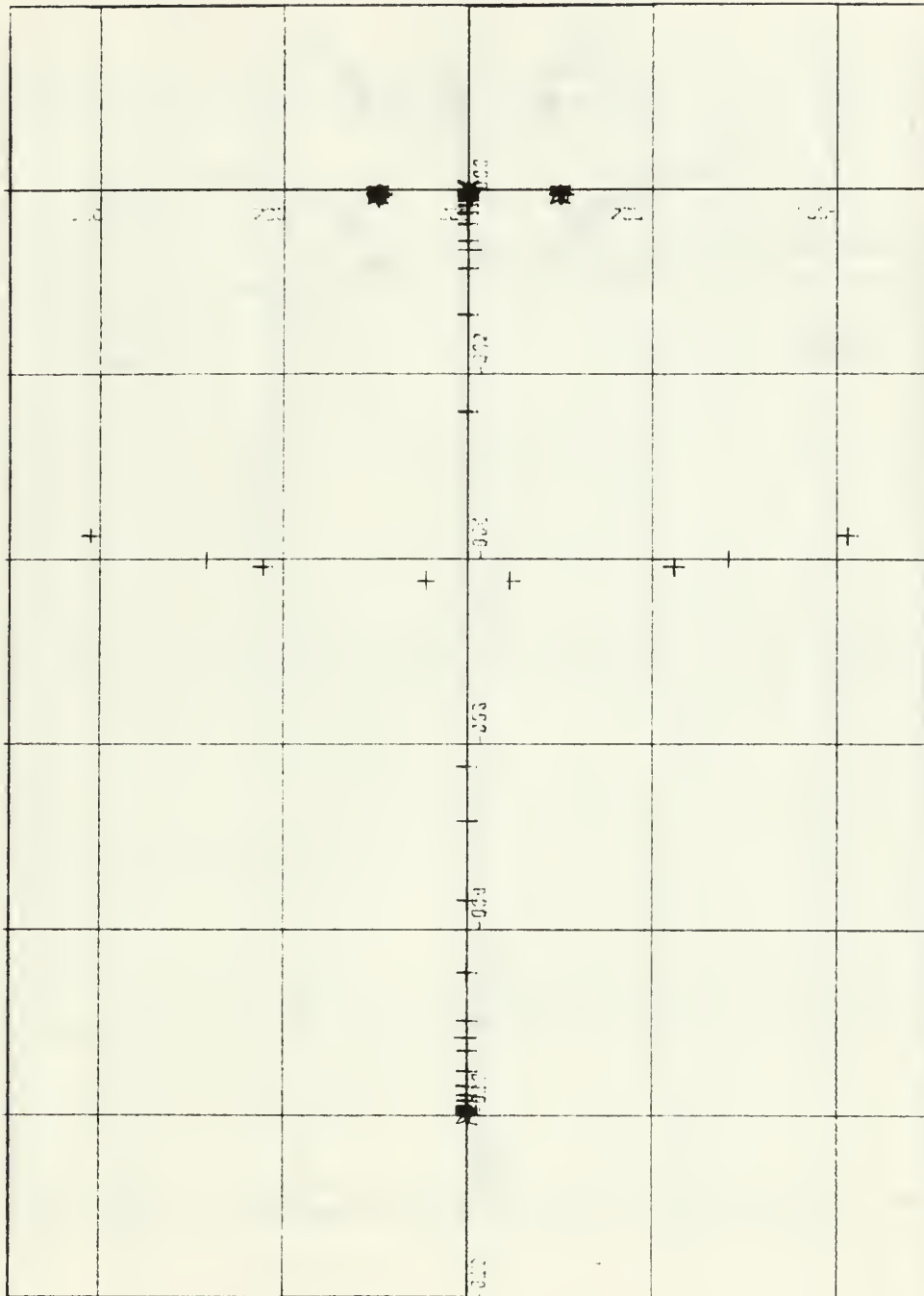


Figure 2.3. Root Locus of the System Showing Exact Compensation

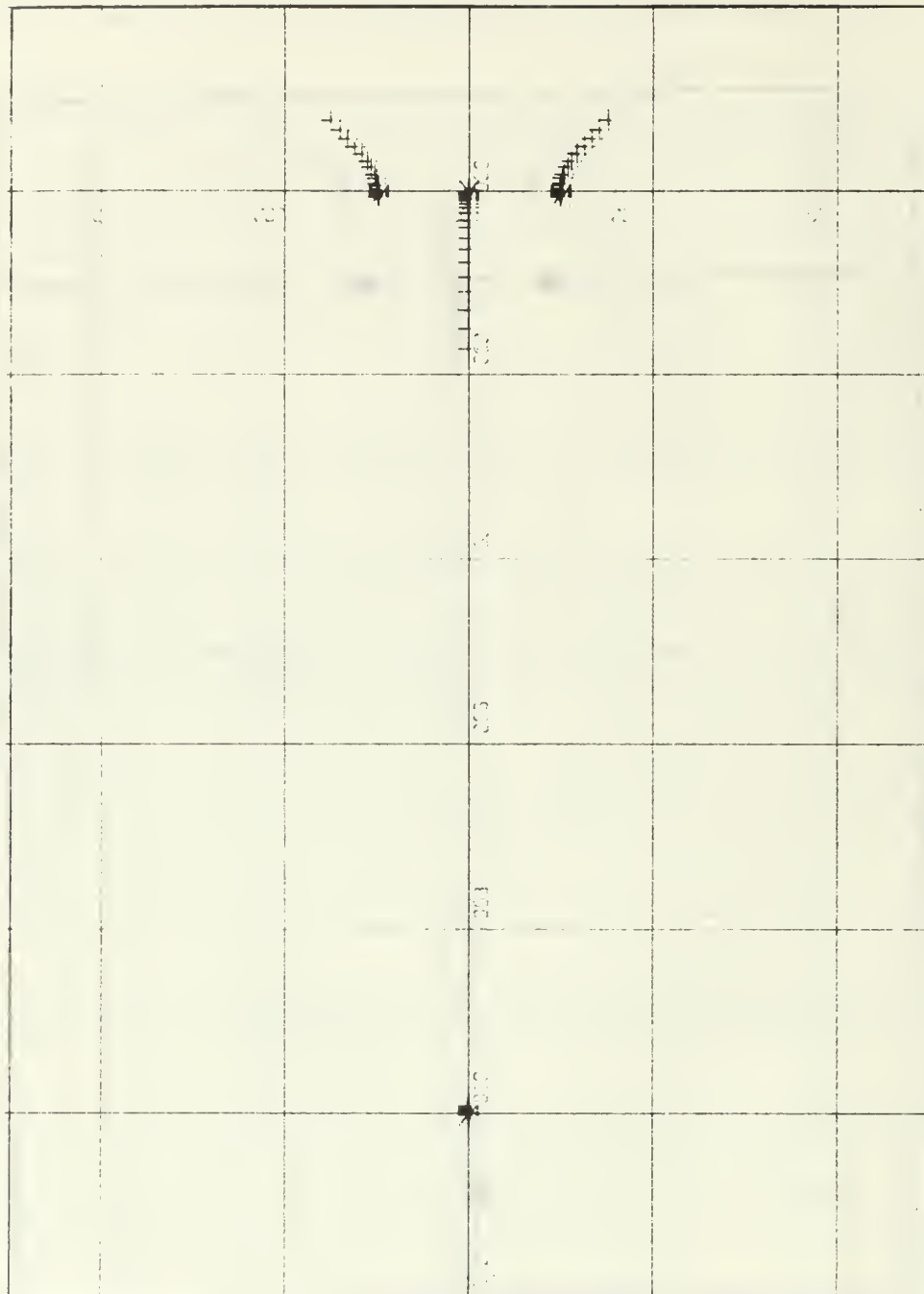


Figure 2.4. Root Locus of the Plant Added the Real Poles of the Compensator.

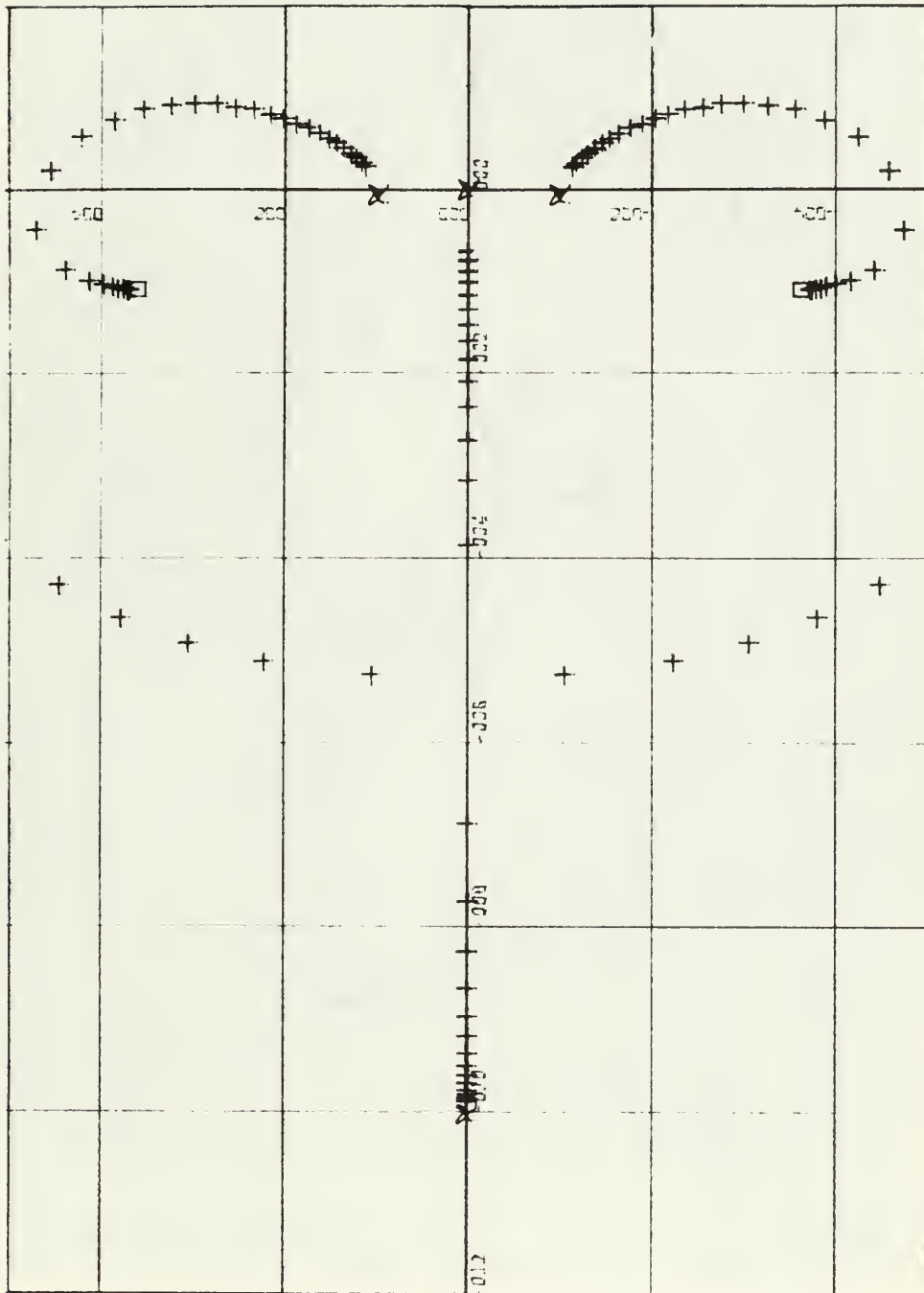


Figure 2.5. Root Locus of a Typically Case Where the Complex Zeros are Away of the Complex Poles.

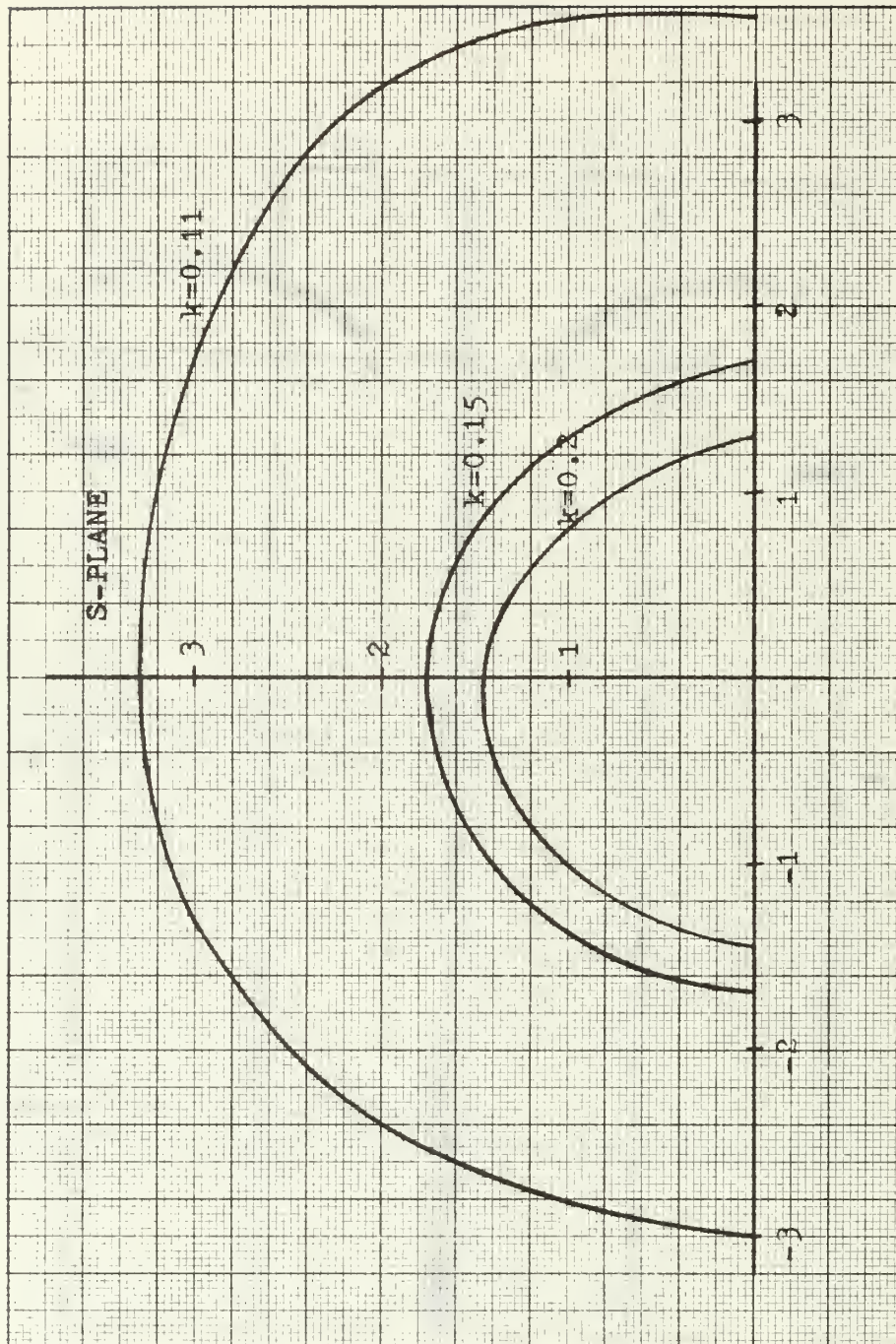


Figure 2.6. Stability Boundaries for Different Gains

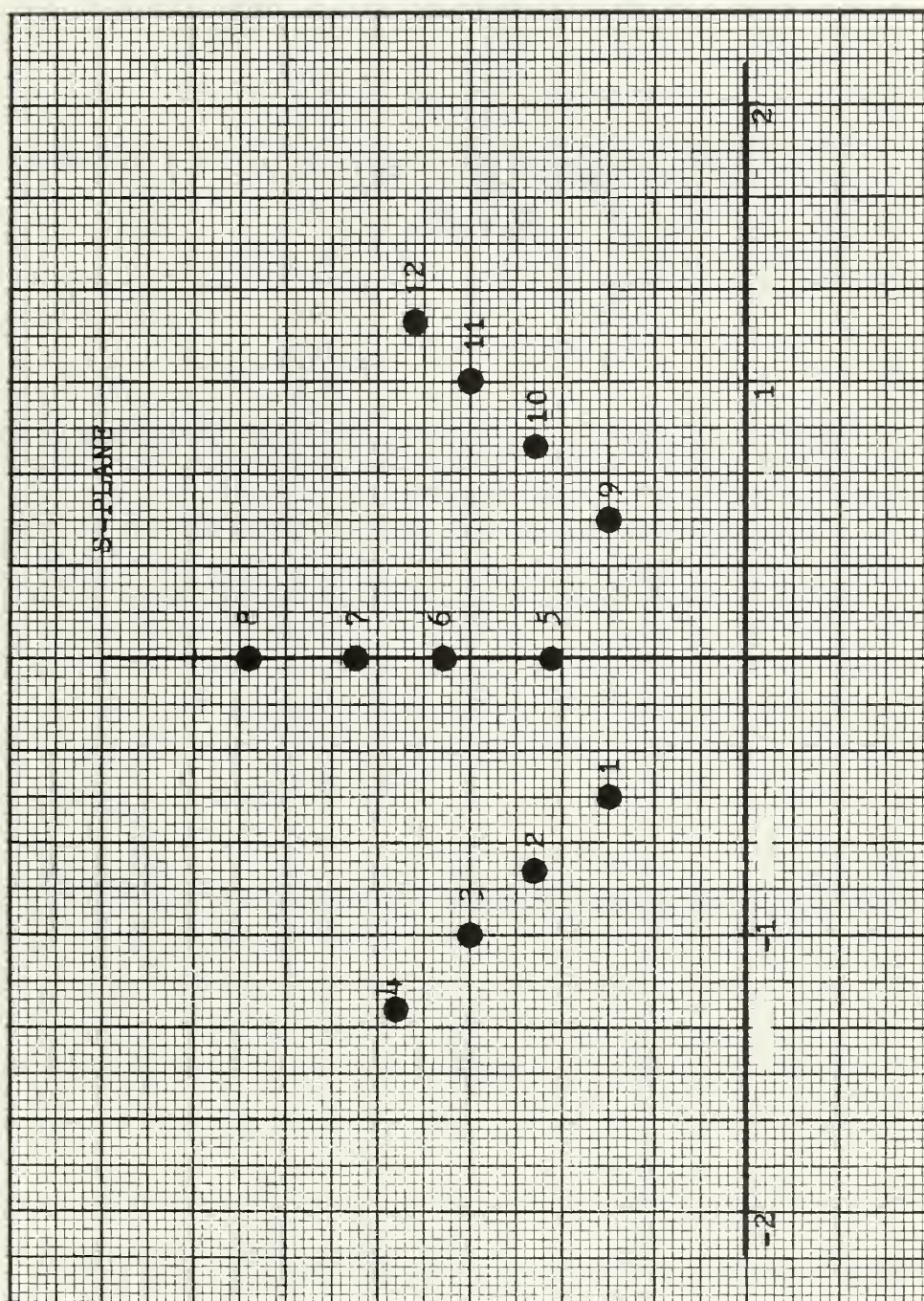
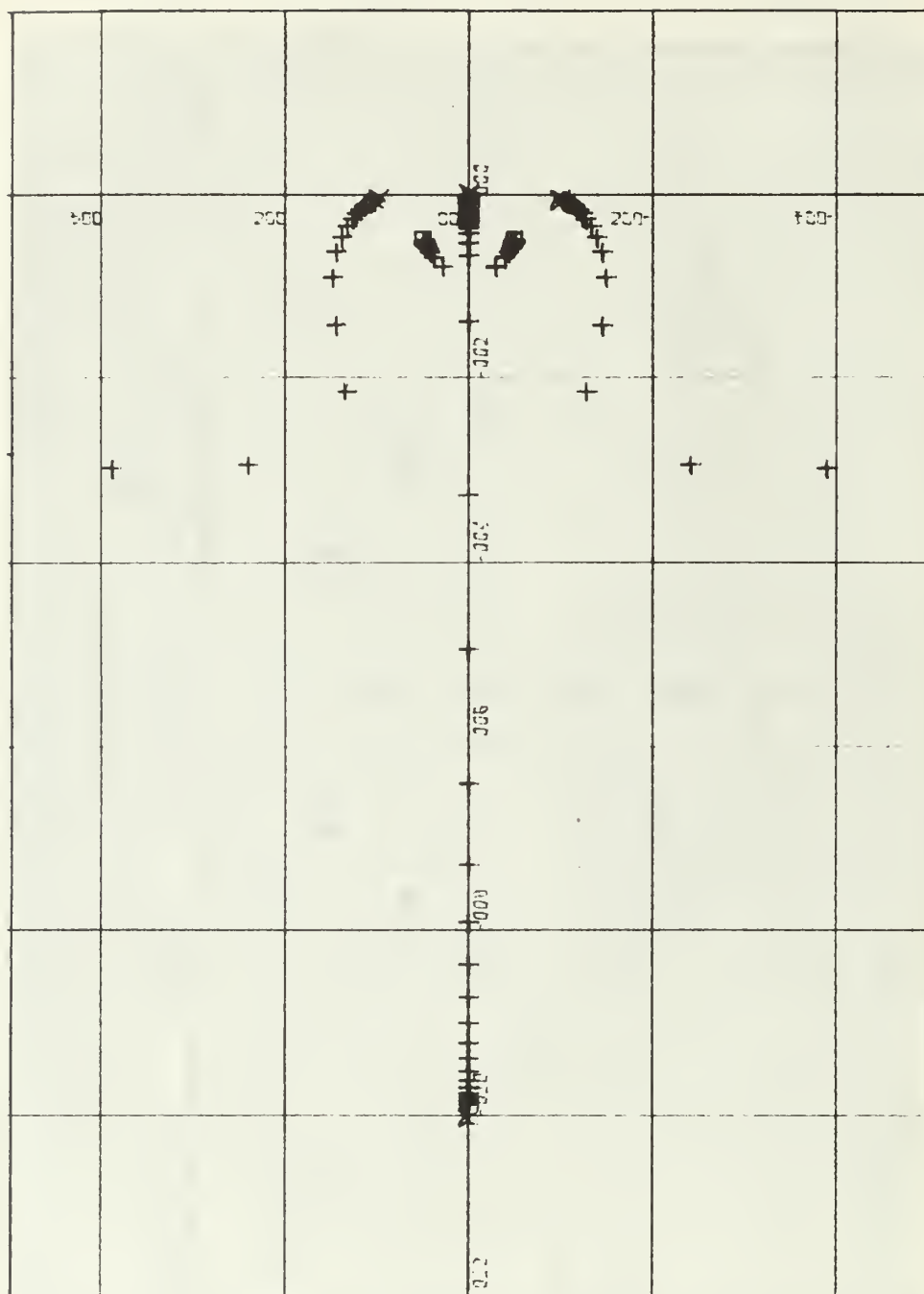


Figure 2.7. Different Location of the Complex Zeros of the Compensator.



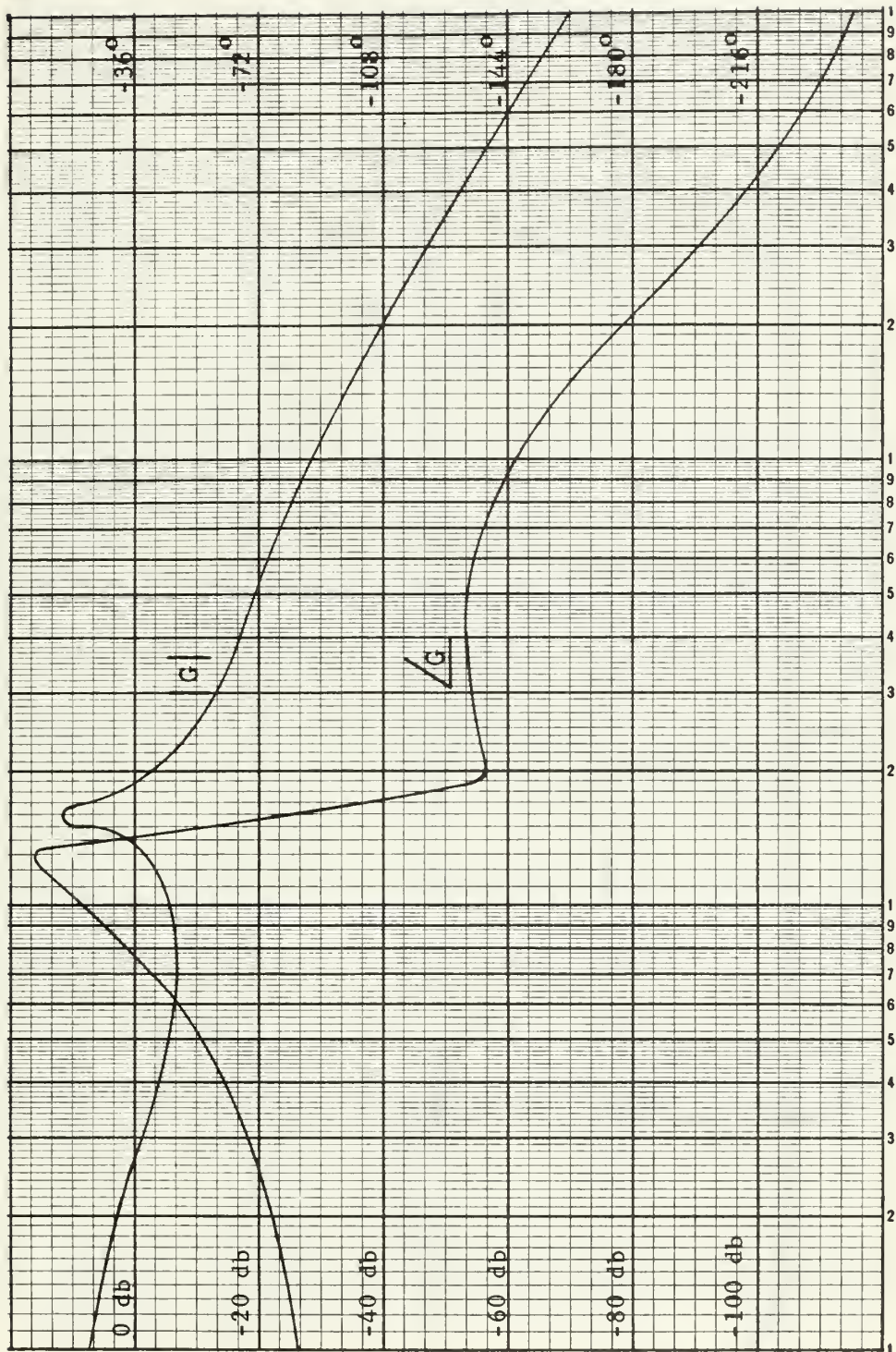


Figure 2.8b. Bode Diagram for Point 1.



Figure 2.8c. Transient Response for Point 1.

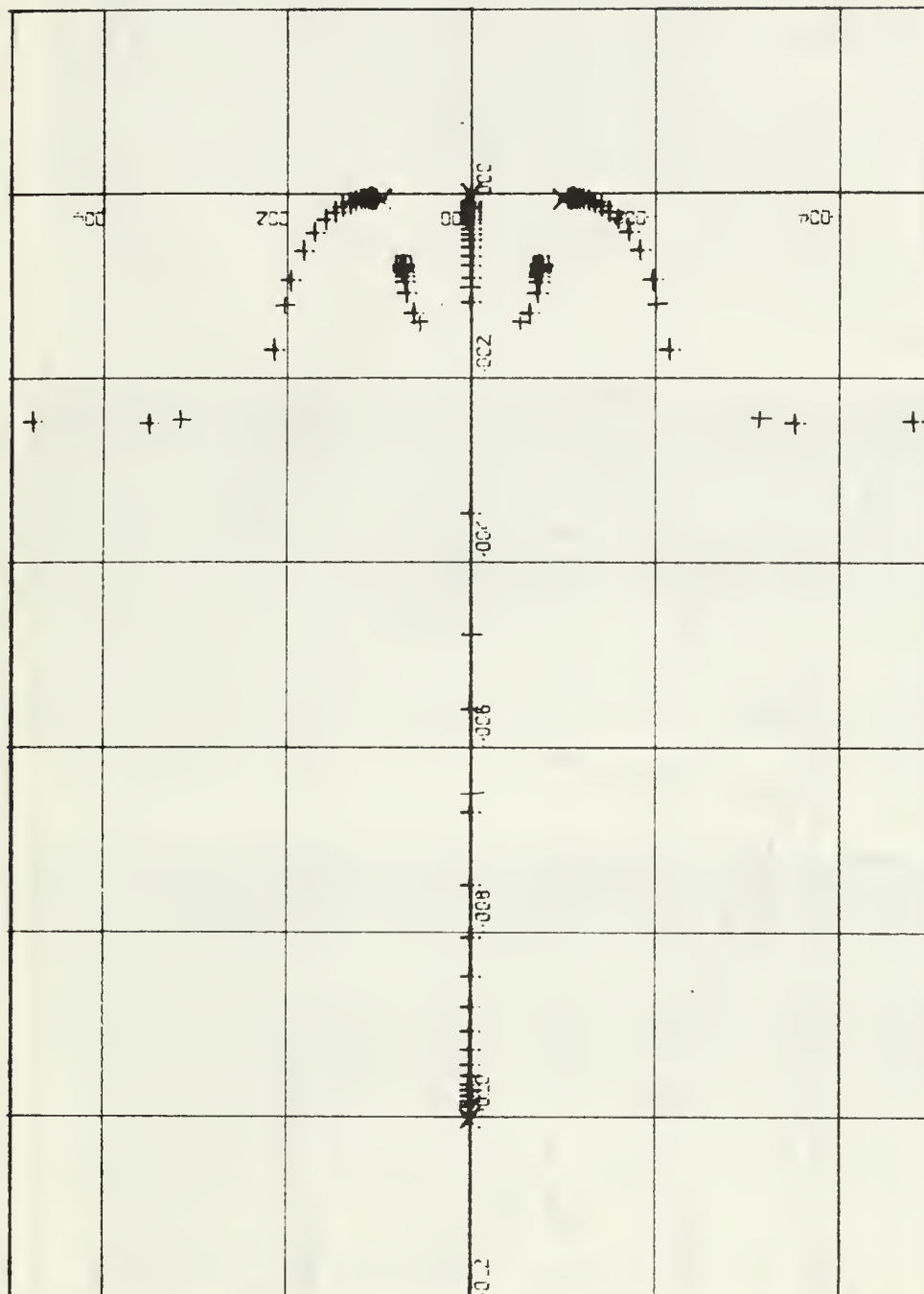


Figure 2.9a. Root Locus for Point 2

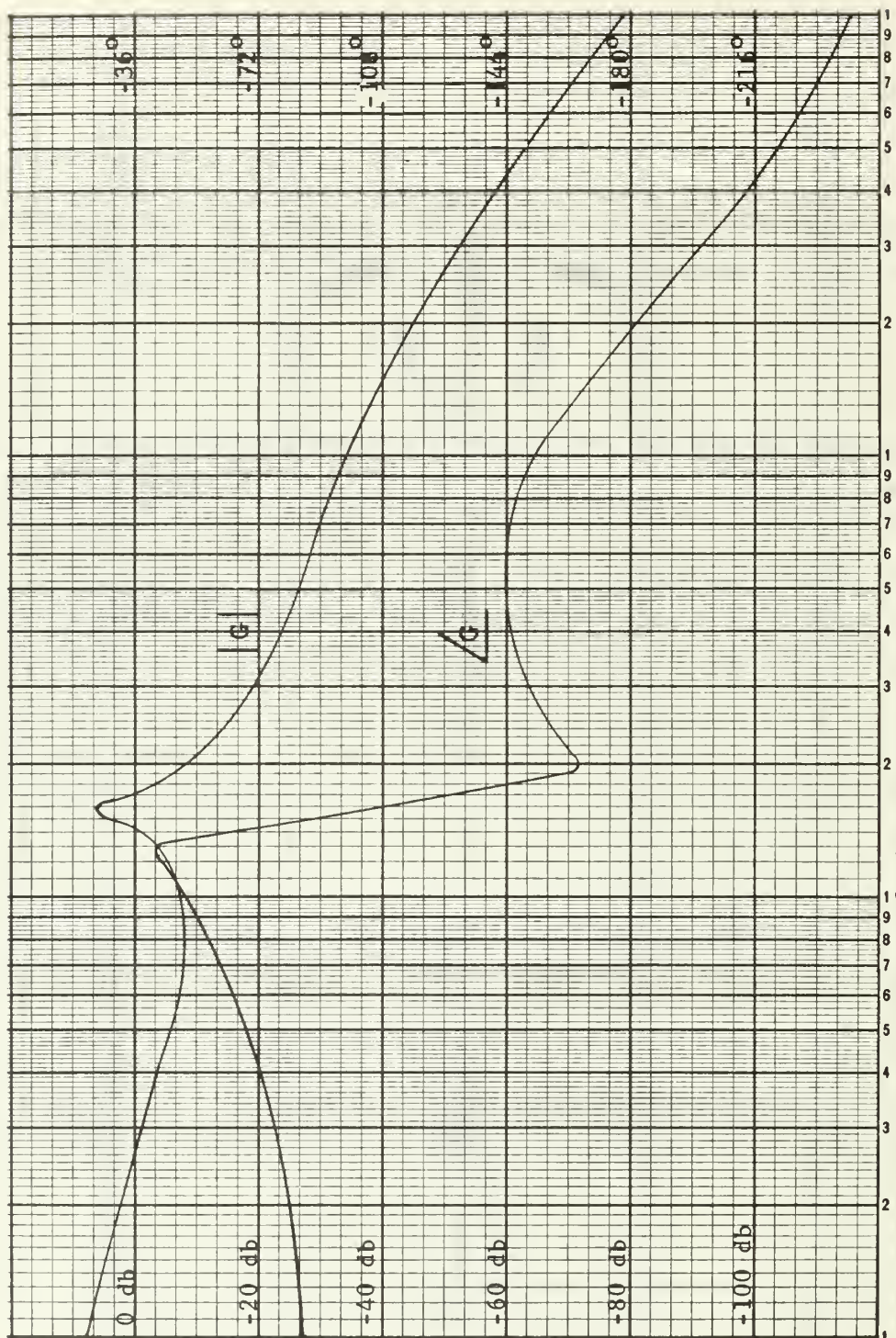


Figure 2.9b. Bode Diagram for Point 2.

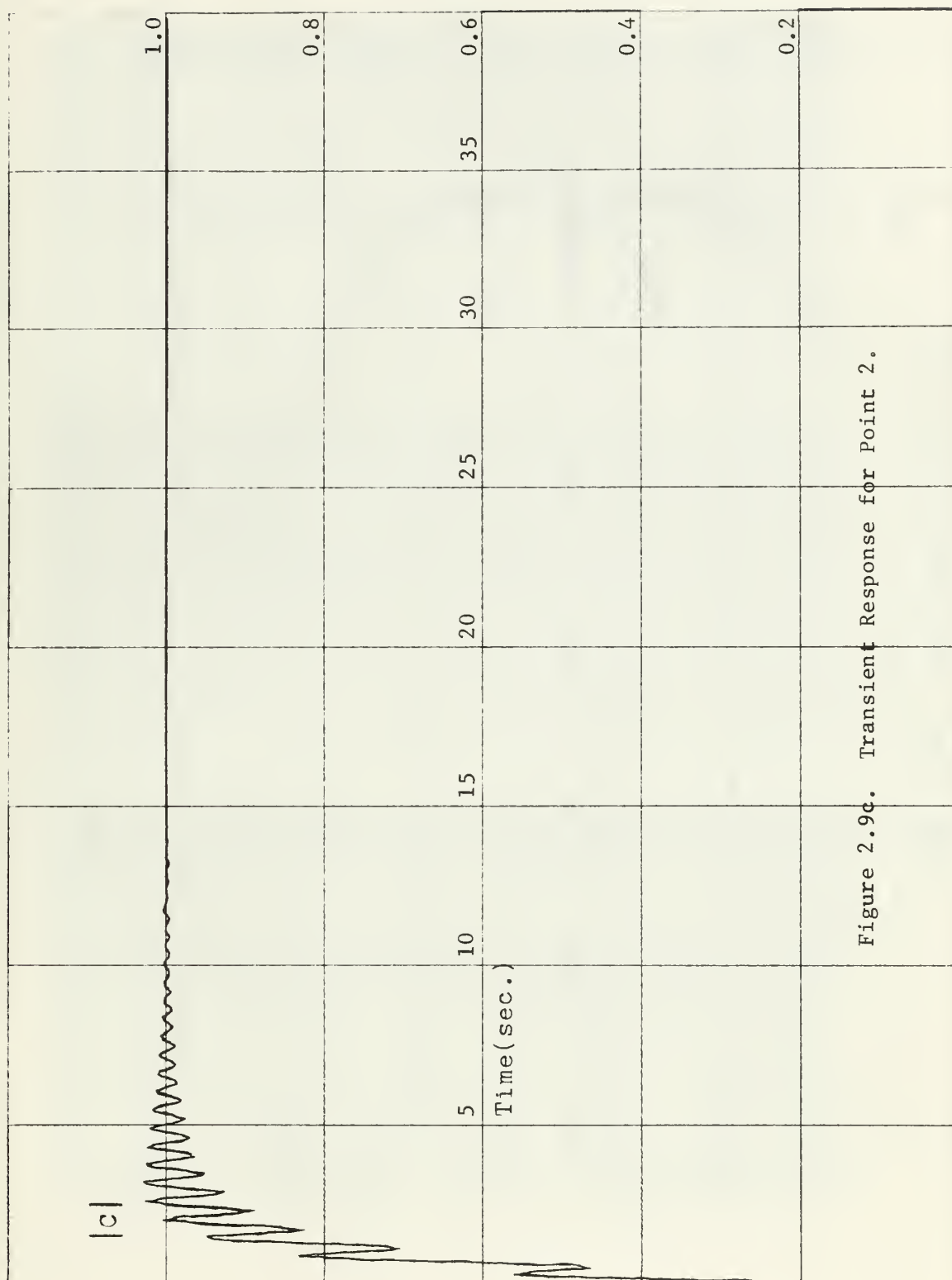


Figure 2.9c. Transient Response for Point 2.

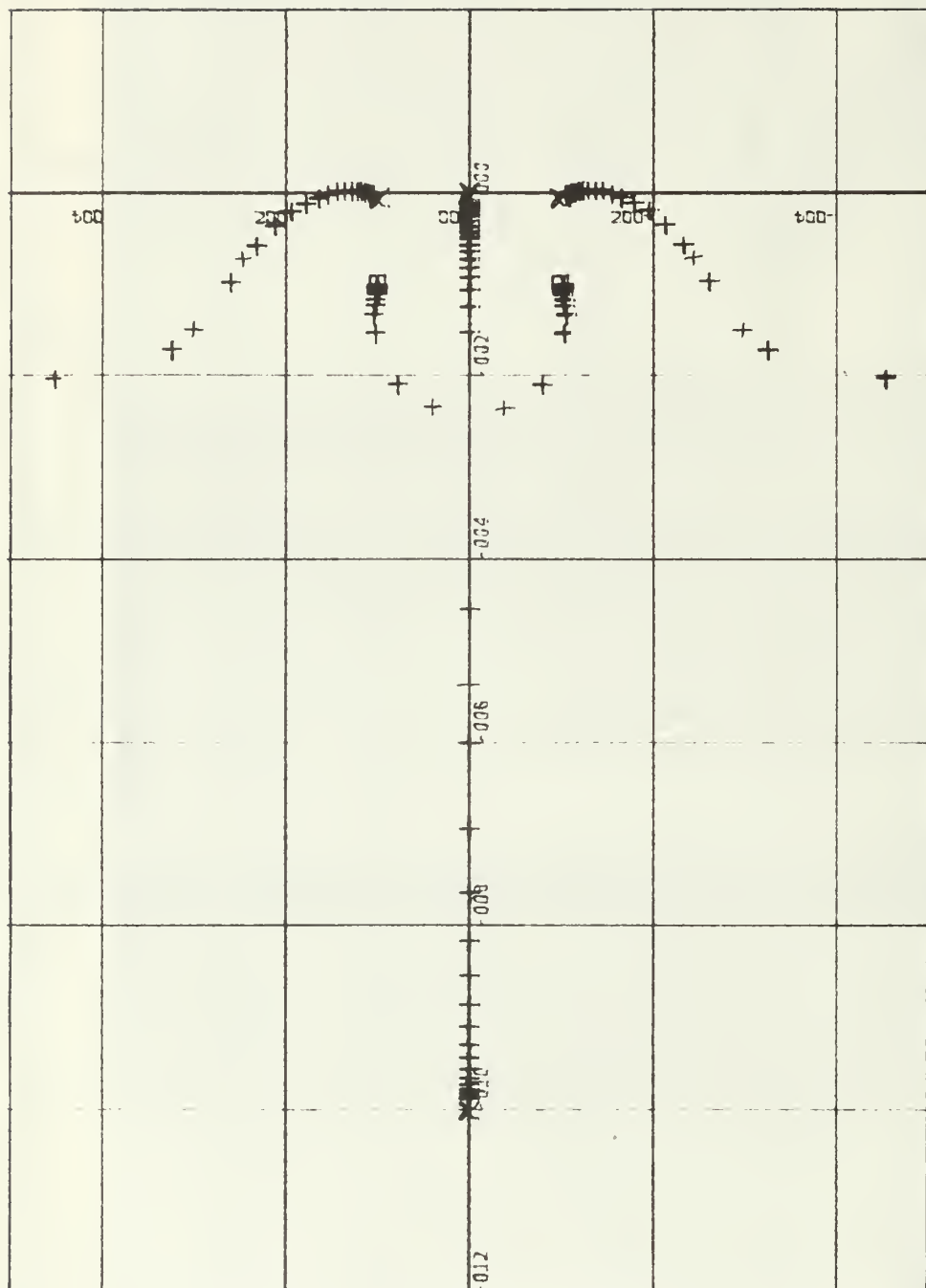


Figure 2.10a. Root Locus for Point 3.

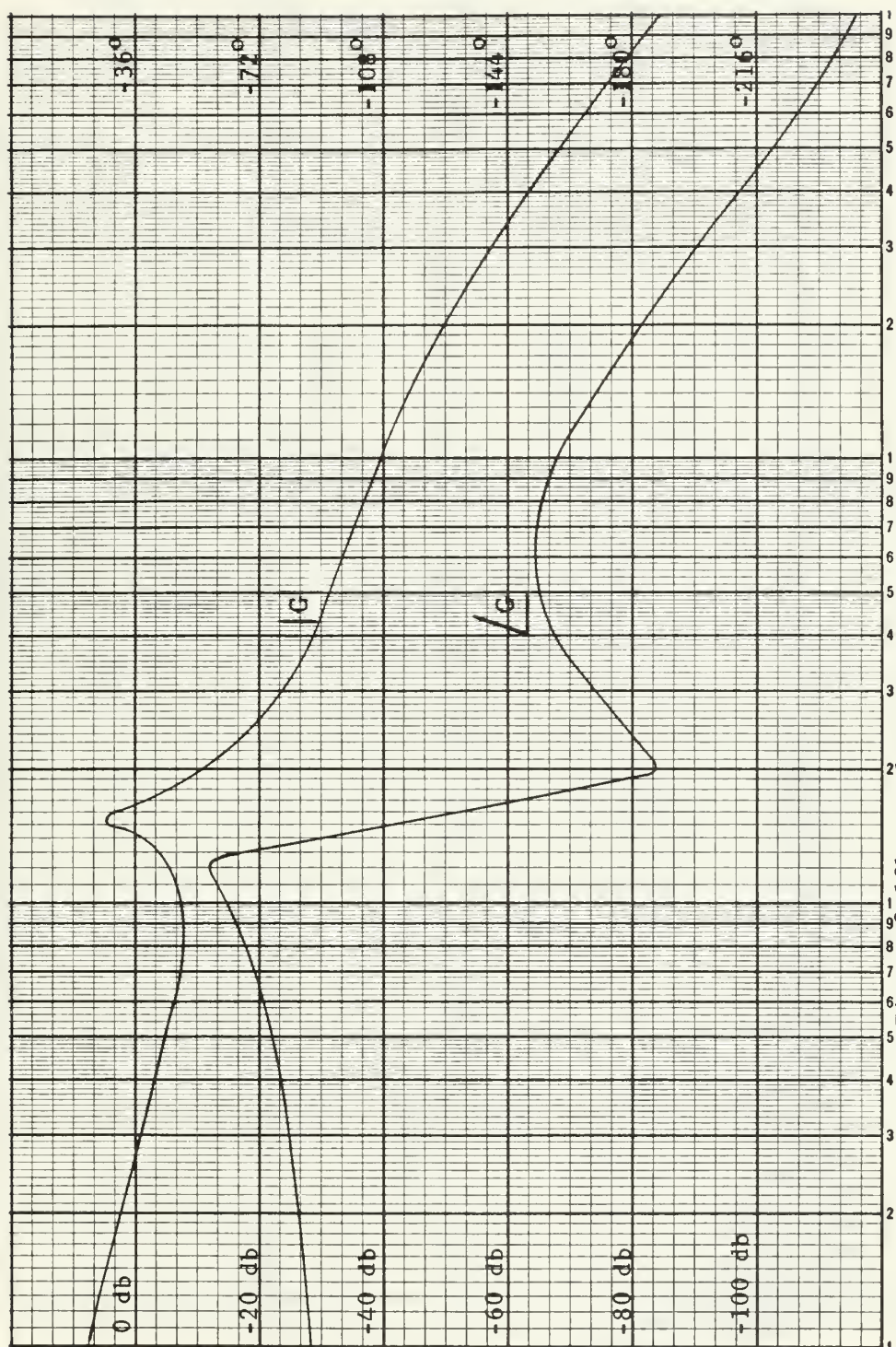


Figure 2.10b. Bode Diagram for Point 3.

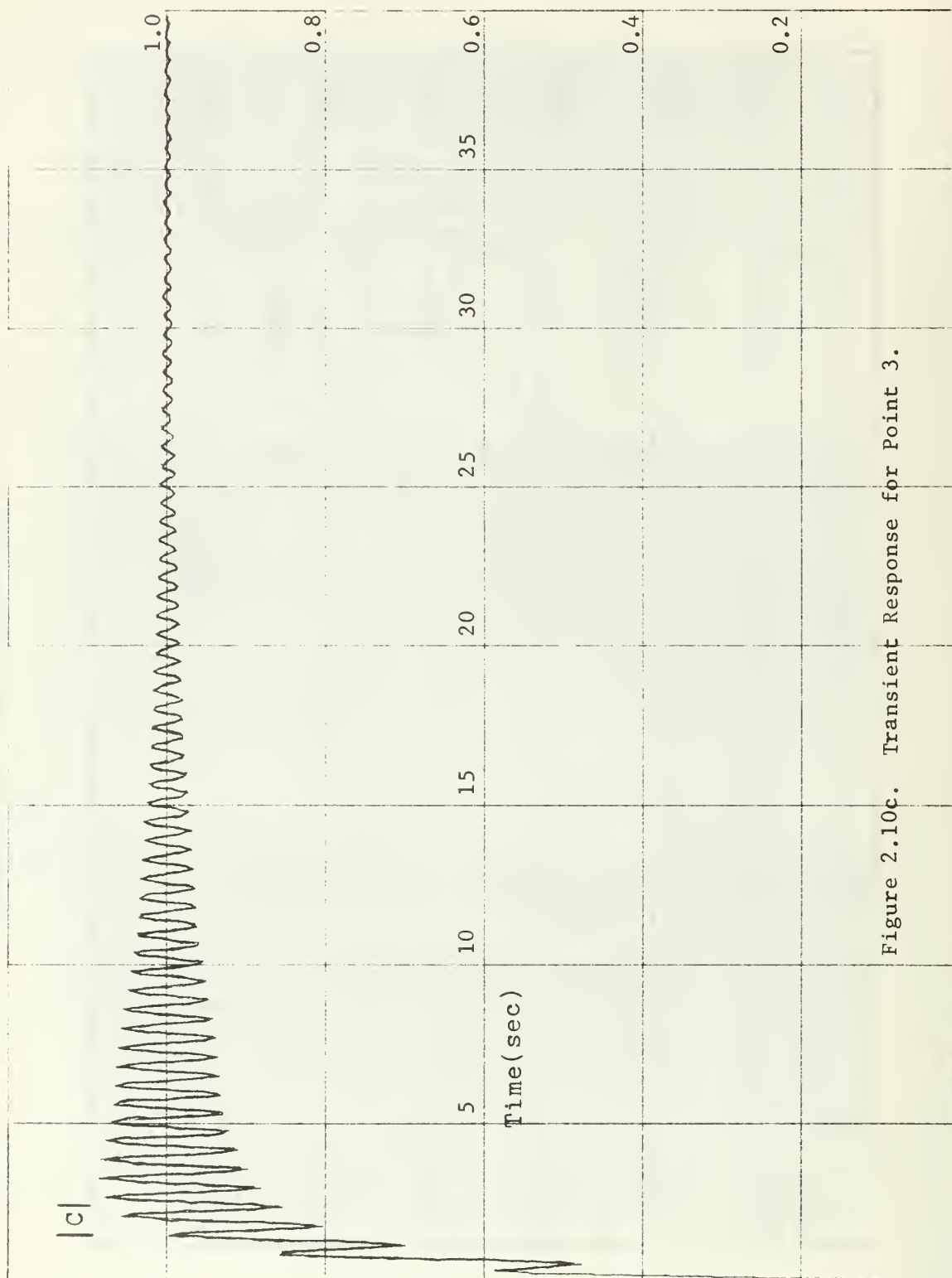


Figure 2.10c. Transient Response for Point 3.

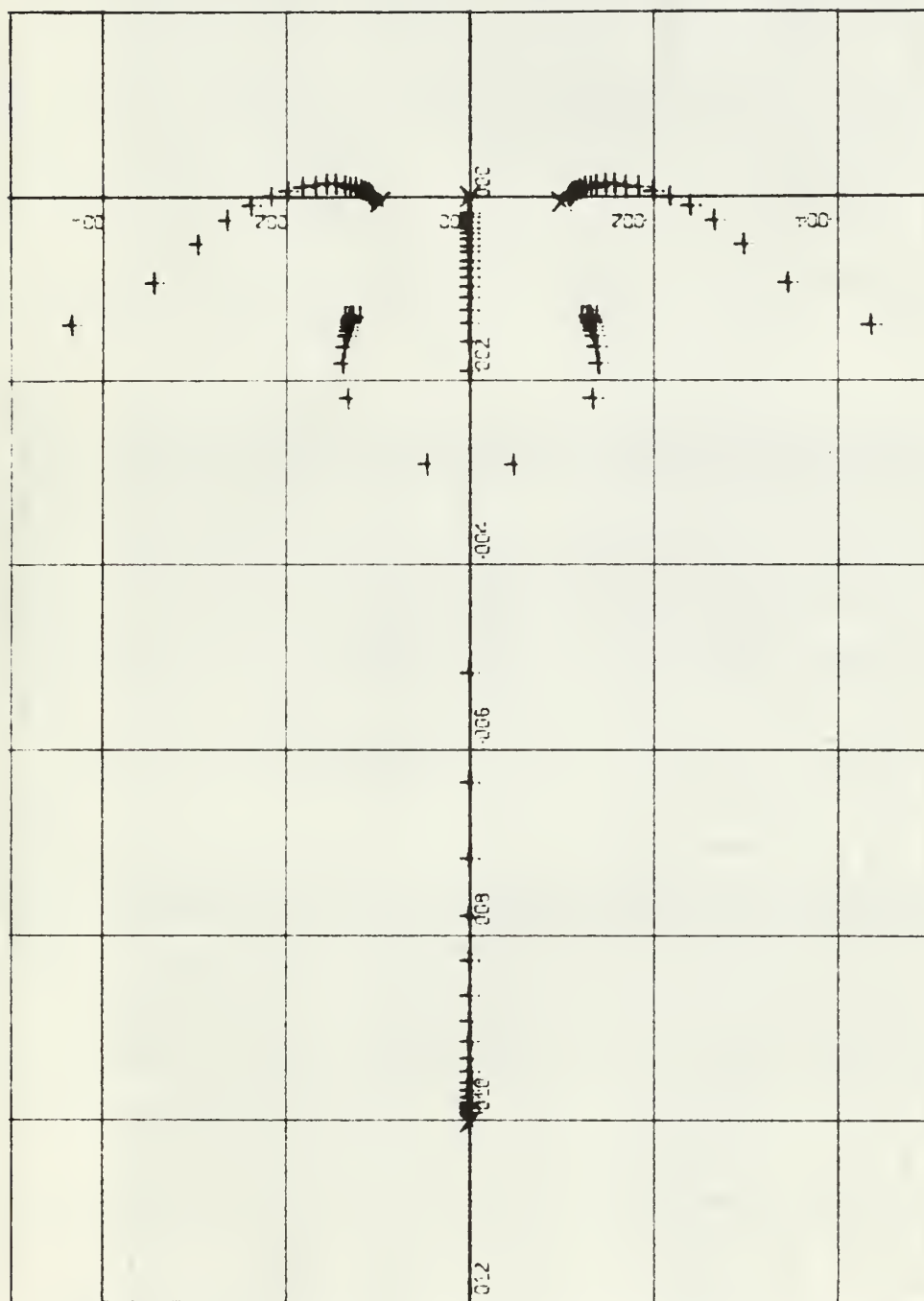


Figure 2.11a. Root Locus for Point 4

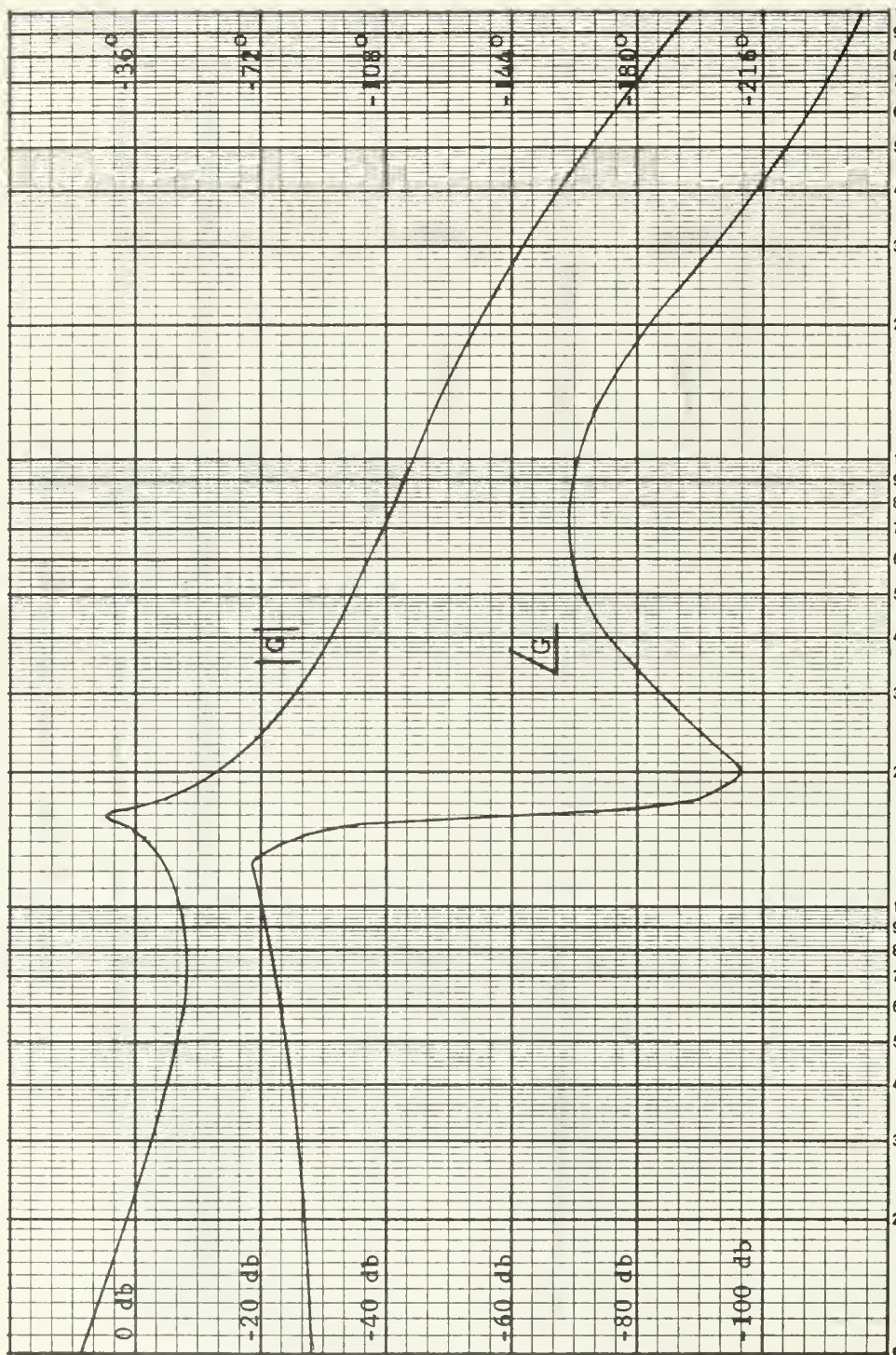


Figure 2.11b. Bode Diagram for Point 4.

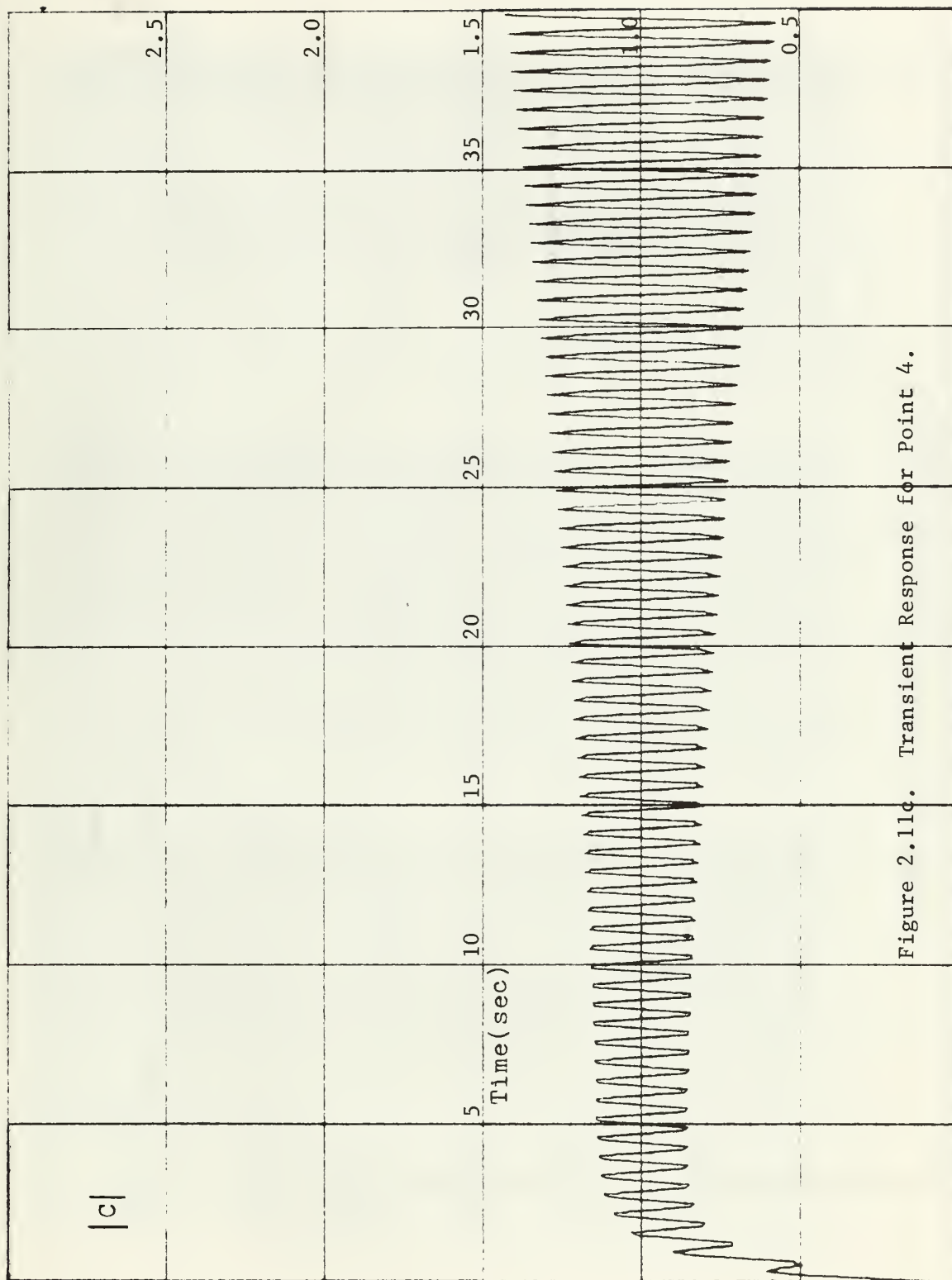


Figure 2.11c. Transient Response for Point 4.

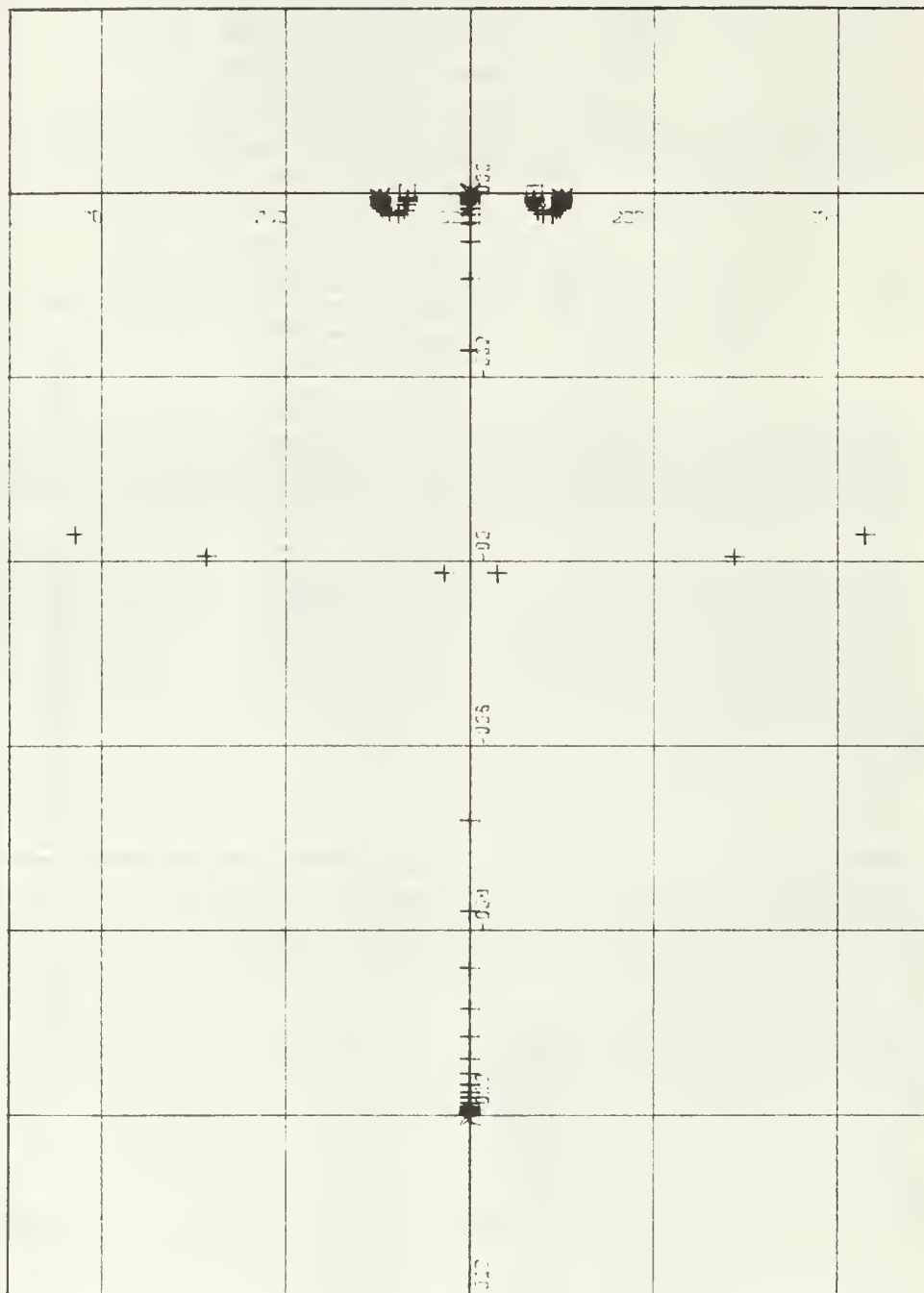


Figure 2.12a. Root Locus for Point 5

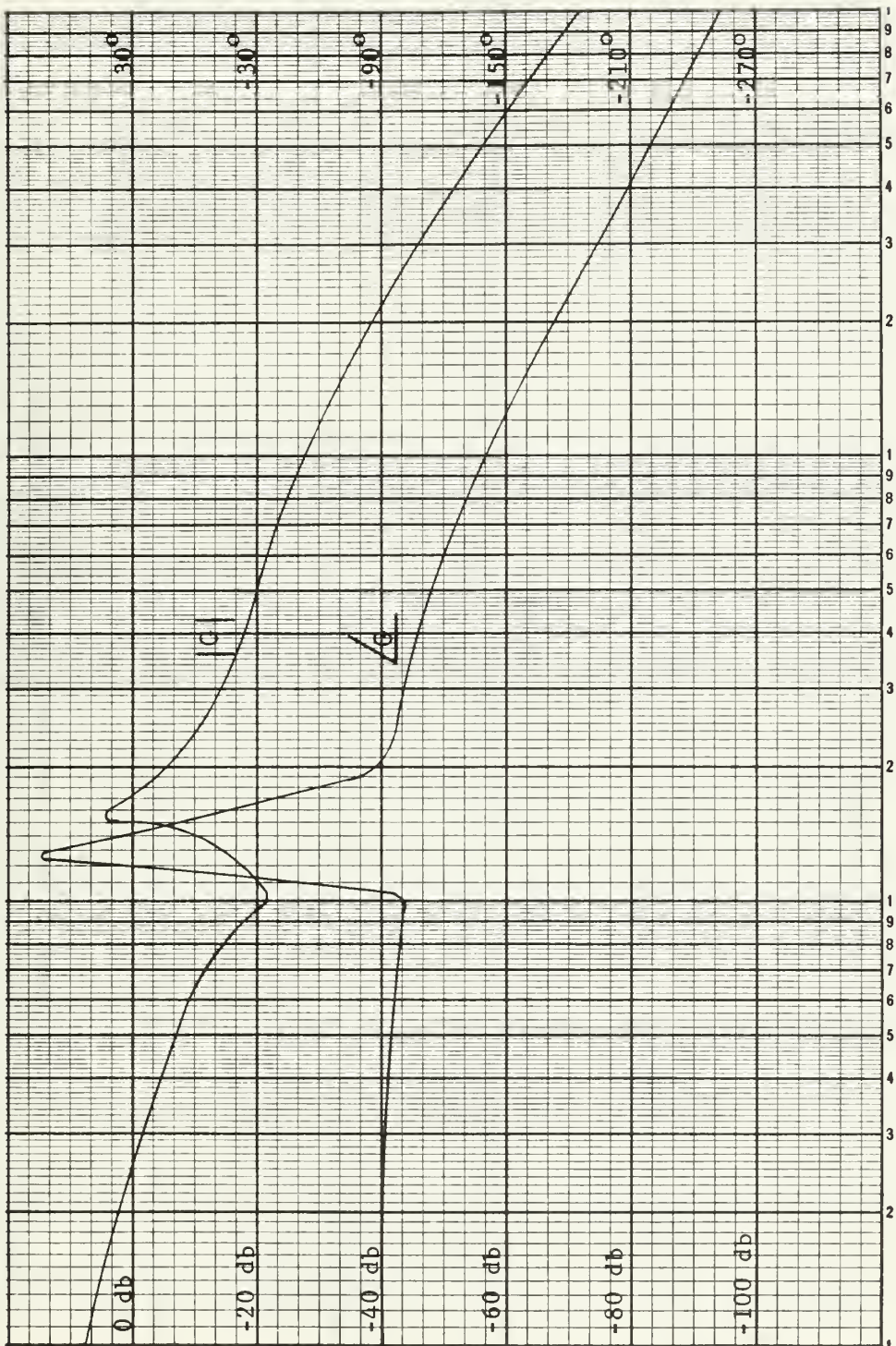


Figure 2.12b. Bode Diagram for Point 5.

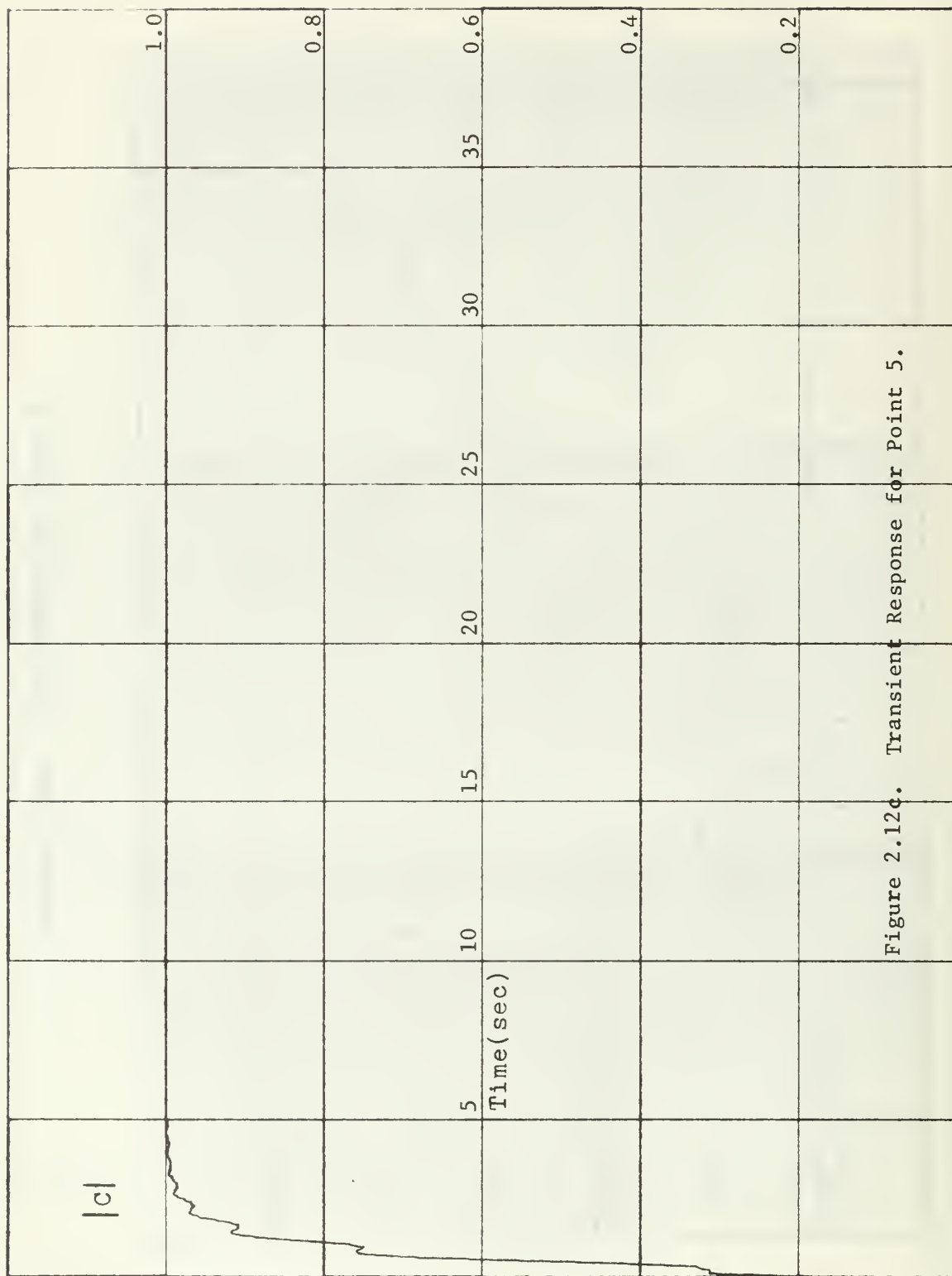


Figure 2.12c. Transient Response for Point 5.

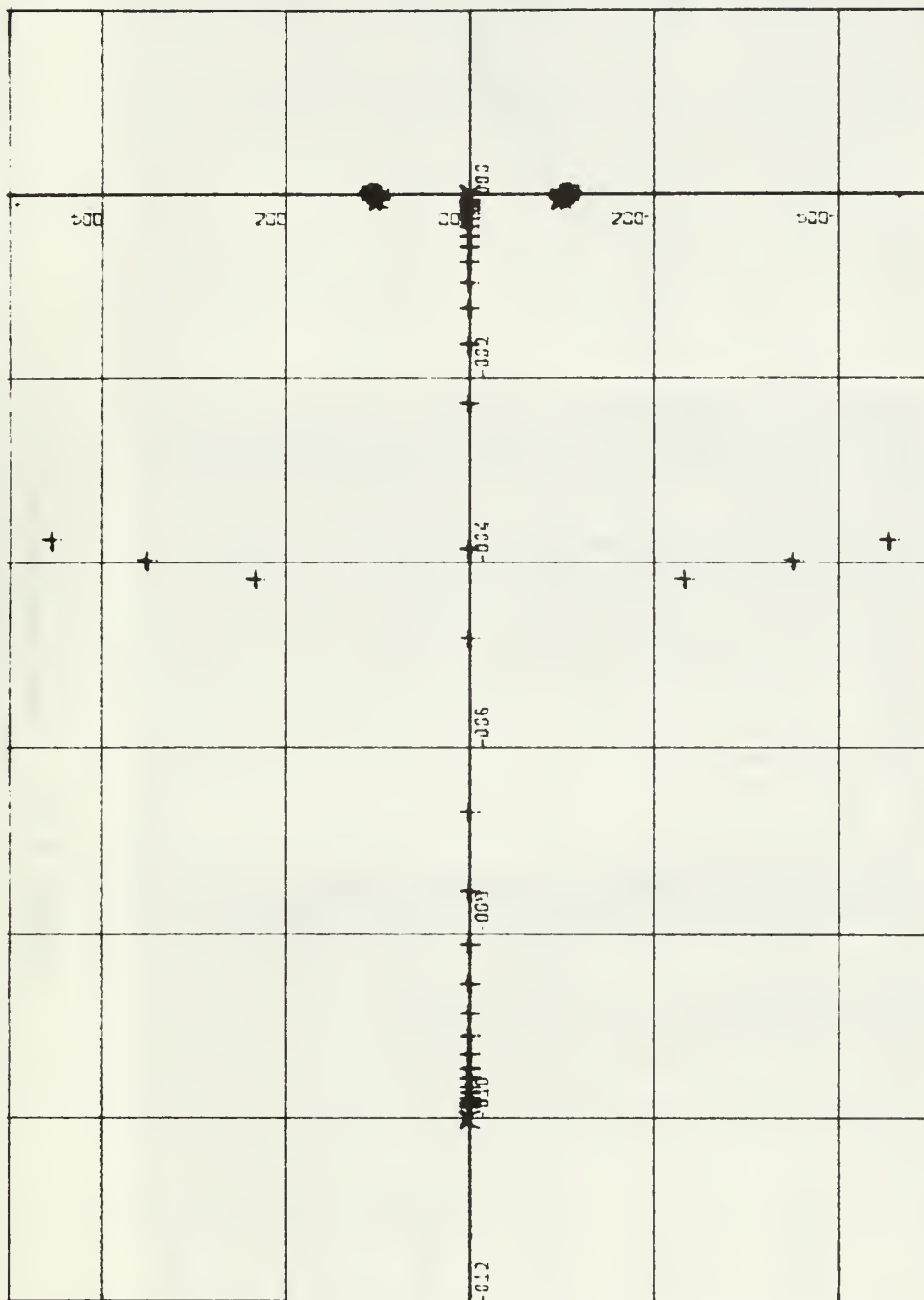


Figure 2.13a. Root Locus for Point 6

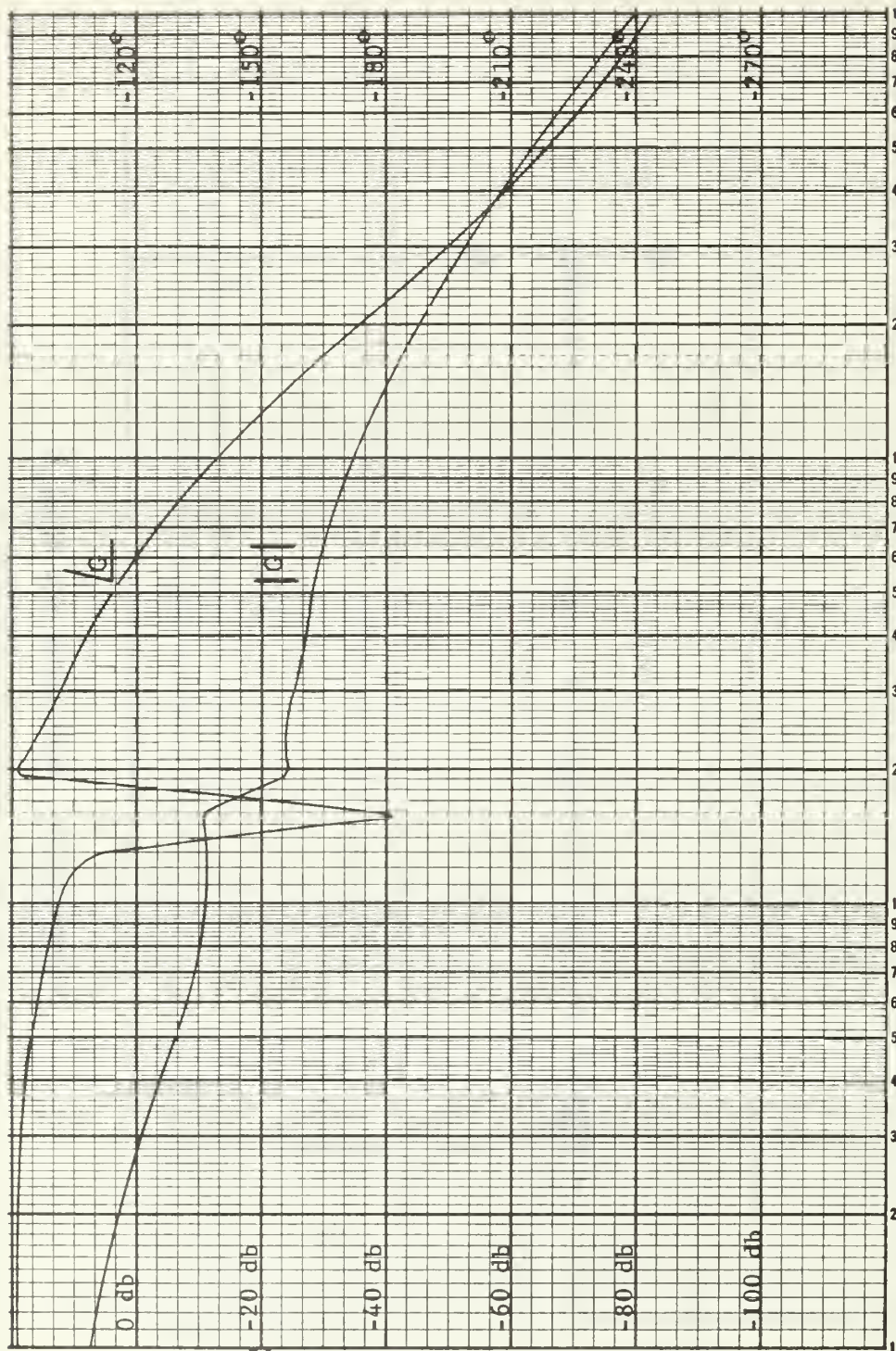


Figure 2.13b. Bode Diagram for Point 6.

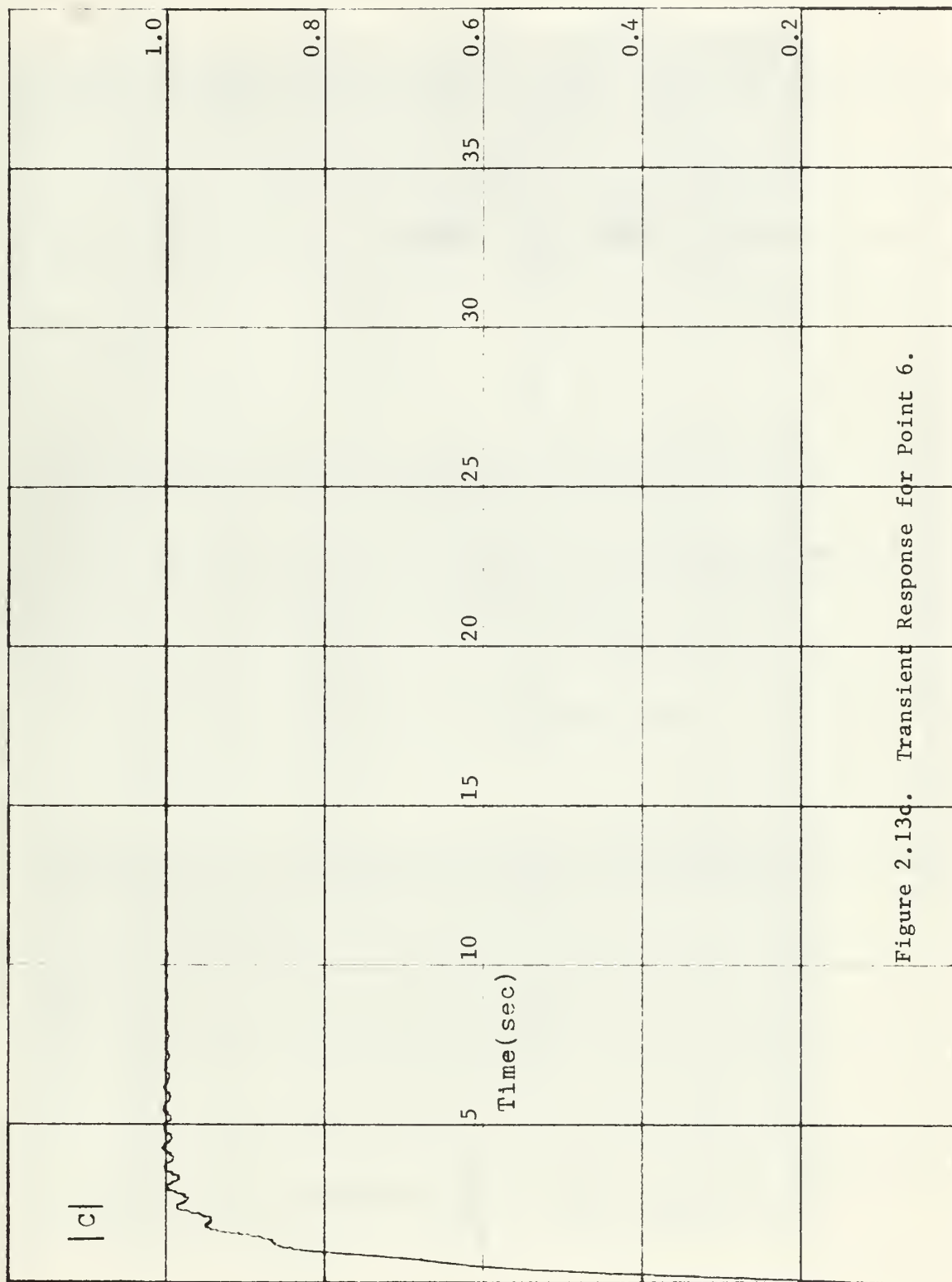


Figure 2.13d. Transient Response for Point 6.

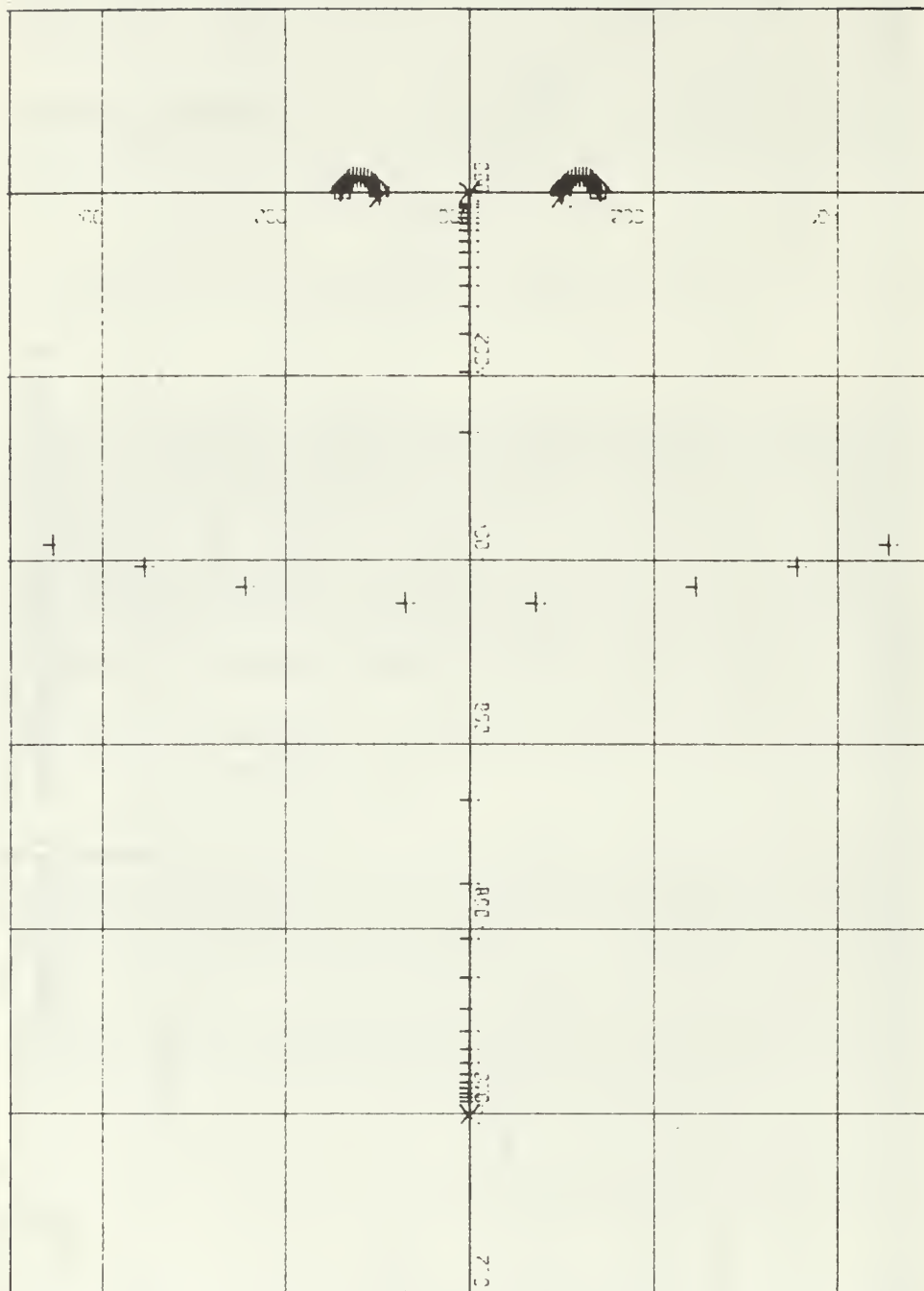


Figure 2.14a. Root Locus for Point 7

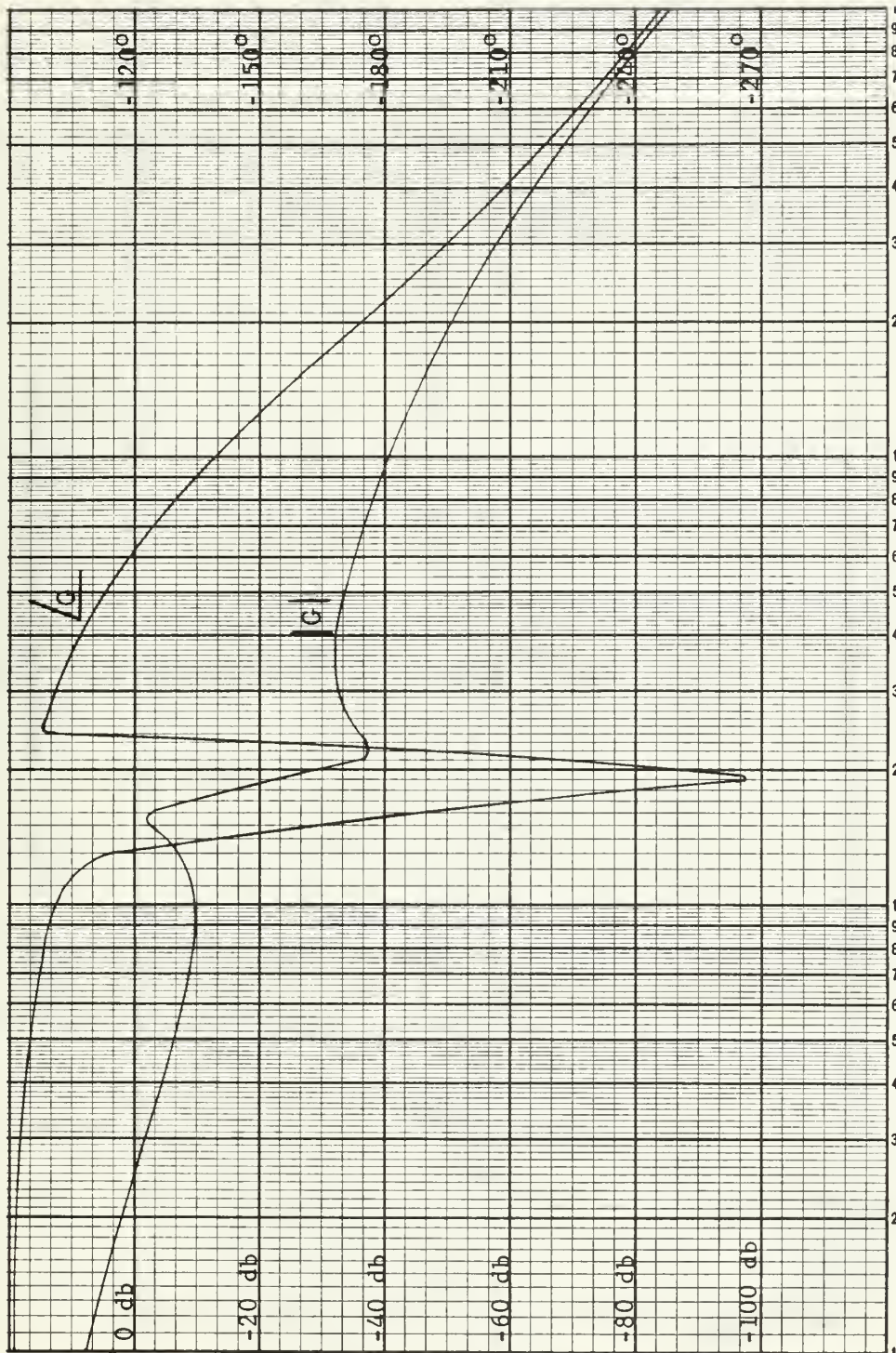


Figure 2.14b. Bode Diagram for Point 7.

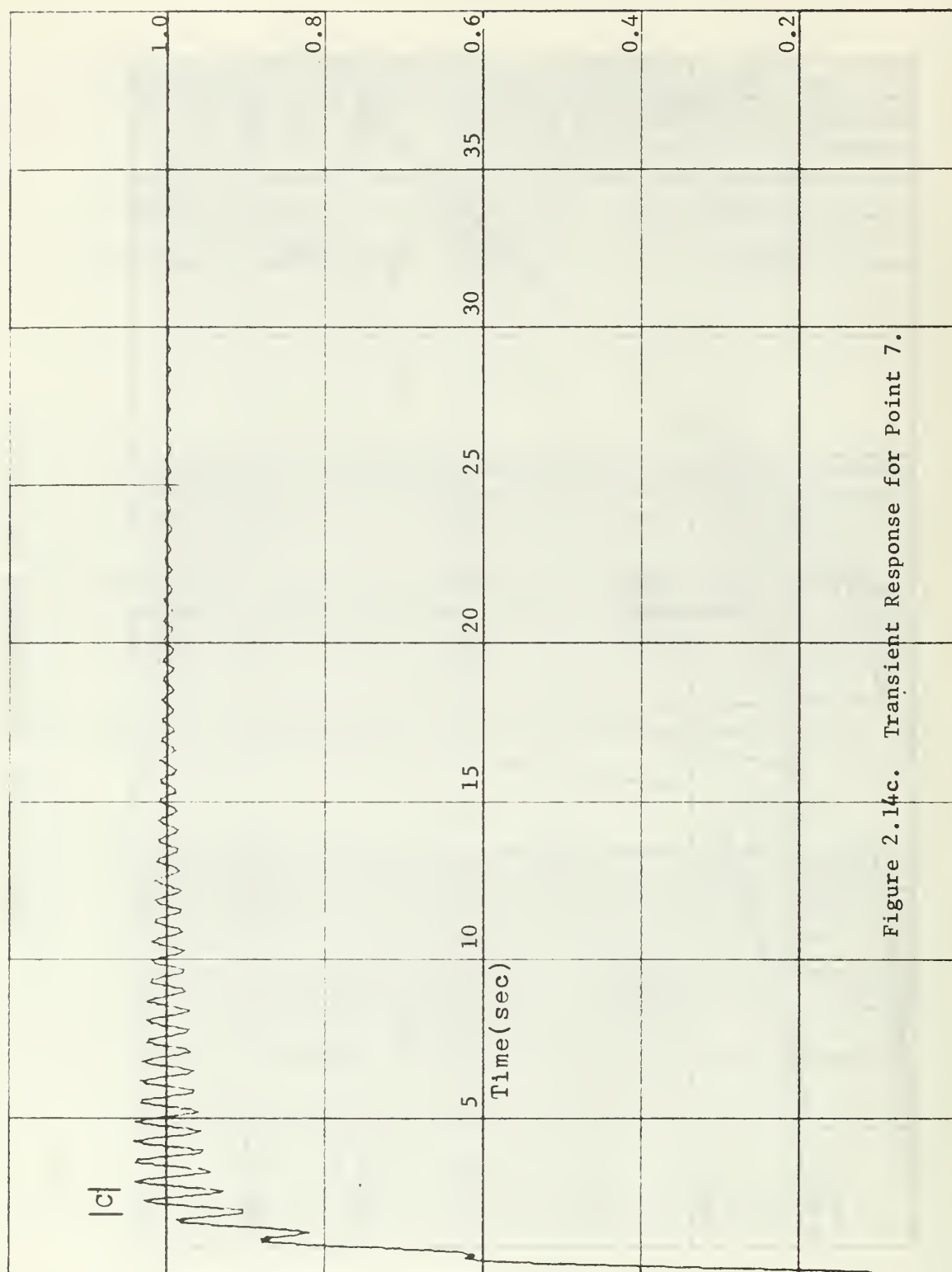


Figure 2.14c. Transient Response for Point 7.

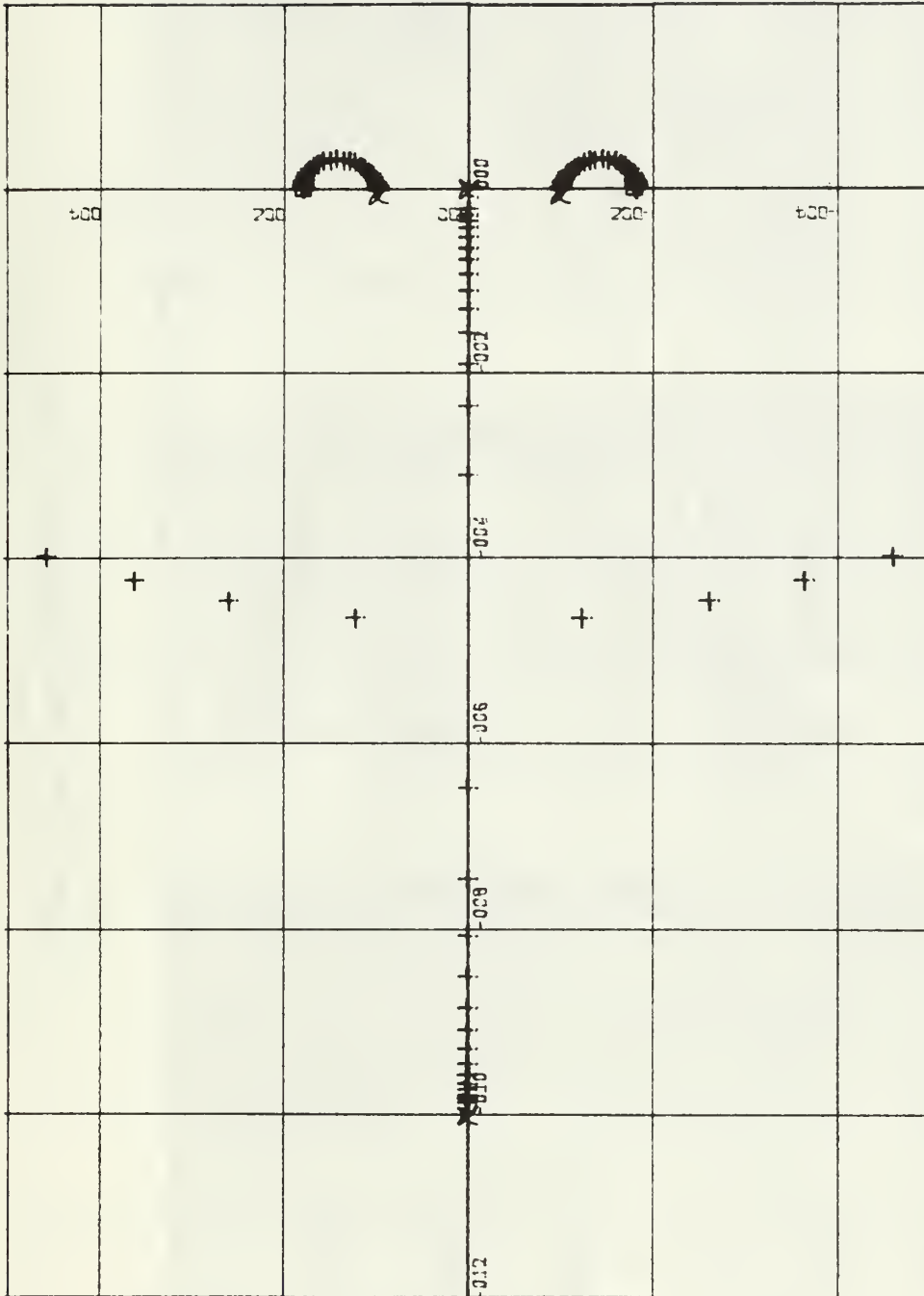


Figure 2.15a. Root Locus for Point 8

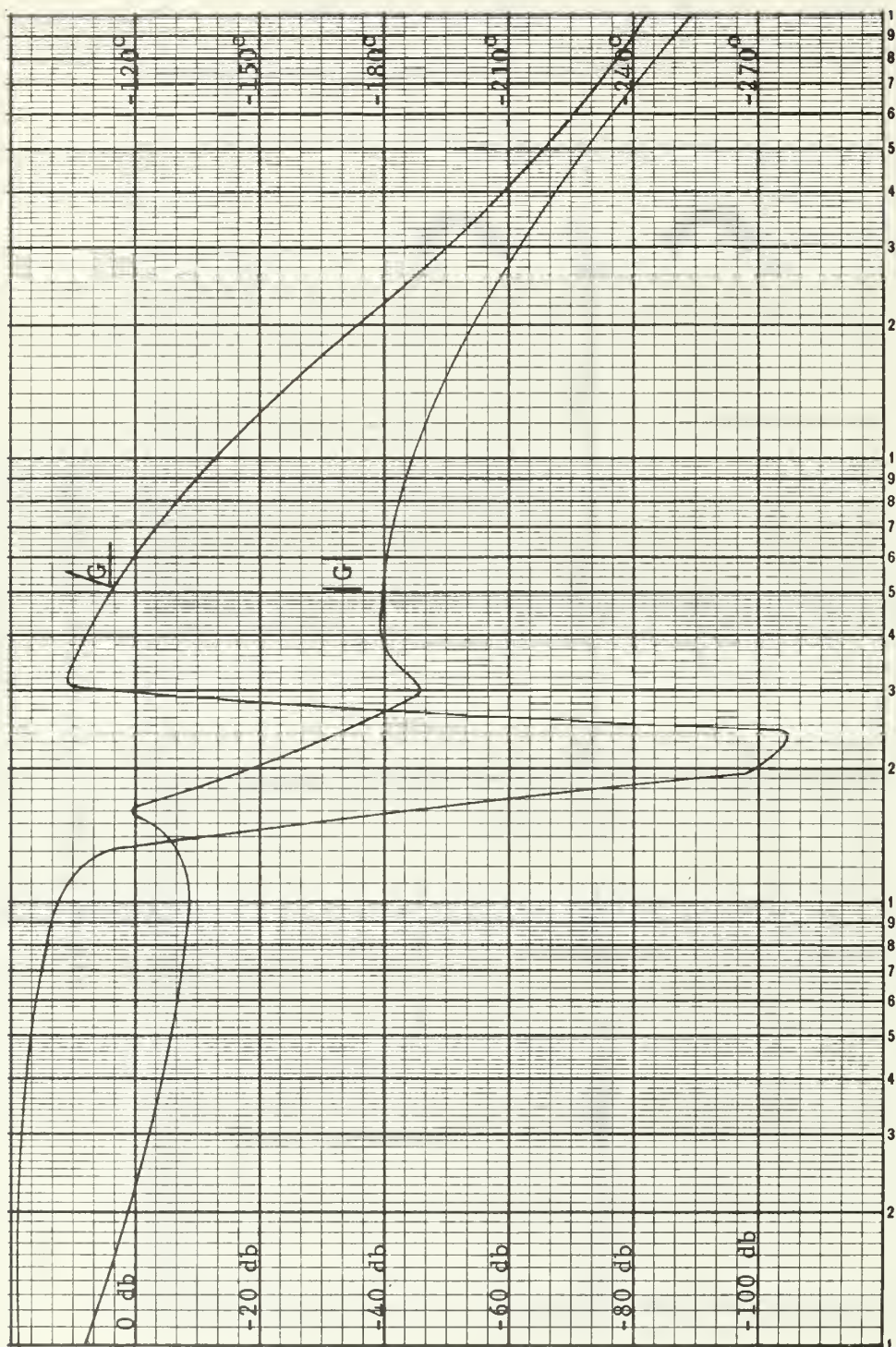


Figure 2.15b. Bode Diagram for Point 8.

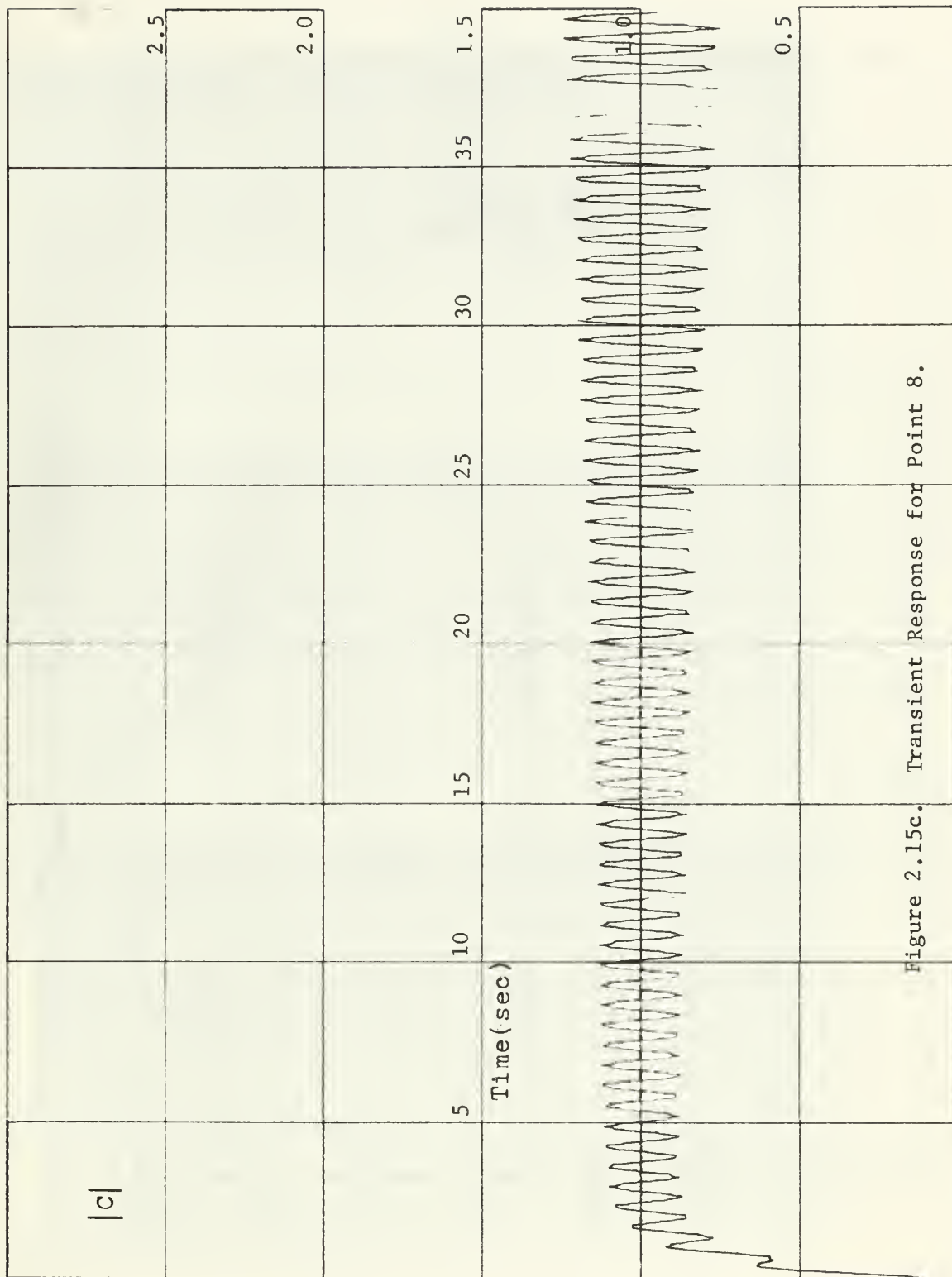


Figure 2.15c. Transient Response for Point 8.

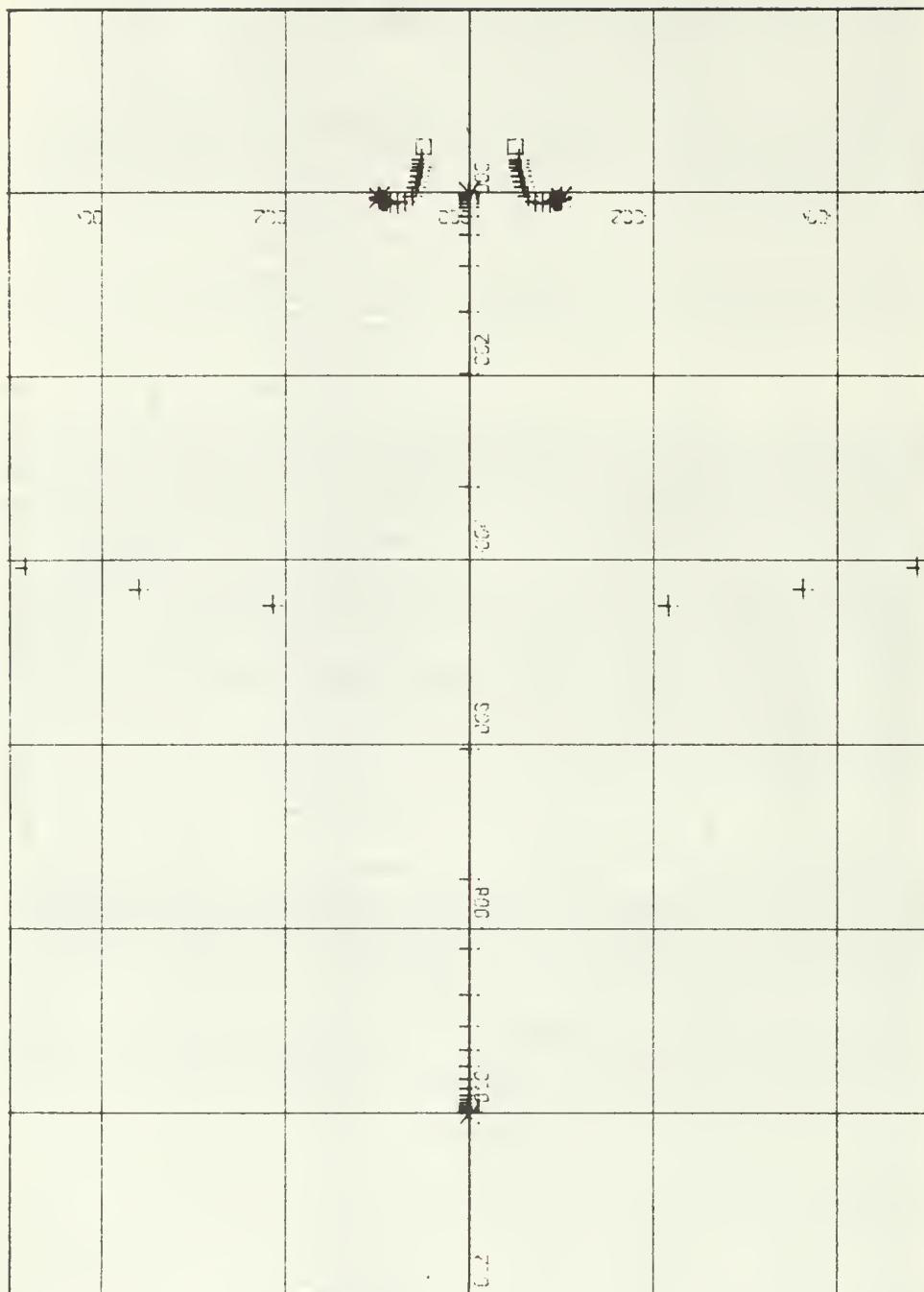


Figure 2.16a. Root Locus for Point 9

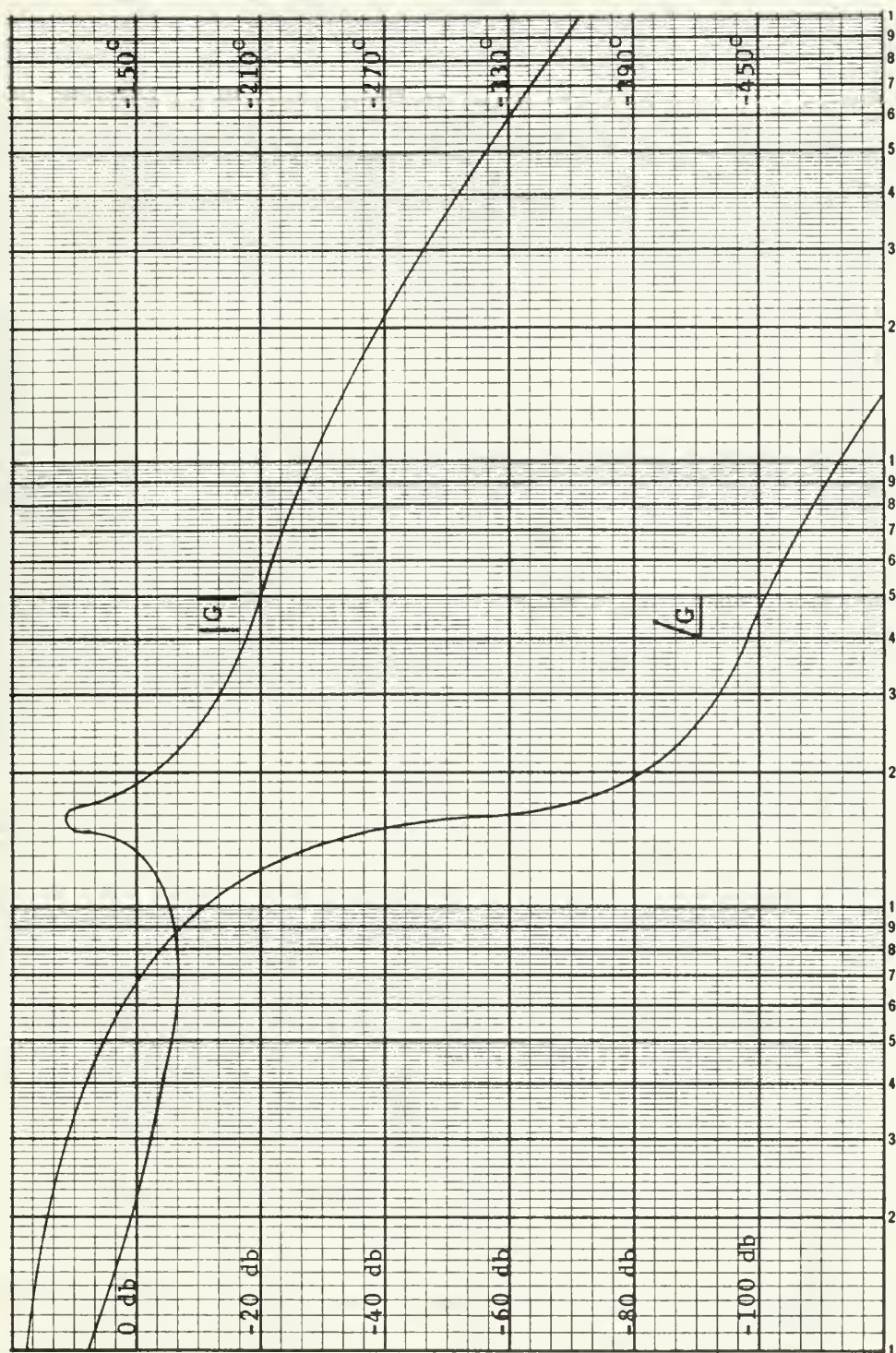


Figure 2.16b. Bode Diagram for Point 9.

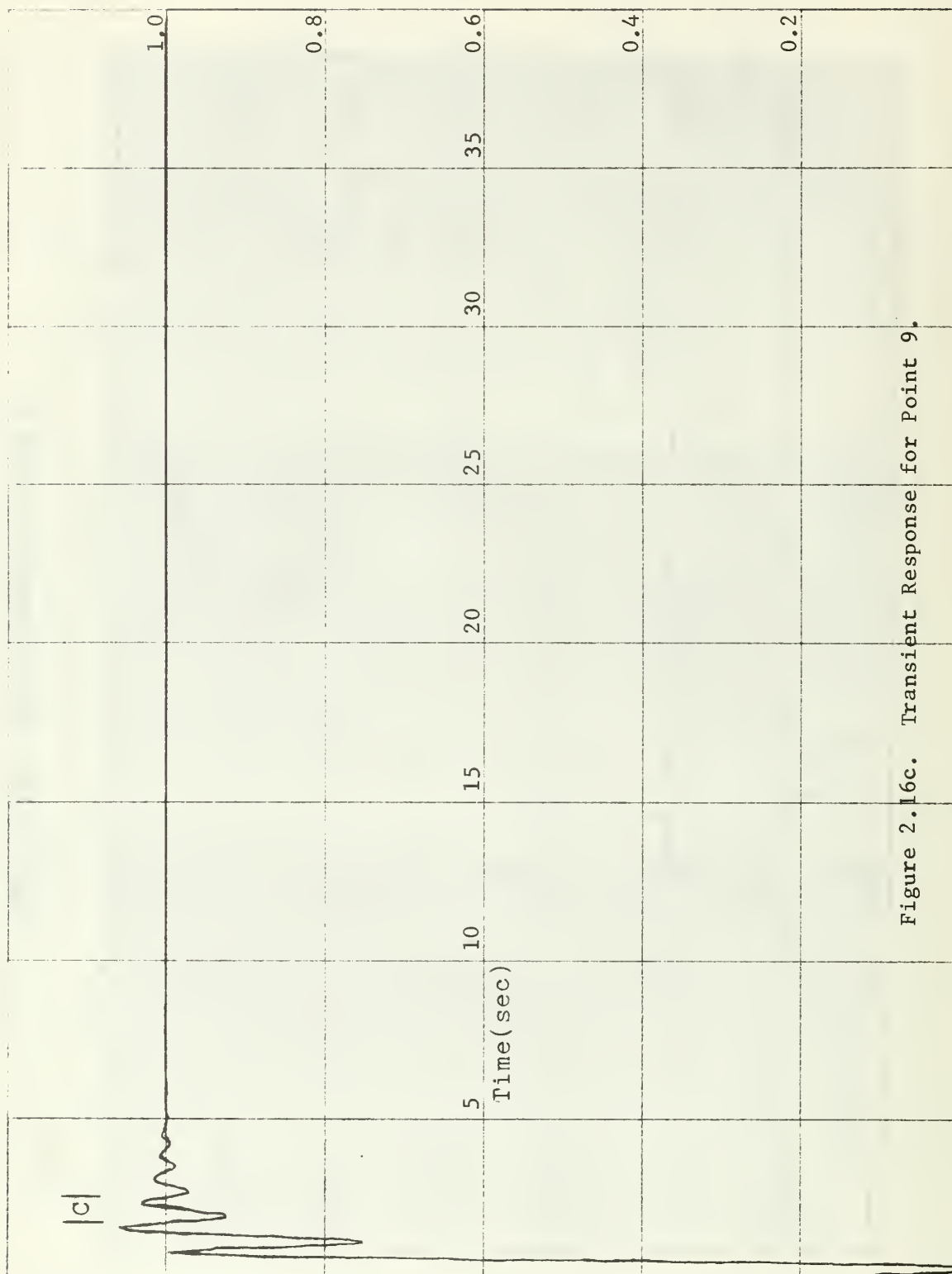


Figure 2.16c. Transient Response for Point 9.

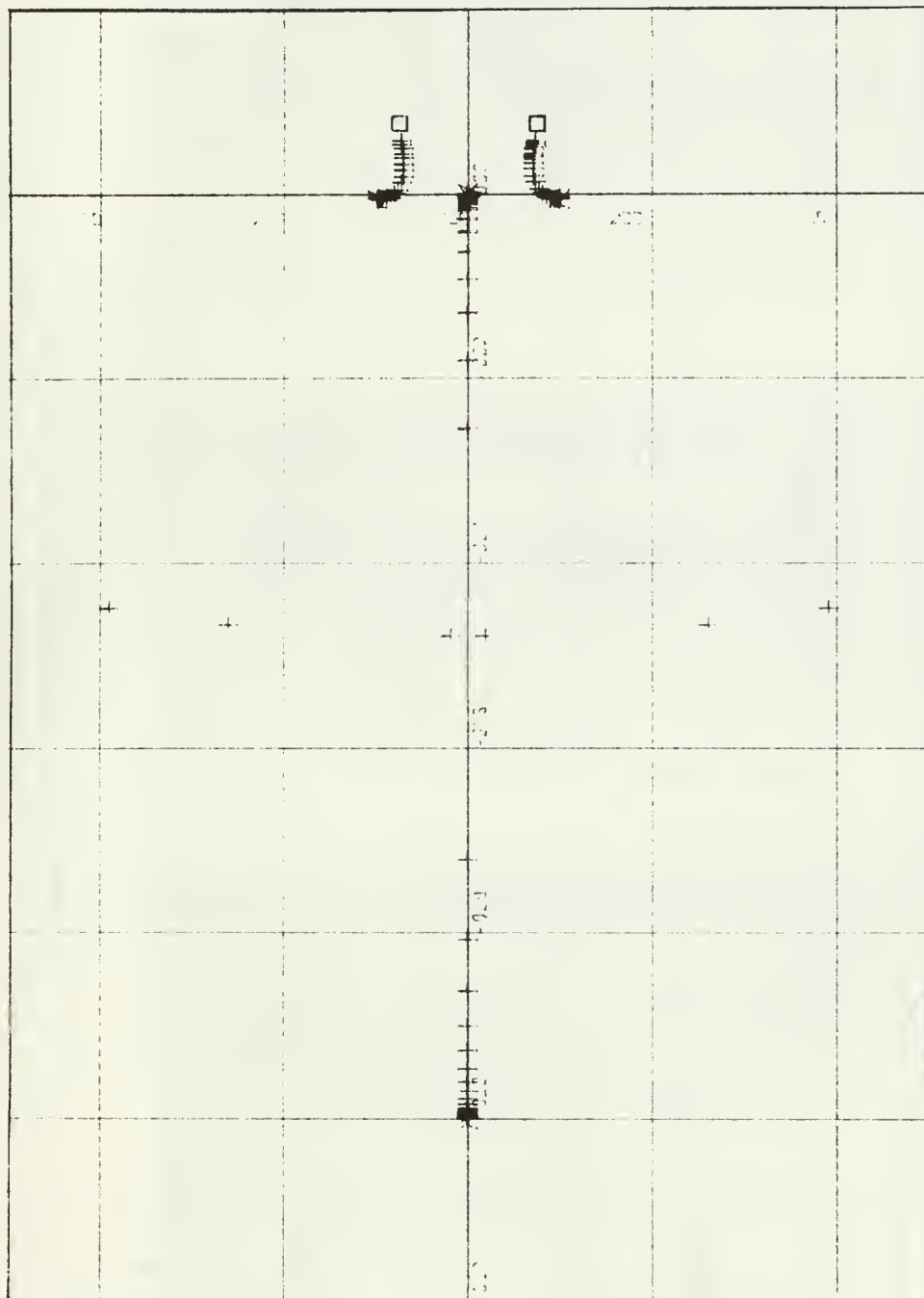


Figure 2.17a. Root Locus for Point 10

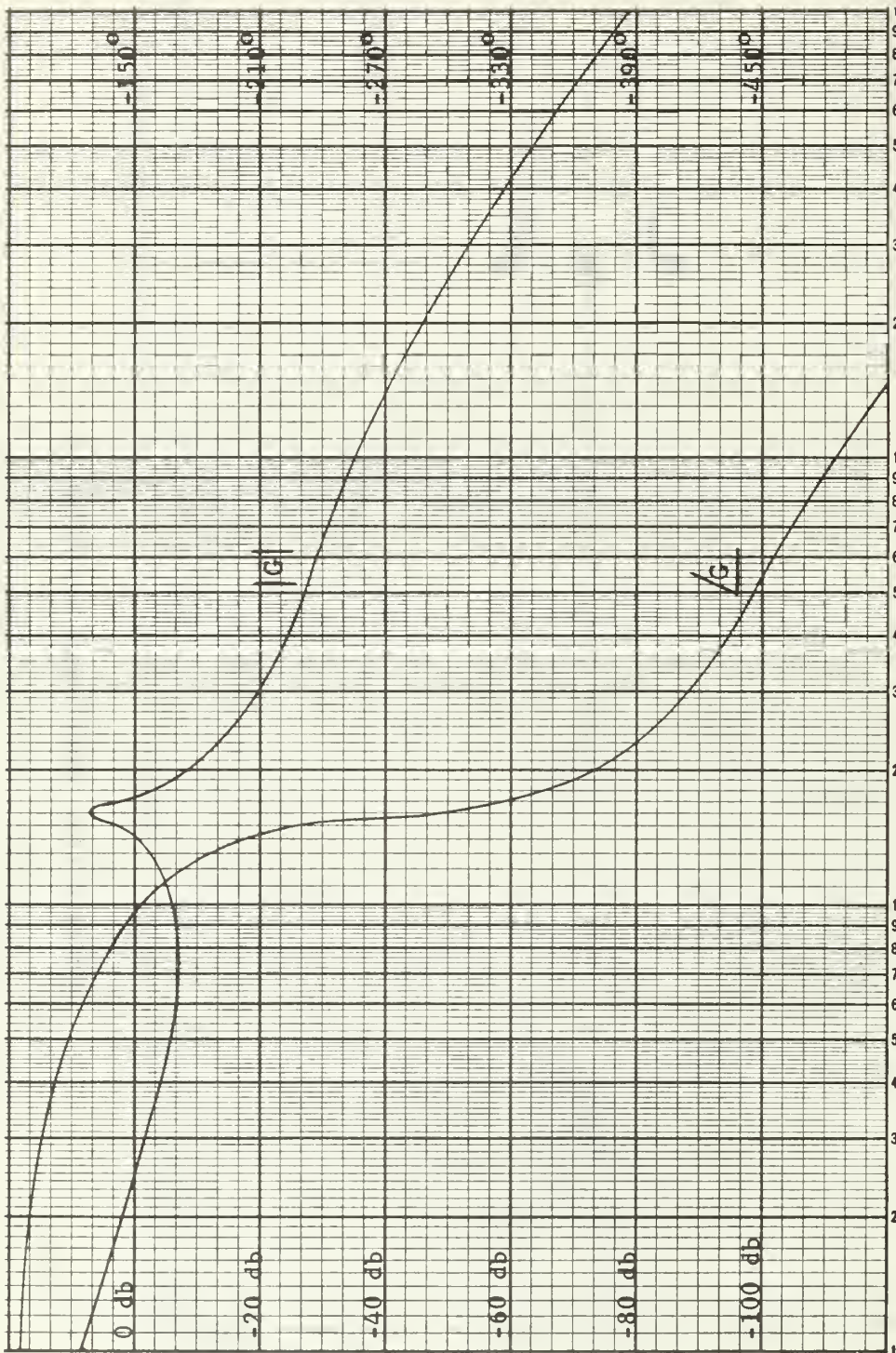


Figure 2.17b. Bode Diagram for Point 10.

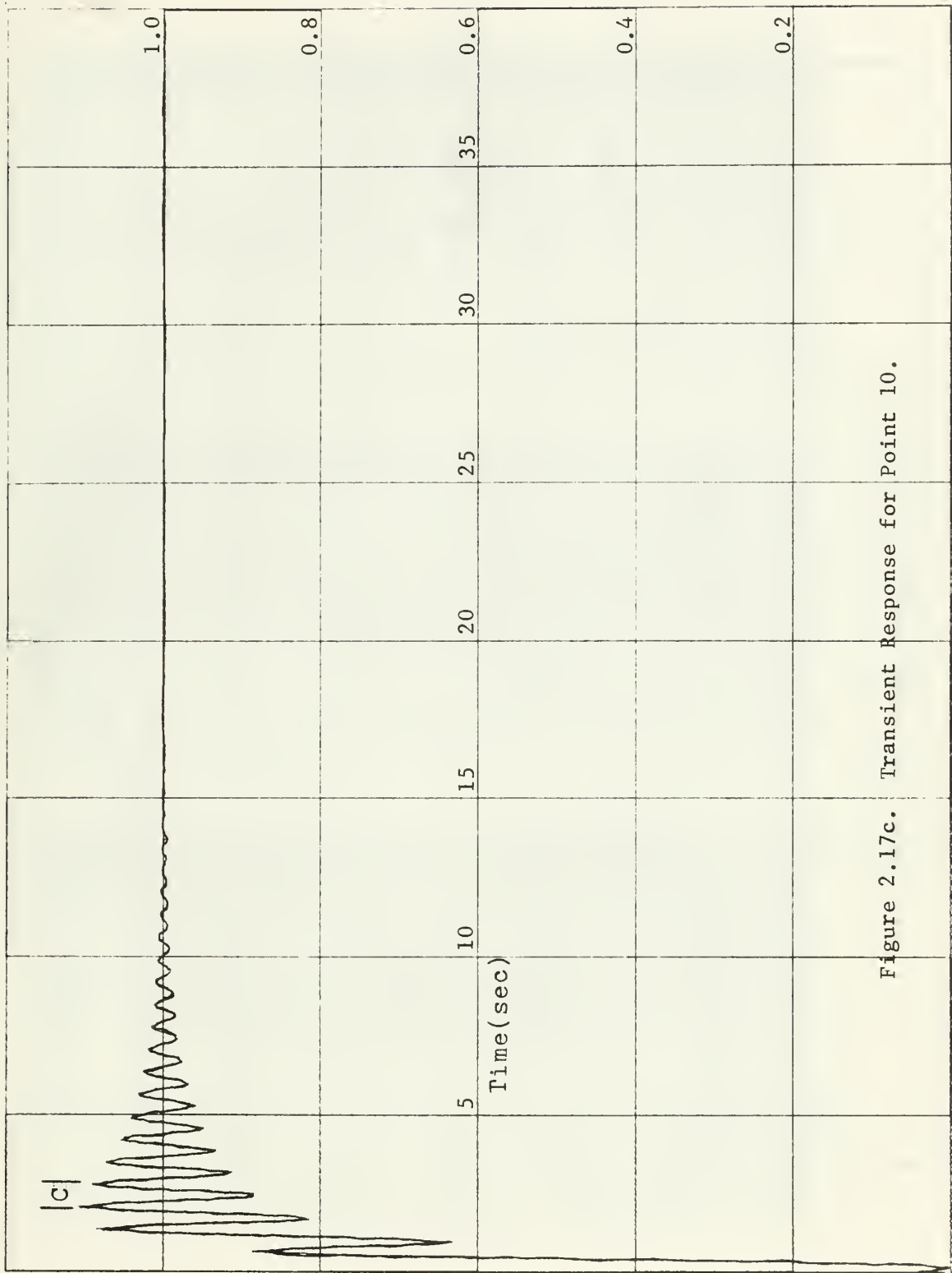


Figure 2.17c. Transient Response for Point 10.

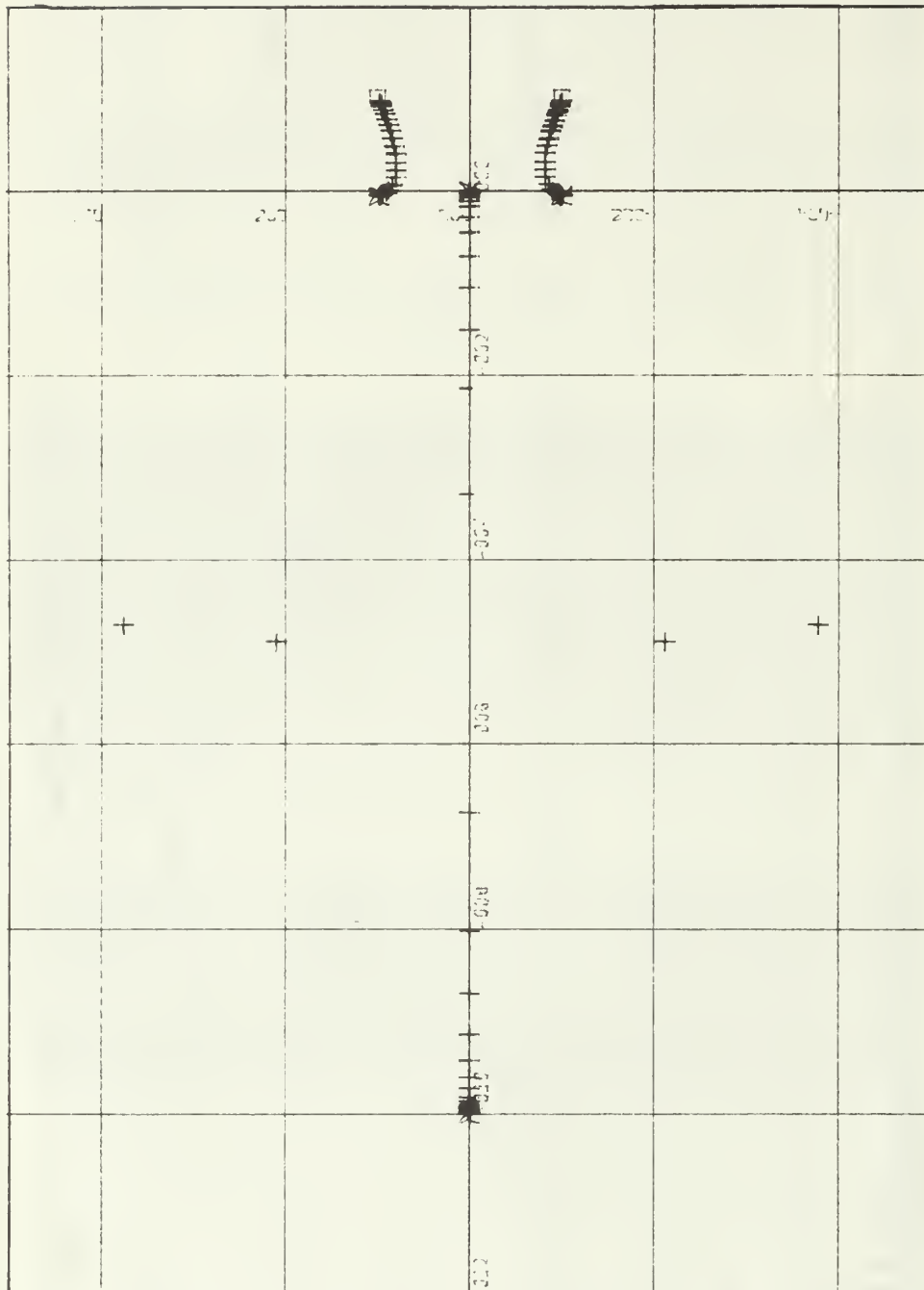


Figure 2.18a. Root Locus for Point 11

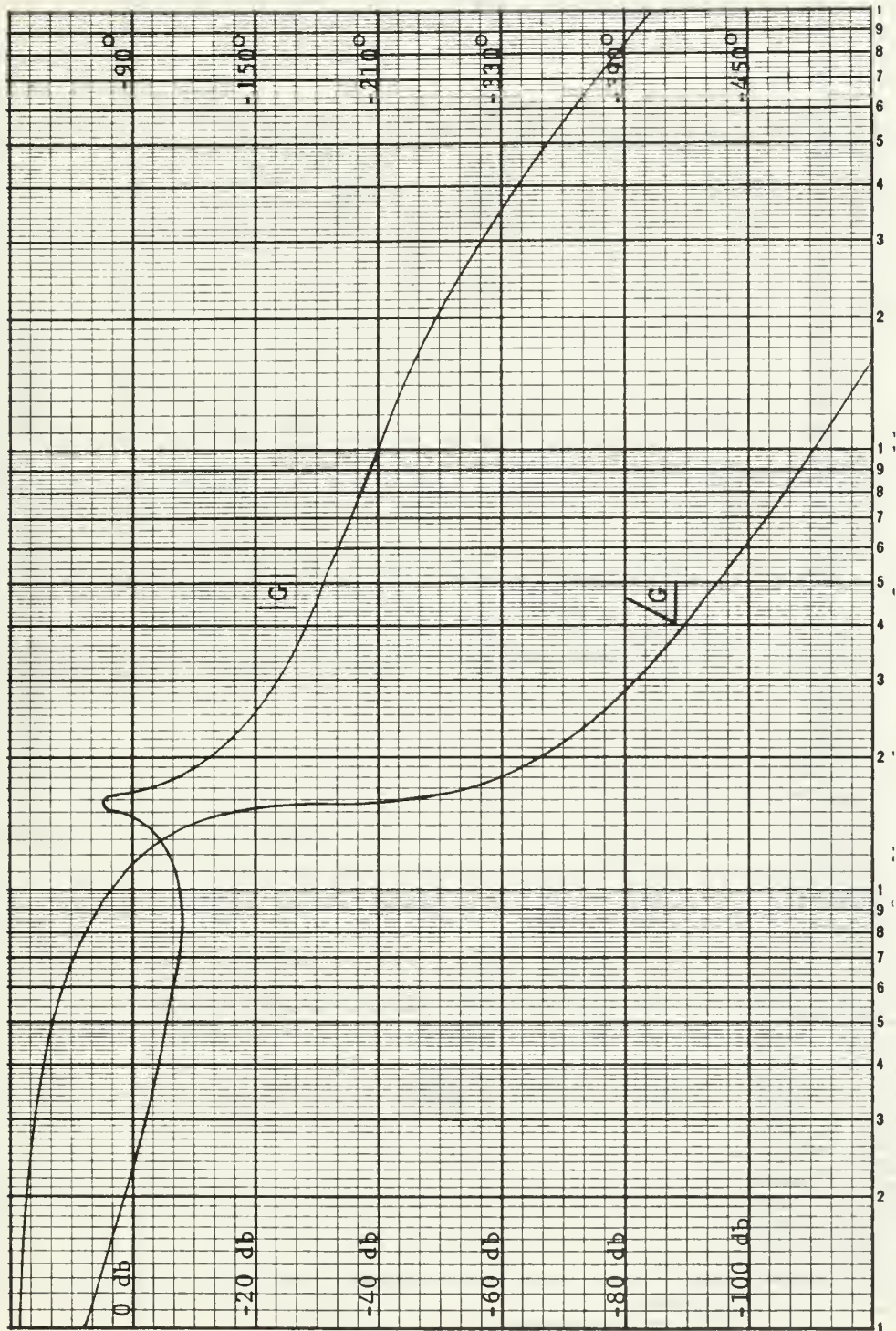


Figure 2.18b. Bode Diagram for Point 11.

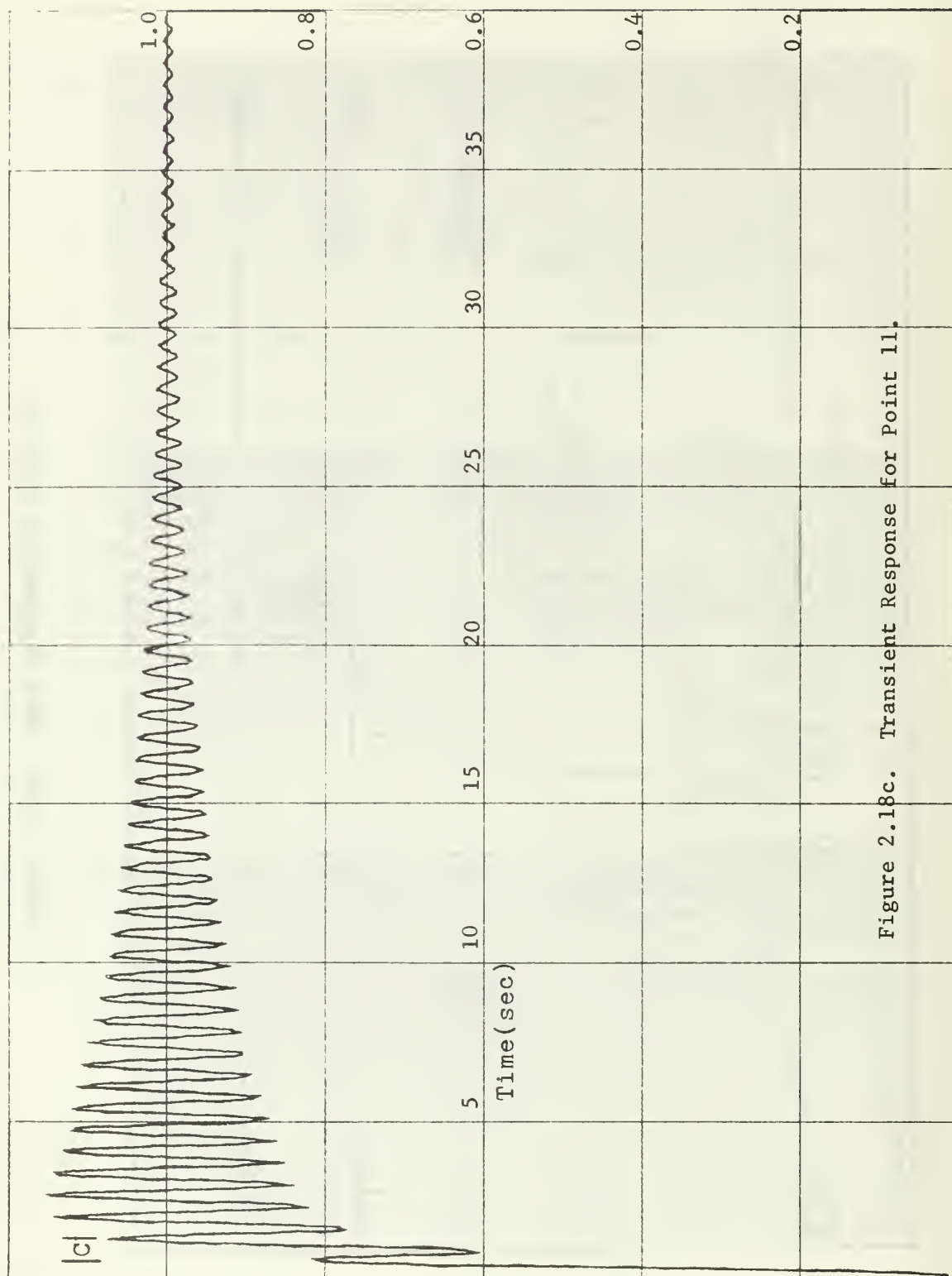


Figure 2.18c. Transient Response for Point 11.

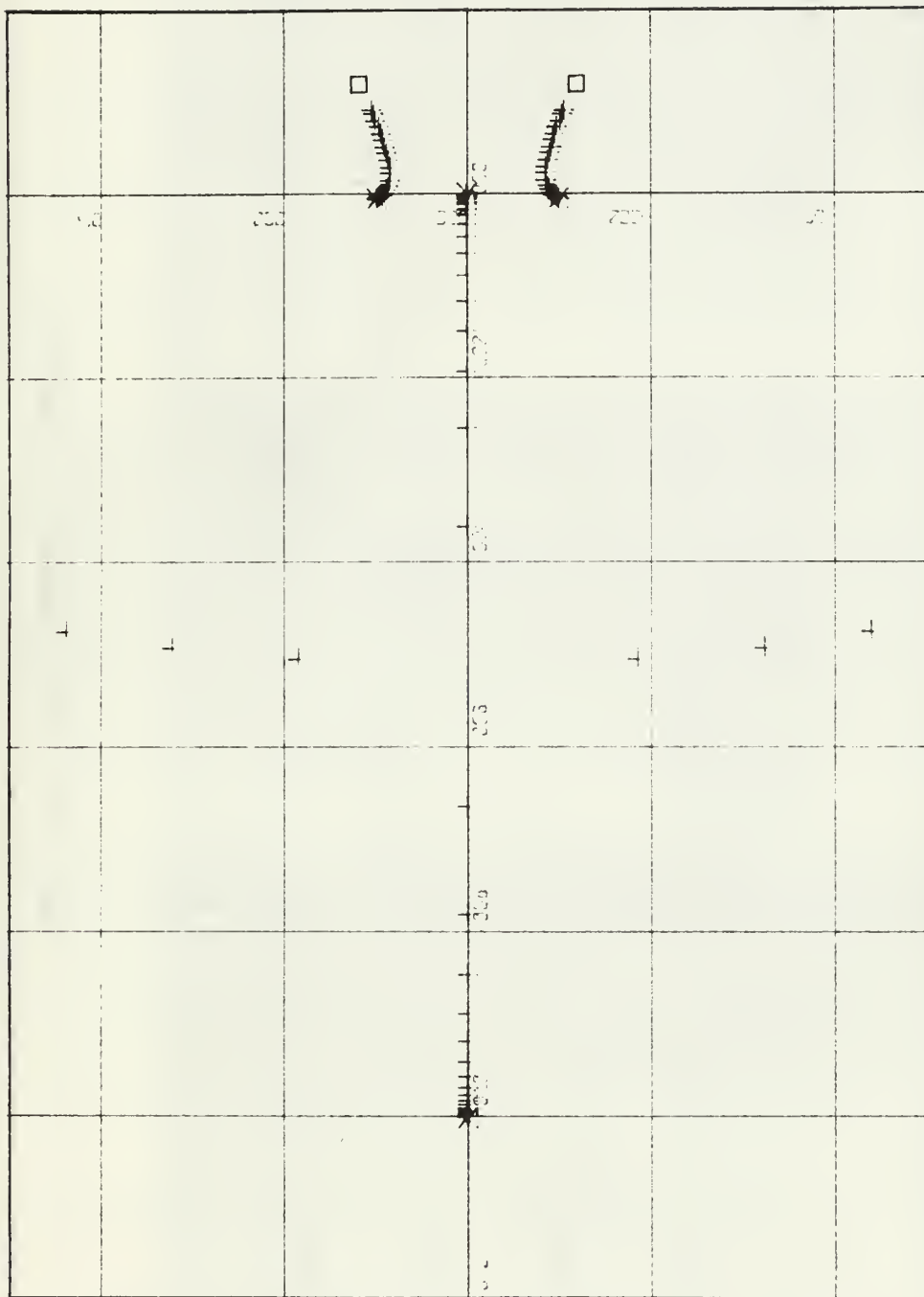


Figure 2.19a. Root Locus for Point 12

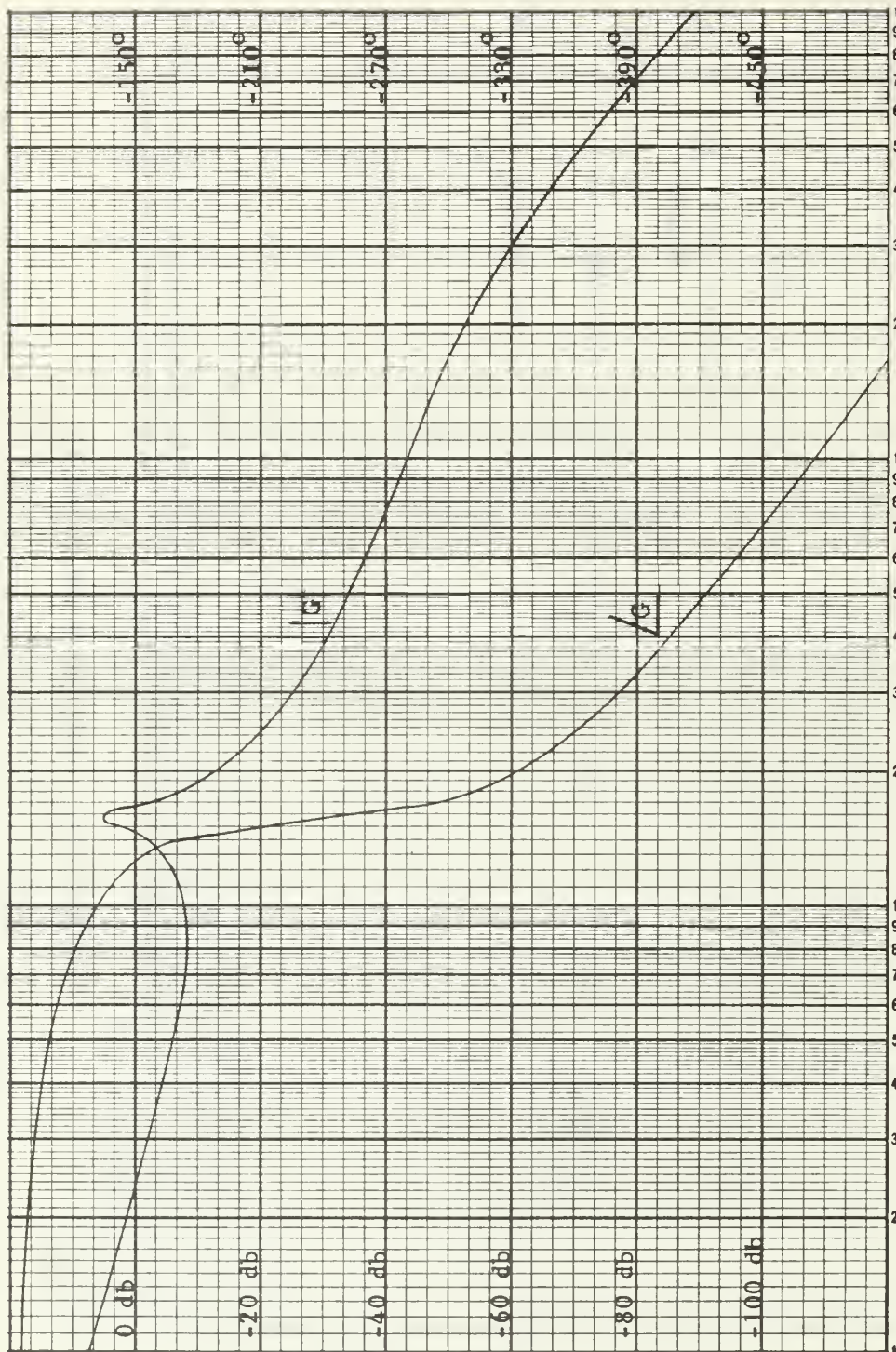
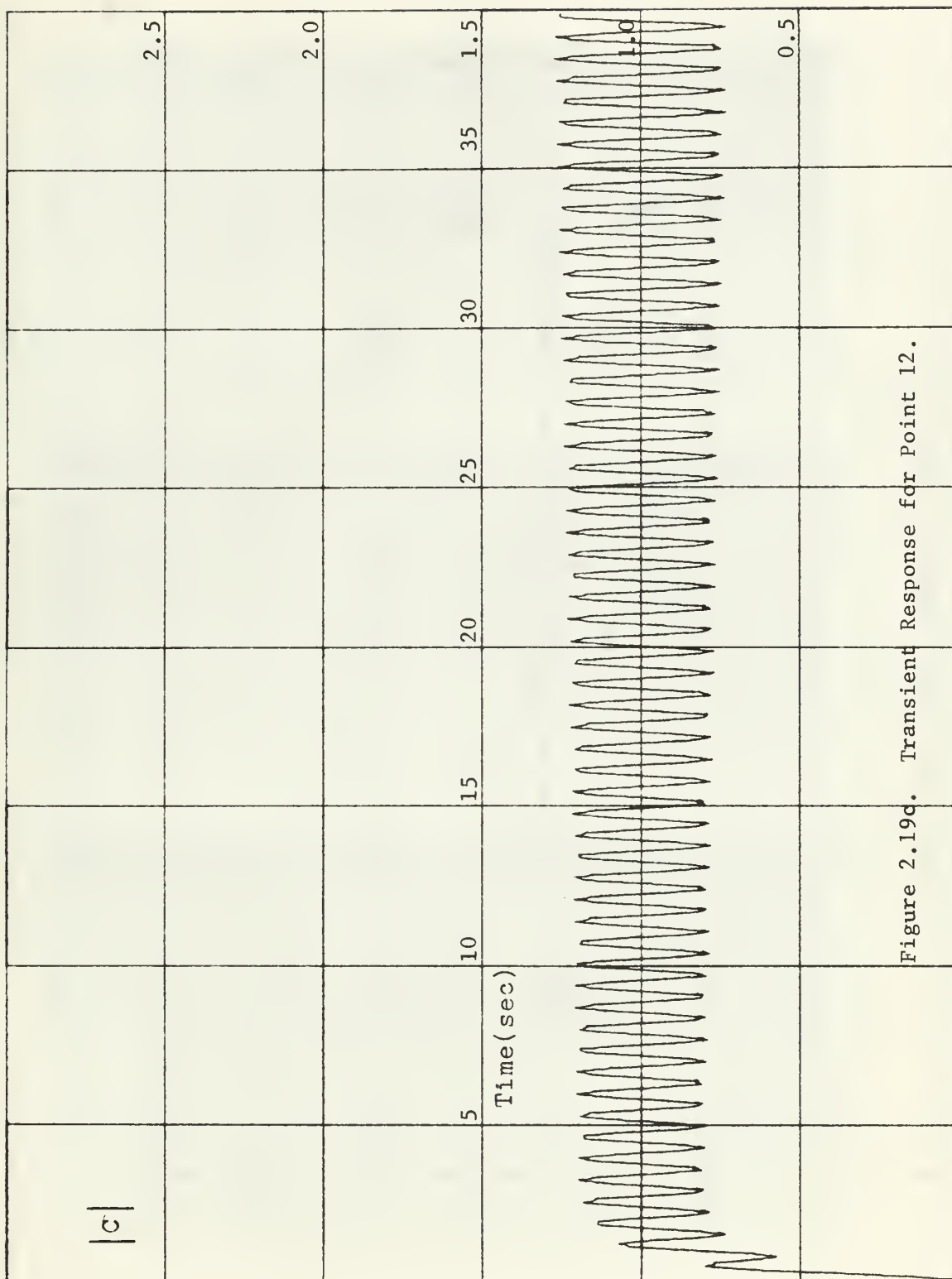


Figure 2.19b. Bode Diagram for Point 12.



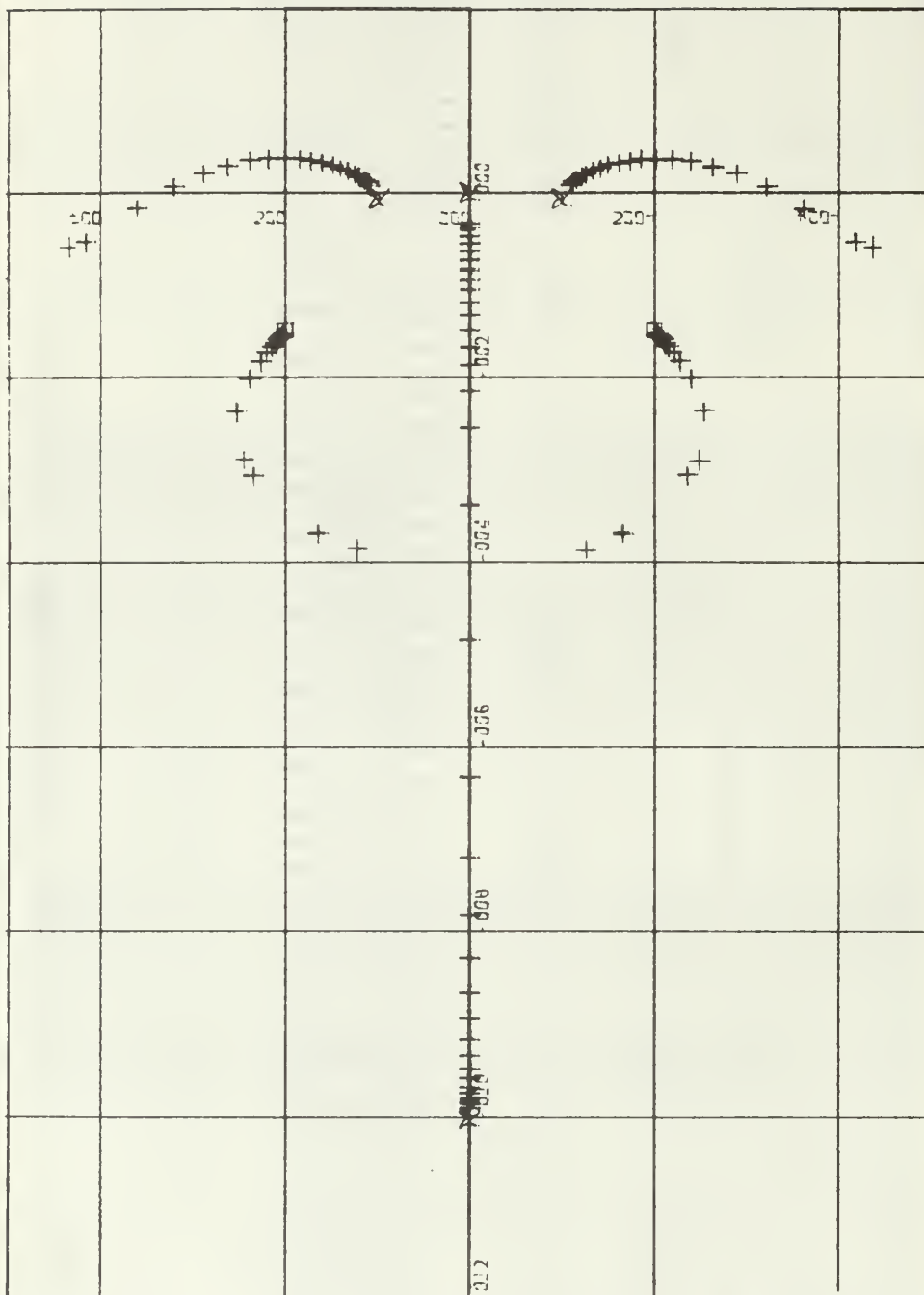


Figure 2.20a. Root Locus for Point 13

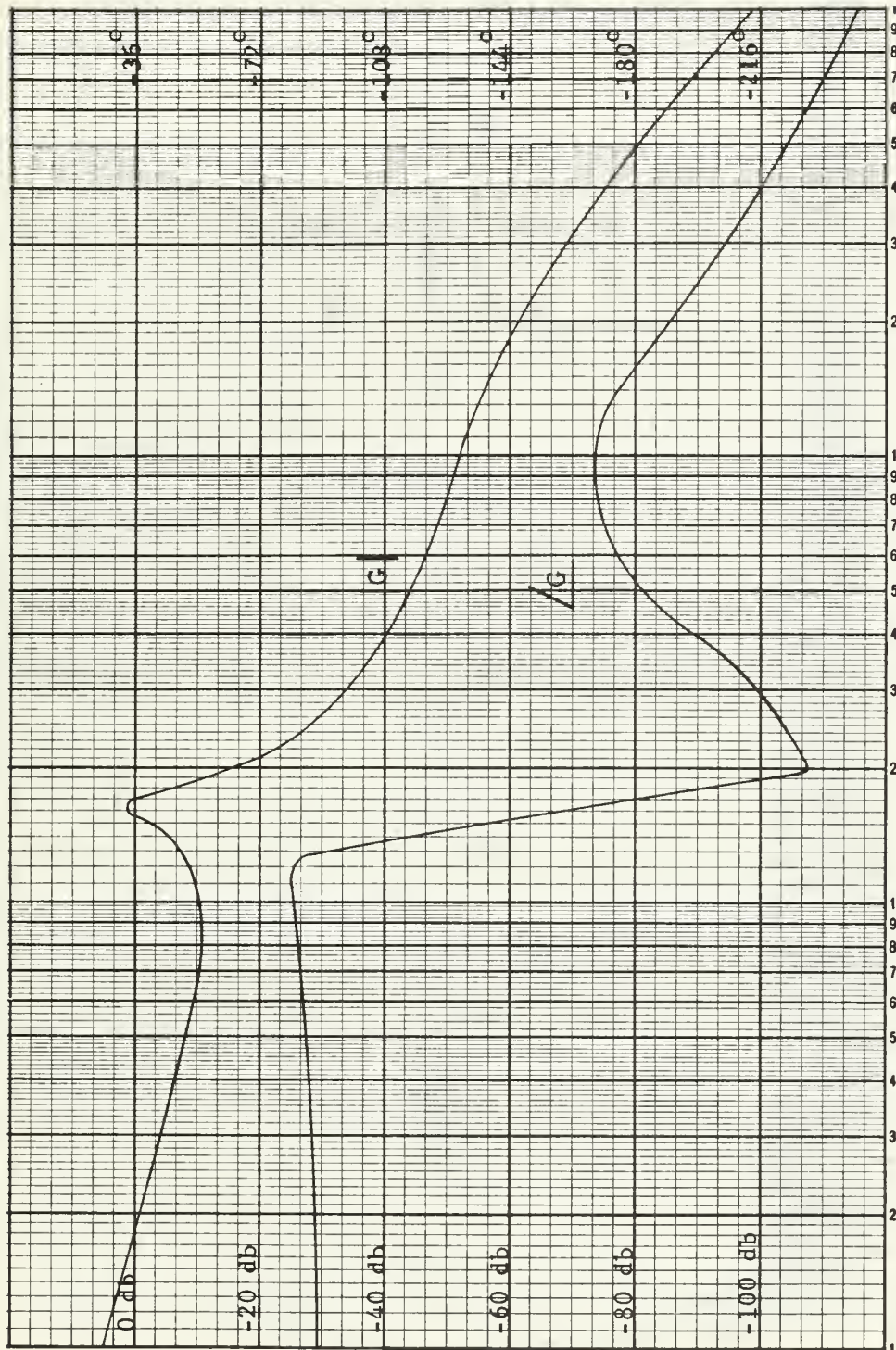


Figure 2.20b. Bode Diagram for Point 13.

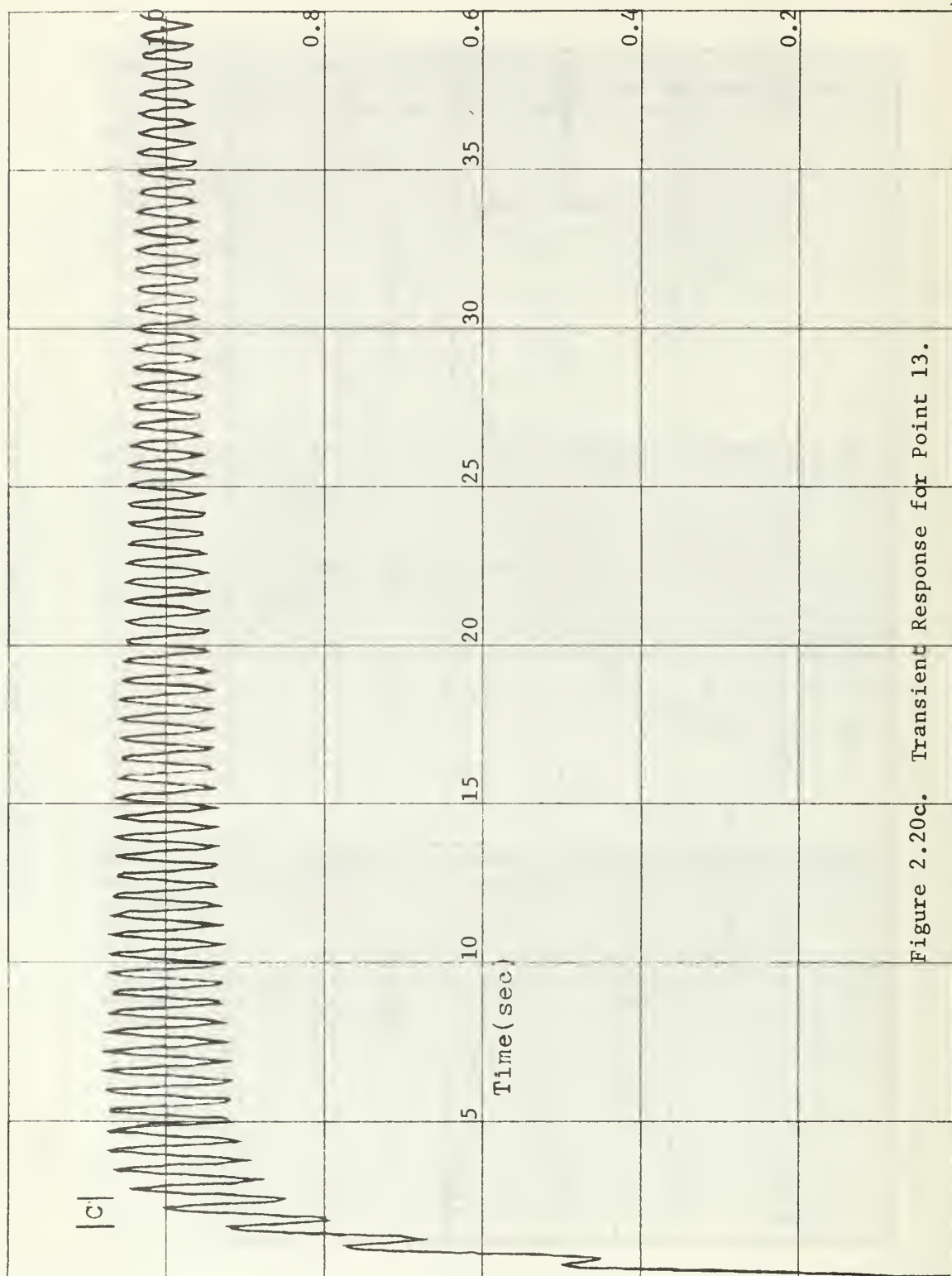


Figure 2.20c. Transient Response for Point 13.

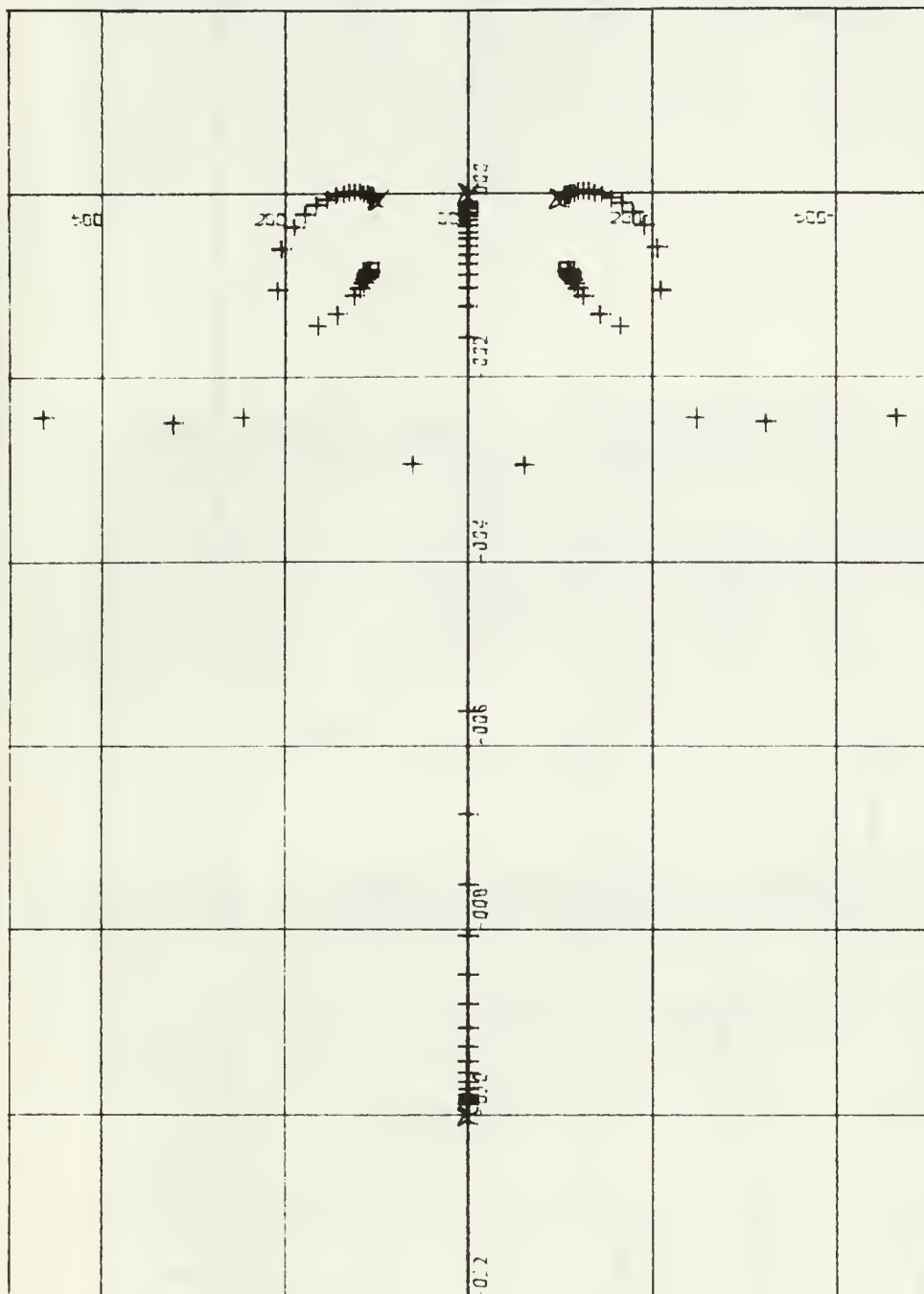


Figure 2.21a. Root Locus for Point 14

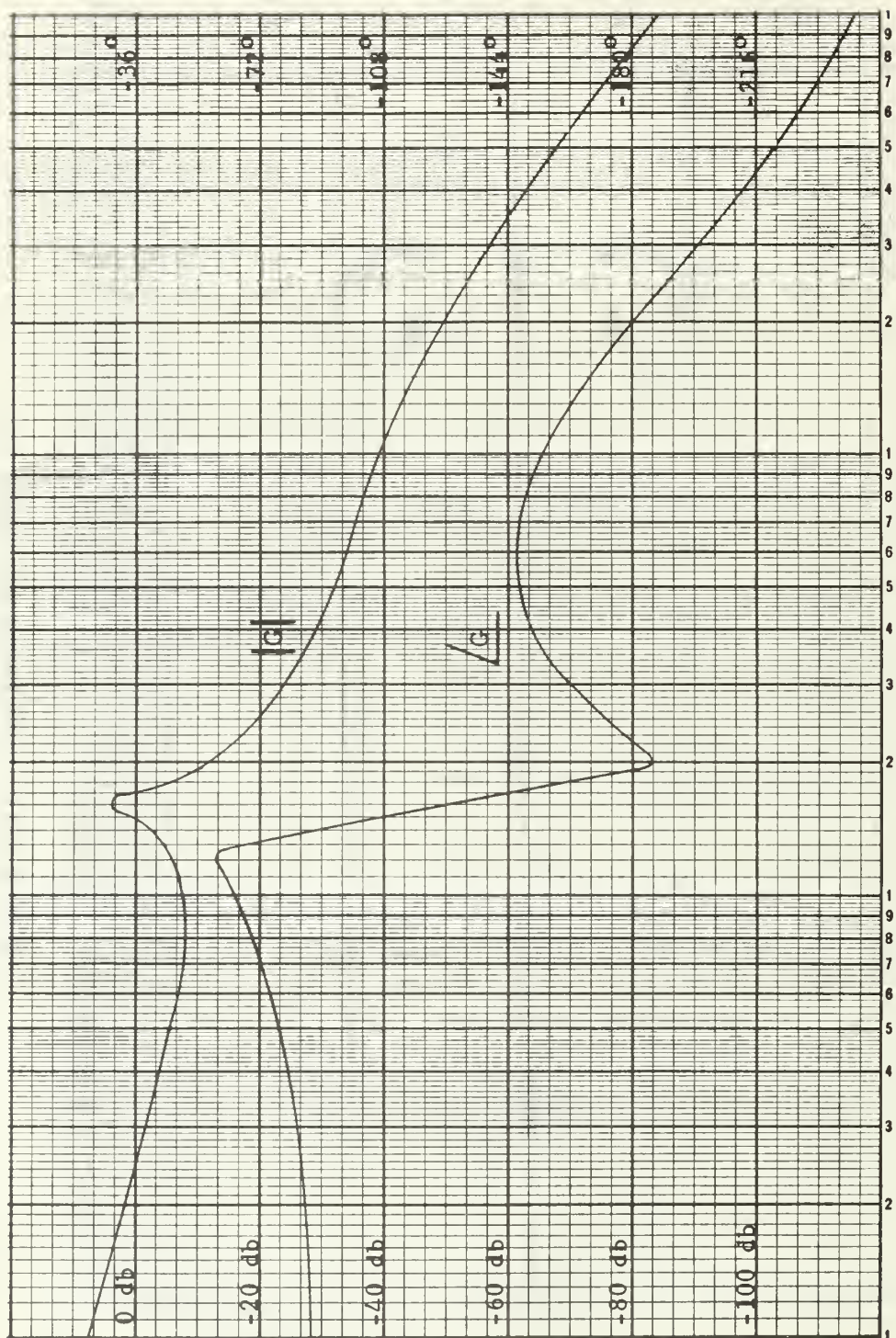


Figure 2.21b. Bode Diagram for Point 14.

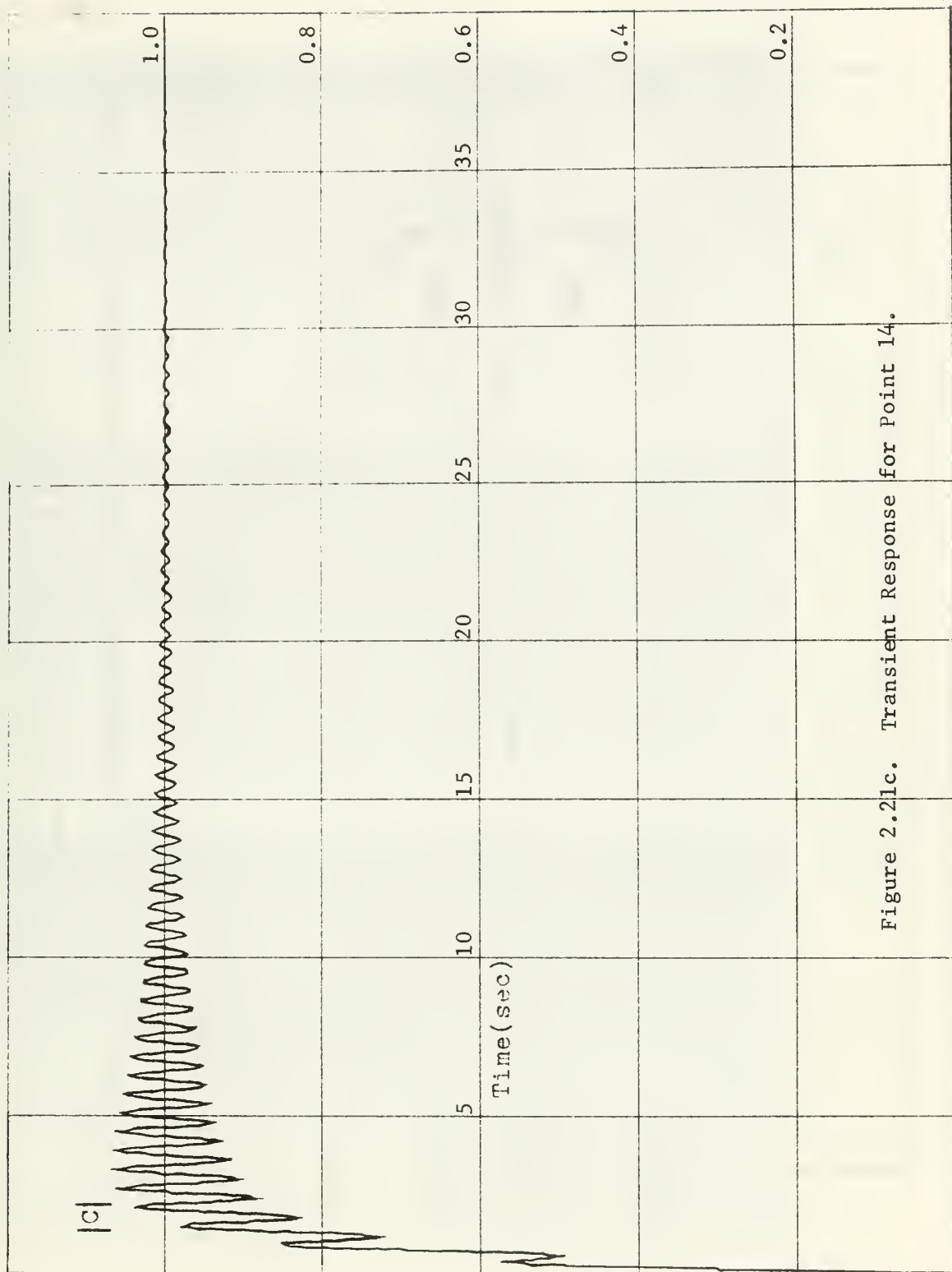


Figure 2.21c. Transient Response for Point 14.

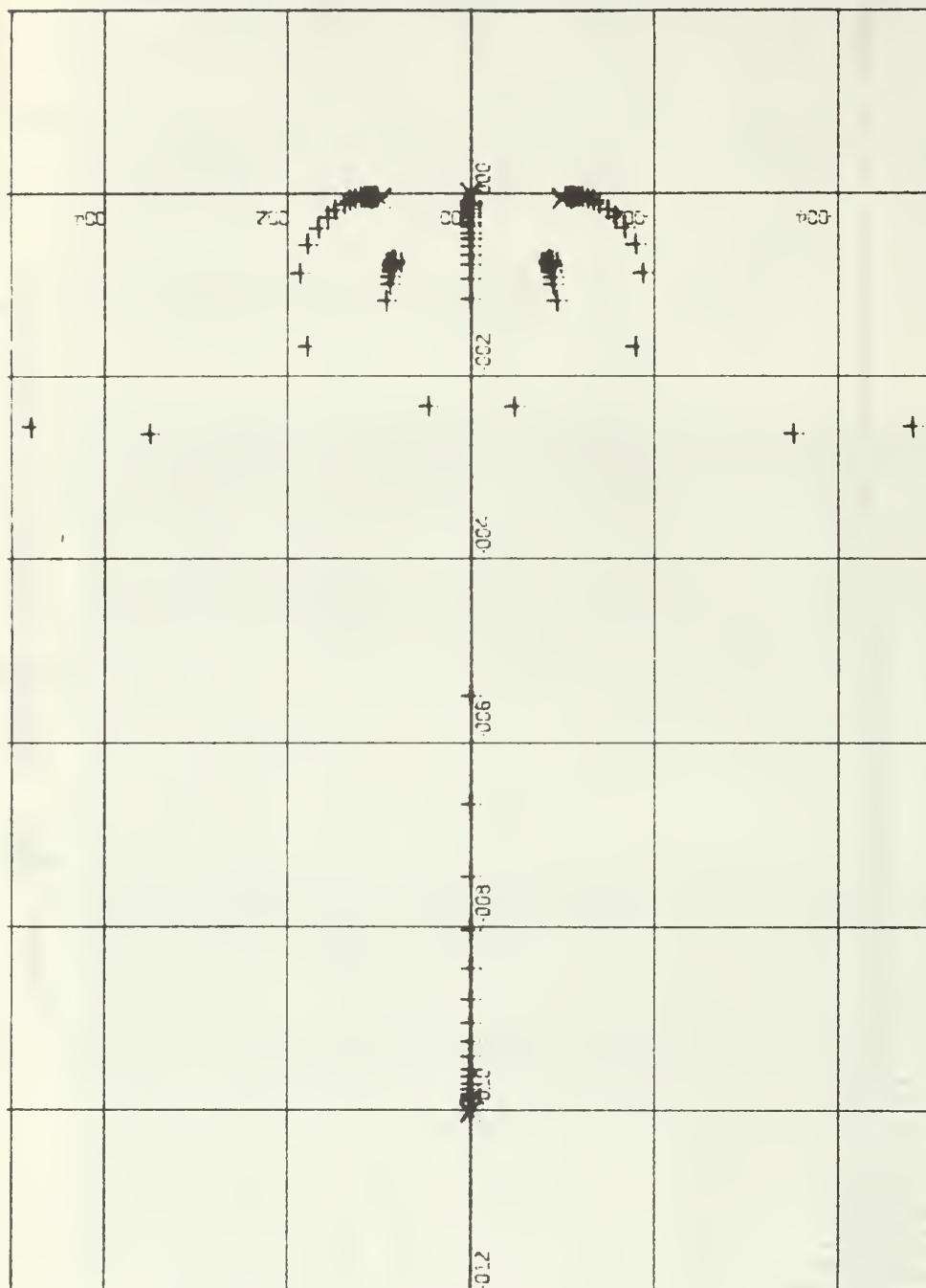


Figure 2.22a. Root Locus for Point 15

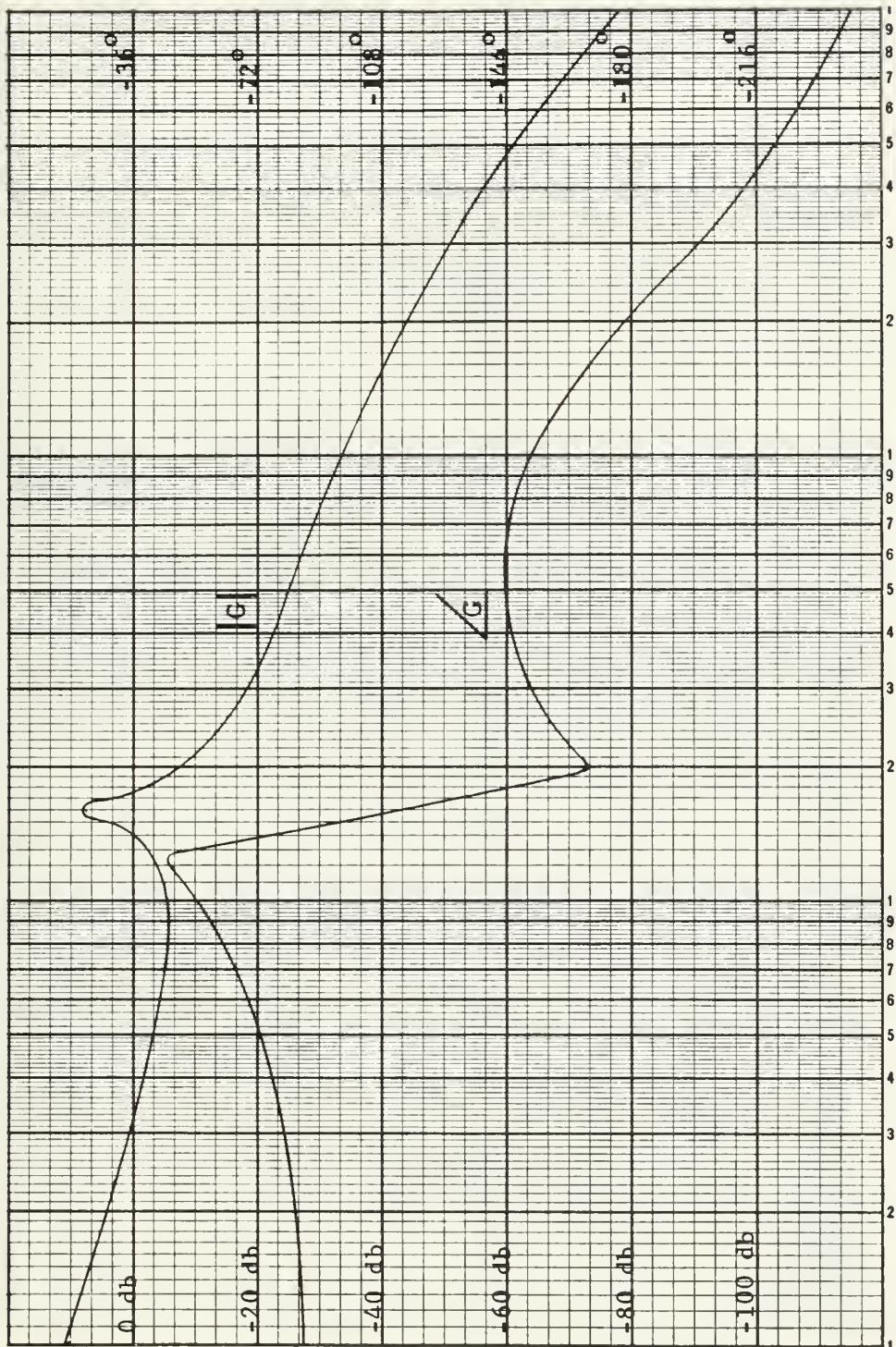


Figure 2.22b. Bode Diagram for Point 15.

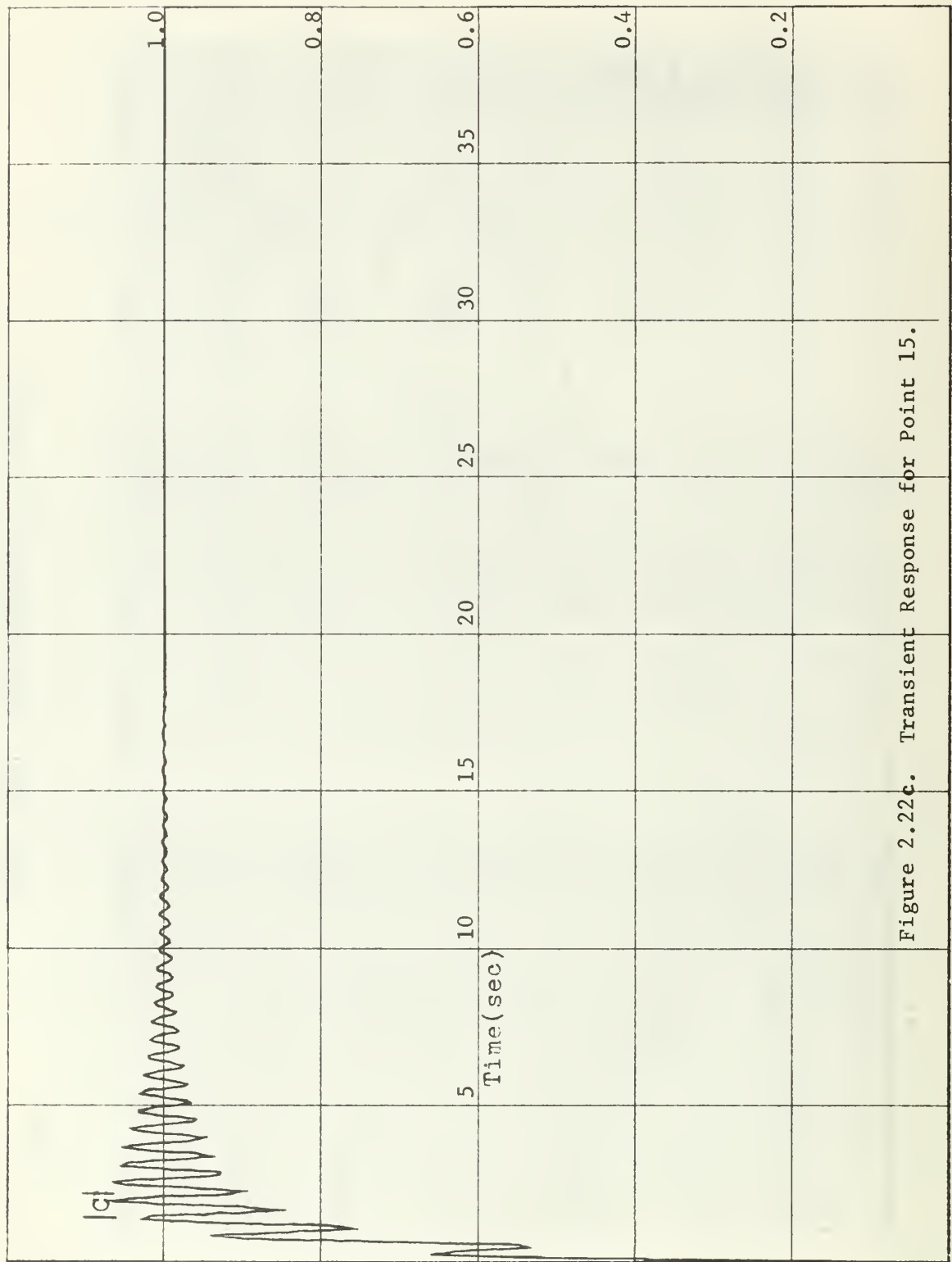


Figure 2.22c. Transient Response for Point 15.

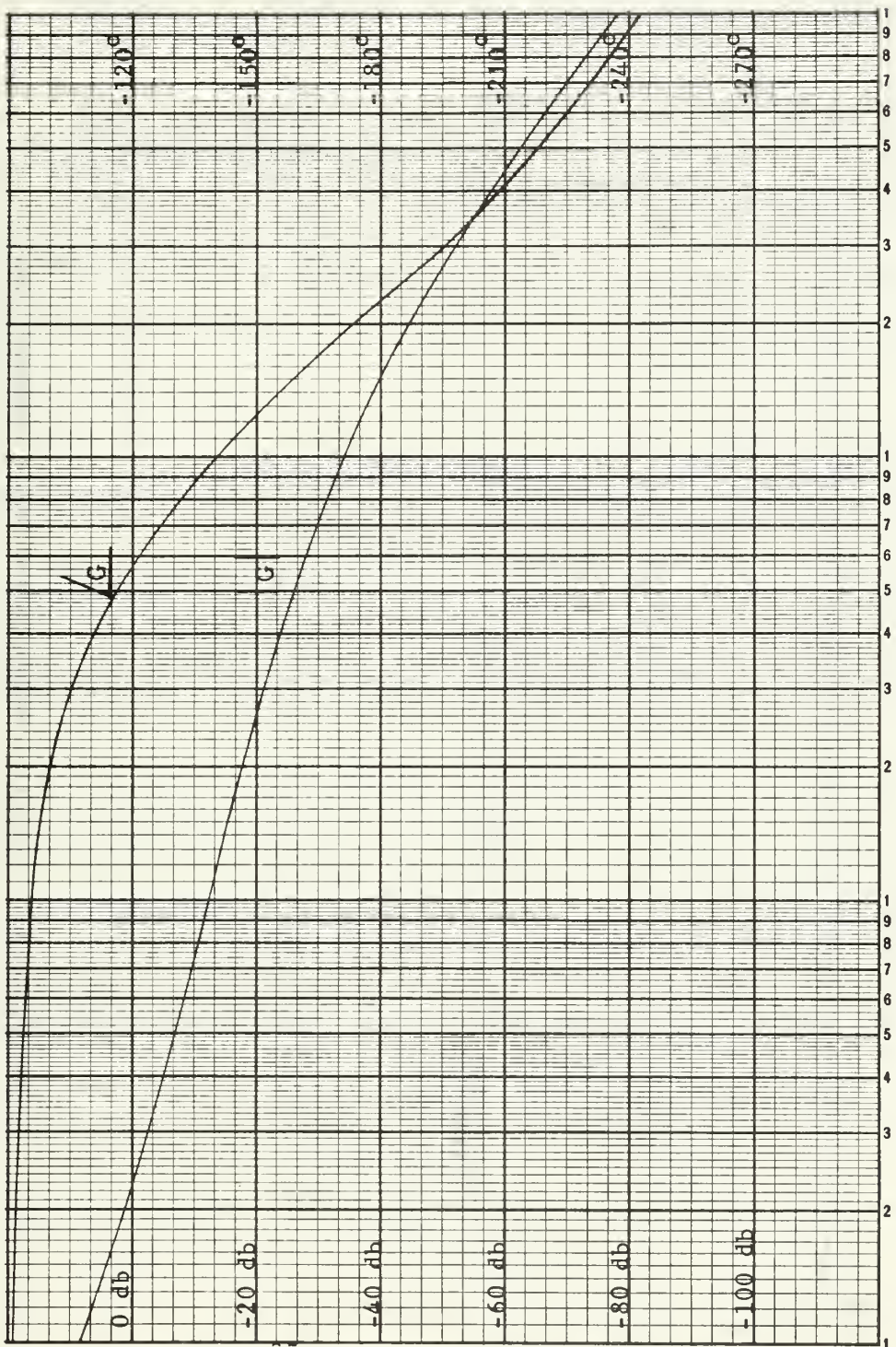


Figure 2.23b. Bode Diagram for Exact Compensation.



Figure 2.23c. Transient Response for Exact Compensation.

BIBLIOGRAPHY

1. Thaler, G. J. and Brown, R. G., Analysis and Design of Feedback Control Systems, 2d ed., McGraw-Hill, 1960.
2. Hsu, J. C. and Meyer, A. U., Modern Control Principles and Applications, McGraw-Hill, 1968.
3. Raven, F. H., Automatic Control Engineering, 2d ed., McGraw-Hill, 1968.
4. Watkins, B. O., Introduction to Control Systems, Macmillan, 1969.

INITIAL DISTRIBUTION LIST

| | No. Copies |
|--|------------|
| 1. Defense Documentation Center Cameron Station Alexandria, Virginia 22314 | 20 |
| 2. Library, Code 0212 Naval Postgraduate School Monterey, California 93940 | 2 |
| 3. Dr. George Thaler Dept. of Electrical Engineering Naval Postgraduate School Monterey, California 93940 | 5 |
| 4. TNFG Ruben Landazuri Primera Zona Naval Guayaquil, Ecuador | 2 |
| 5. Commander, Naval Ordnance Systems Command Department of the Navy Washington, D. C. 20360 | 1 |

DOCUMENT CONTROL DATA - R & D

(Security classification of title, body of abstract and indexing annotation must be entered when the overall report is classified)

1. ORIGINATING ACTIVITY (Corporate author)

Naval Postgraduate School
Monterey, California 93940

2a. REPORT SECURITY CLASSIFICATION

Unclassified

2b. GROUP

3. REPORT TITLE

Servo Compensation for Mechanical Resonances and Feedback Loops

4. DESCRIPTIVE NOTES (Type of report and inclusive dates)

Master's Thesis; December 1969

5. AUTHOR(S) (First name, middle initial, last name)

Ruben Jaime Landazuri

6. REPORT DATE

December 1969

7a. TOTAL NO. OF PAGES

89

7b. NO. OF REFS

4

8a. CONTRACT OR GRANT NO.

b. PROJECT NO.

c.

d.

9a. ORIGINATOR'S REPORT NUMBER(S)

9b. OTHER REPORT NO(S) (Any other numbers that may be assigned this report)

10. DISTRIBUTION STATEMENT

This document has been approved for public release and sales; its distribution is unlimited.

11. SUPPLEMENTARY NOTES

12. SPONSORING MILITARY ACTIVITY

Naval Postgraduate School
Monterey, California 93940

13. ABSTRACT

When the transfer function of a system has at least one pair of complex poles, resonant peaks will occur in the open-loop frequency response at the frequency determined by these complex poles. The resonant peaks may produce instability in the closed-loop system. Cascaded complex-zero compensators are studied in order to cancel the effect produced by the complex poles. Circles of stability are developed and if the complex zeros of the compensator are located inside the circles the system stability is guaranteed. Several locations for the complex zeros in the s-plane are studied and a correlation among frequency-response, transient-response and root-locus techniques is described to aid in the design of the compensator. (Complex poles are often generated by mechanical resonances)

KEY WORDS

Stability

Mechanical Resonances

Compensation Design

LINK A

LINK B

LINK C

ROLE

WT

ROLE

WT

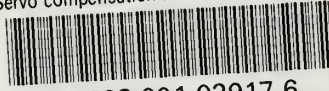
ROLE

WT



thesL2563

Servo compensation for mechanical resona



3 2768 001 02917 6

DUDLEY KNOX LIBRARY